Université d'Ottawa · University of Ottawa

Université d'Ottawa · University of Ottawa

FACULTÉ DES ÉTUDES SUPÉRIEURES ET POSTDOCTORALES

FACULTY OF GRADUATE AND POSTDOCTORAL STUDIES

VLASKALIN, Tatjana

AUTEUR DE LA THÈSE - AUTHOR OF THESIS

M.Sc. (Cellular and Molecular Medicine)

GRADE - DEGREE

Cellular and Molecular Medicine

FACULTÉ, ÉCOLE, DÉPARTEMENT - FACULTY, SCHOOL, DEPARTMENT

TITRE DE LA THÈSE - TITLE OF THE THESIS

Profiling Apoptotic Patterns during Forelimb Development and Regeneration in the Newt, *Notophthalmus viridescens*

Catherine Tsilfidis

DIRECTEUR DE LA THÈSE - THESIS SUPERVISOR

EXAMINATEURS DE LA THÈSE - THESIS EXAMINERS

Martin Holcik

David Park

J.-M. De Koninck, Ph.D.

LE DOYEN DE LA FACULTÉ DES ÉTUDES SUPÉRIEURES ET POSTDOCTORALES

SIGNATURE

DEAN OF THE FACULTY OF GRADUATE AND POSTDOCTORAL STUDIES

Profiling Apoptotic Patterns during Forelimb Development and Regeneration in the newt, *Notophthalmus viridescens*

by

Tatjana Vlaskalin

This thesis is submitted to the School of Graduate Studies and Research

in partial fulfillment of the Masters of Science program in

Growth and Development

Department of Cellular and Molecular Medicine

Faculty of Medicine

University of Ottawa

June 9, 2003

Your file Votre référence
ISBN: 0-612-90354-0
Our file Notre référence
ISBN: 0-612-90354-0

Abstract

Recent studies have found that many of the genes involved in the initial development of the limb in higher vertebrates are also expressed during regeneration of the limb in urodeles. These similarities have lead researchers to conclude that the regeneration process is a recapitulation of development and that patterning of the regenerate mimics pattern formation in development. In this work, we address the issue of whether regeneration and development are similar by examining patterns of apoptosis during these processes. In contrast to higher vertebrates, forelimb development in the newt, *Notophthalmus viridescens*, does not follow conventional pattern formation utilizing interdigital apoptosis as the method of individualization of the digits. Similarly, forelimb regeneration does not undergo interdigital apoptosis during cartilage condensation and digit formation in the adult. Apoptosis seems to play an important role during the wound healing stage of regeneration and again during cartilage to bone turnover during digit and radius/ulna regeneration. We suggest that urodeles have adapted a mechanism of forelimb regeneration that may re-activate developmental pathways similar to higher vertebrates, yet without cell death between the digits, and furthermore, undergo a unique mechanism of limb development in which apoptosis plays a minor role.

TABLE OF CONTENTS

LIST OF FIGURES

CHAPTER ONE

CHAPTER TWO

CHAPTER THREE

LIST OF ABBREVIATIONS

AEC – Apical epidermal cap
AER – Apical epithelial ridge
Apaf-1 – Apoptosis protease activating factor-1
Hox – Homeobox
Lmx 1 – LIM-homeodomain
FGF – Fibroblast growth factor
ZPA – Zone of polarizing activity
Shh – Sonic hedgehog
DNA – Deoxyribonucleic acid
NrFrg – Newt radical fringe
N-shh – Newt sonic hedgehog
Bhh – Banded hedgehog
Ihh – Indian hedgehog
PCD – Programmed cell death
TNF – Tumour necrosis factor
DD – Death domain
DED – death effector domain
FADD – Fas-associated death domain
IAPs – Inhibitor of apoptosis proteins
BIR – Baculoviral IAP repeat
CARD – Caspase recruitment domain
BMP – Bone morphogenetic protein
PBS – Phosphate buffered saline
PBT – PBS with Tween 20
TdT – Terminal deoxynucleotidyl transferase
TUNEL – TdT – mediated dUTP nick end labelling
PFA – Paraformaldehyde
MS-222 – Tricaine methane sulphonate/3-aminobenzoic acid ethyl ester
OCT – Optimal cutting temperature
AP – Alkaline Phosphate
MAB – Maleic acid buffer
BSA – Bovine serum albumen
EG – Embryonic gills
MAB-B – MAB with BSA
MABT – MAB with Tween 20

ACKNOWLEDGEMENTS

I would like to send my deepest gratitude and thank my supervisor, Catherine Tsilfidis, for not only taking me into her lab and under her guidance, but taking me into her home and making me feel as part of her family during and after work hours. I would also like to thank her for her constant support and the trust she had instilled in my work, which allowed me the ability to take creative new directions in my experimentation. The experiences I have gained in her hands will go along with me in all my future endeavours.

I would like to thank my professor, Richard A. Liversage, and fellow graduate Christine Wong, for introducing me to the fascinating field of regeneration. I am indebted to them for all their help. Thank you for making yourselves available for answering the many questions I came across during my period of study.

To my fellow lab folk, you made the time in our lab enjoyable and I will cherish the memories we've created. Thank you all for your support and sharing your experiences with me. Particular thanks to Adam and Sandy, for your teachings, technical advice and unconditional assistance. Life in Ottawa would not have been the same without you.

Exceptional thank you goes out to my family. Reaching my educational goals has come from having their outstanding support. Thank you to my parents for giving me the drive to persevere and being my mentors; thank you to my brothers for the much needed comic relief whenever I made the long journey home for a visit.

Special thank you to my husband John for being by my side and going the distance. Thank you for your extended patience, constant love and undeniable support. I am grateful to have shared this experience with you.

Lastly, I am so proud of my little baby daughter, Sanja, who was born into the final crucial days of my work. Quietly, you pondered while I wrote, and listened selflessly, as the keys typed away during the write up of this long enduring thesis. Thank you so much for patiently waiting... Mommy's unconditional devotion to *our* time begins now.

CHAPTER 1
INTRODUCTION

1.1 General Introduction

The ability to replace lost or injured appendages such as limbs and fins during adulthood is restricted to some classes of vertebrates like fish and amphibians. The degree of regeneration among different species varies. For example, anurans (tailless amphibians like frogs) regenerate lost structures that are hypomorphic, their structure is replaced but not functionally equivalent to the original. Urodeles (tailed amphibians like newts and salamanders) regenerate their lost structures by a process that leads to the complete re-growth of a replacement that is anatomically and functionally identical to the original. This includes complex paired appendages like the limbs, which involve many different tissue types. This capability is unique to urodeles and is non-existent in higher vertebrates like birds and mammals, although recent evidence has linked many factors involved in the initial set up of the mammalian limb to that of development of the urodele limb and furthermore, regeneration.

1.2 Epimorphic Regeneration in the Urodele, *Notophthalmus viridescens*

Forelimb regeneration can be classified into two forms. The first is tissue regeneration or morphallaxis, which involves the reorganization of stump tissue at the site of injury as the sole source of cells for the regeneration of the replacement. Limbs that undergo tissue regeneration do not form a structure equivalent to the original; instead the result is a heteromorphic spike with little complexity and no evidence of digit formation. The second type of limb regeneration is referred to as Epimorphic regeneration. During limb regeneration in urodeles, the cells beneath the wound epithelium undergo dedifferentiation, which involves the reversion of differentiated cells (like bone, muscle, nerve, blood and connective tissue), to an unspecialized "embryonic-like" state. These cells undergo rapid proliferation by re-entering the cell cycle until a mesenchymal mass is formed, known as the blastema. The undifferentiated blastema cells subsequently re-differentiate and undergo morphogenesis to give rise to the new limb. This type of regeneration is a rare phenomenon that demonstrates the use of a developmental programme in an adult organism where reversal of cell fate and re-entry into the cell cycle does not lead to tumorigenesis (Figure 1).

Most studies of limb regeneration have involved newts (e.g. *Notophthalmus viridescens, Cynops pyrrhogaster*) and axolotls (e.g. *Ambystoma mexicanum*). Limb regeneration proceeds through a series of stages each containing specific factors that contribute to the success or failure of the regeneration process. The first event that must take place for regeneration to occur is an initial stimulus or injury. Immediately following injury or amputation, a fibrous plasma clot forms above the wound and wound healing begins (Repesh and Oberpriller, 1978). During the first 6-12 hrs of wound healing,

Figure 1. Stages and timeline of forelimb regeneration in the urodele, *Notophthalmus viridescens*.
Following an initial injury at day 0, the regeneration process proceeds through the following stages during its development: wound healing and dedifferentiation, blastema, cone, palette, early digit and advanced digitation and growth. Image modified from Goss, 1969.

Epimorphic Regeneration in the urodele, *Notophthalmus viridescens*

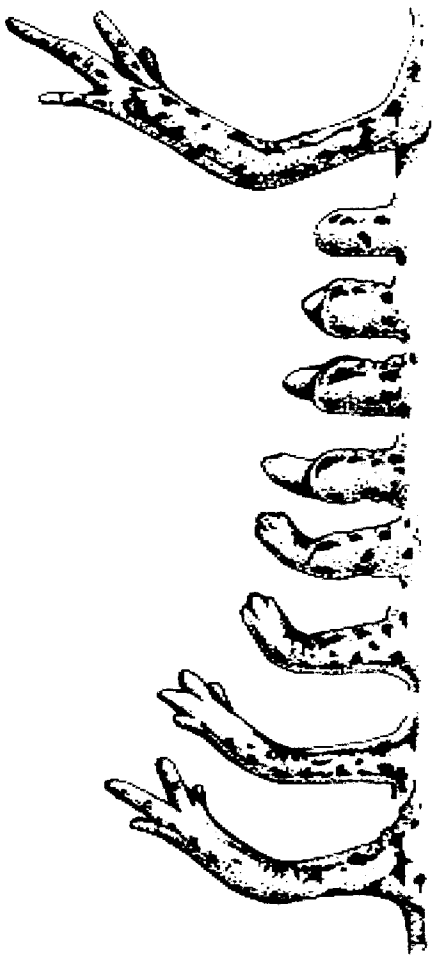

Stages	Timeline
1) amputation/injury	**day 0**
2) wound healing & dedifferentiation	**0-5 days**
3) blastema	**7-14 days**
4) cone	**15-21 days**
5) palette-differentiation/ morphogenesis	**21-28 days**
6) early digit	**28-60 days**
7) advanced digit & growth	**28-60 days**

epithelial cells migrate distally from the stump epidermis to cover the cut surface and seal off the wound (Hay and Fischman, 1961). Evidence for this epithelial cell migration was shown by cellular marking experiments using triploidy and tritiated thymidine (Hay, 1952; Rose, 1965). Wound healing is key to the progression of regeneration. Normal wound healing proceeds without cicatrization (formation of a scar), but should a scar form, regeneration will fail to commence (Schmidt, 1968). Wound healing is accompanied by a typical inflammatory response in the damaged area. Phagocytes remove any tissues that have become disorganized among the cellular debris. Over the next few days, the initial stratified epithelium consisting of a couple of cell layers, thickens and forms a specialized wound epithelium of 10-15 cell layers called the apical epithelial cap (AEC) (Ferretti, 2001). Removal of the AEC results in the cessation of regeneration (Butler, 1935). Suturing of a skin flap over the wound inhibits the formation of the AEC, and regeneration does not occur (Stocum, 1985). The AEC is thought to be homologous to the apical ectodermal ridge (AER) of developing limb buds in higher vertebrates. The AER is also critical for limb bud outgrowth and its removal results in truncated limbs. One of the major differences between epimorphic regeneration in urodeles and that of typical wound healing in other vertebrates, is that formation of the basement membrane beneath the wound epidermis is postponed until the blastema has been established, thereby allowing direct contact of the AEC with the mesenchymal cells of the blastema (Salpeter and Singer, 1960a). This mesenchymal-epithelial interaction is also the key to limb outgrowth and differentiation during limb development in higher vertebrates with an AER, which similarly lacks a basement membrane (reviewed in Ferretti, 2001).

The appearance of blastemal cells beneath the wound epithelium 3-5 days post-amputation is characterized by the phenotypic loss of mature stump tissue, like muscle and bone, through dedifferentiation. All the mesodermal tissues of the limb, including connective tissue and cartilage, contribute to the blastema (Chalkley, 1954; Chalkely, 1959). Recent cellular and molecular studies have contributed further support to the occurrence of dedifferentiation. When cultured myotubes are injected with a lineage tracer or labeled with an integrated retrovirus and transplanted into a blastema *in vivo*, labeled mononucleate cells can be found re-entering the cell cycle (Lo *et al.*, 1993), and more specifically entering S phase (Tanaka *et al.*, 1999; Kumar *et al.*, 2000). Similar experiments have also confirmed labeled chondrocytes contribute to the proliferating blastema (Steen, 1968). Gene expression analysis has identified two sources of myogenic cells in the regenerating limb, a reserve 'satellite' cell population for muscle repair which may be functionally homologous to those found in mammals (Cameron *et al.*, 1986), and a progenitor-like cell population originating from dedifferentiated muscle (Corcoran and Ferretti, 1999). Metaplasic transformation has been documented through triploidy, irradiation and nucleolar marker experiments as evidence that dermis, epidermis and muscle do undergo a conversion (re-differentiation) into cell types other than their own (Hay, 1952; Steen, 1968; Namenwirth, 1974; Dunis and Namenwirth, 1977).

Following dedifferentiation, cells proliferate to form the blastema. A critical role for peripheral innervation has been shown during cell proliferation of the blastema. If the nerves supplying the limb (nerves 3, 4 and 5 of the brachial plexus in the forelimb) are severed prior to or concomitantly with amputation, the initial stages of wound healing and dedifferentiation take place, but subsequent cell proliferation is abrogated and

regeneration is inhibited (Singer, 1952). These observations demonstrate that there exists a nerve-dependent phase early during regeneration, but the [growth] factor(s) responsible has yet to be identified. After the formation of the blastema, nerves seem to play a minimal role in the continuation of regeneration. If a limb is denervated after the late blastema stage, regeneration proceeds normally with the limb being slightly smaller than normal (Schotte and Butler, 1944). Morphologically, the blastema stage can be recognized by the rounding off of the wound stump and elongation of the blastemal mass into a cone (Iten and Bryant, 1973).

The final stage of regeneration begins following cell proliferation when differentiation and histogenesis commence and progress in a proximodistal direction. The cone-shaped regenerate flattens out into a palette and the digit cartilage including a network of capillaries is seen to have formed by this stage. Within 6 weeks, all the structures distal to the plane of amputation are replaced and the pattern of the limb is restored through morphogenesis. Depending on factors such as temperature and nutritional intake, typically, growth of the fully differentiated limb proceeds up to two months post-amputation, at which time the size of the regenerate reaches the equivalent size of the original, and regeneration is complete.

Knowledge of the mechanisms involved in urodele forelimb regeneration would have tremendous clinical applications for regeneration and repair in higher vertebrates such as man. In order to apply the knowledge which we gain from urodele regeneration to regeneration in higher vertebrates, we must first understand the similarities or differences between urodele limb development and limb development in higher vertebrates.

1.3 Forelimb development in higher vertebrates

The vertebrate limb is a complex structure whose proper patterning and development is dependent on a large number of factors and specific interactions between these factors. This is the reason why the limb is one of the most studied organs as a model for patterning and cell-cell interactions. In vertebrates, there are four limb fields that develop opposite each other respectively to the midline (reviewed in Ruvinsky and Gibson-Brown, 2000). Homeobox (Hox) genes are a family of proteins involved in the anterior-posterior pattern formation of developing systems along the body. The position of limb bud outgrowth is determined by Hox gene expression on the anterior-posterior axis (Duboule, 1992). For example, in fish, amphibians, birds and mammals, forelimb buds form at the anterior most region of *hoxc-6* expression (Oliver *et al.*, 1988; Sharpe *et al.*, 1988; Molven *et al.*, 1990; Nelson *et al.*, 1996). Classical embryologic transplantation experiments have demonstrated that within the presumptive forelimb field, mesenchymal cells proliferate from the lateral plate mesoderm, and migrate distally toward the overlying layer of ectodermal cells (Figure 2A). As the limb bud grows, the mesodermal cells signal the overlying ectoderm to induce the formation of the Apical Ectodermal Ridge (AER) (Saunders, 1948; Figure 2B,C). The AER is a multi-cell layered structure that lies along the outermost distal part of the limb bud and is known to be the major signalling centre for the development of the limb (Summerbell *et al.*, 1973; Saunders and Reuss, 1974). The removal of the AER leads to the cessation of limb development (Saunders, 1948). The known functions of the AER are i) to maintain the proliferation of the mesoderm within the limb bud for proximal-distal growth of the limb, and ii)

Figure 2. Induction of the AER in higher vertebrate limb development.
Prior to limb bud outgrowth, mesodermal cells proliferate from the somatic region of the lateral plate mesoderm (A). Proliferation causes the limb bud to bulge outward and the mesodermal cells signal the overlying ectoderm between the dorsal and ventral surfaces (cross-hatch, B) to induce the AER (C). The AER forms at the dorsal-ventral boundary at the distal margin of the limb bud. NT: neural tube; N: notochord: LPM: lateral plate mesoderm; S: somite; D: dorsal; V: ventral; AER: apical ectodermal ridge.

AER induction during limb development in higher vertebrates

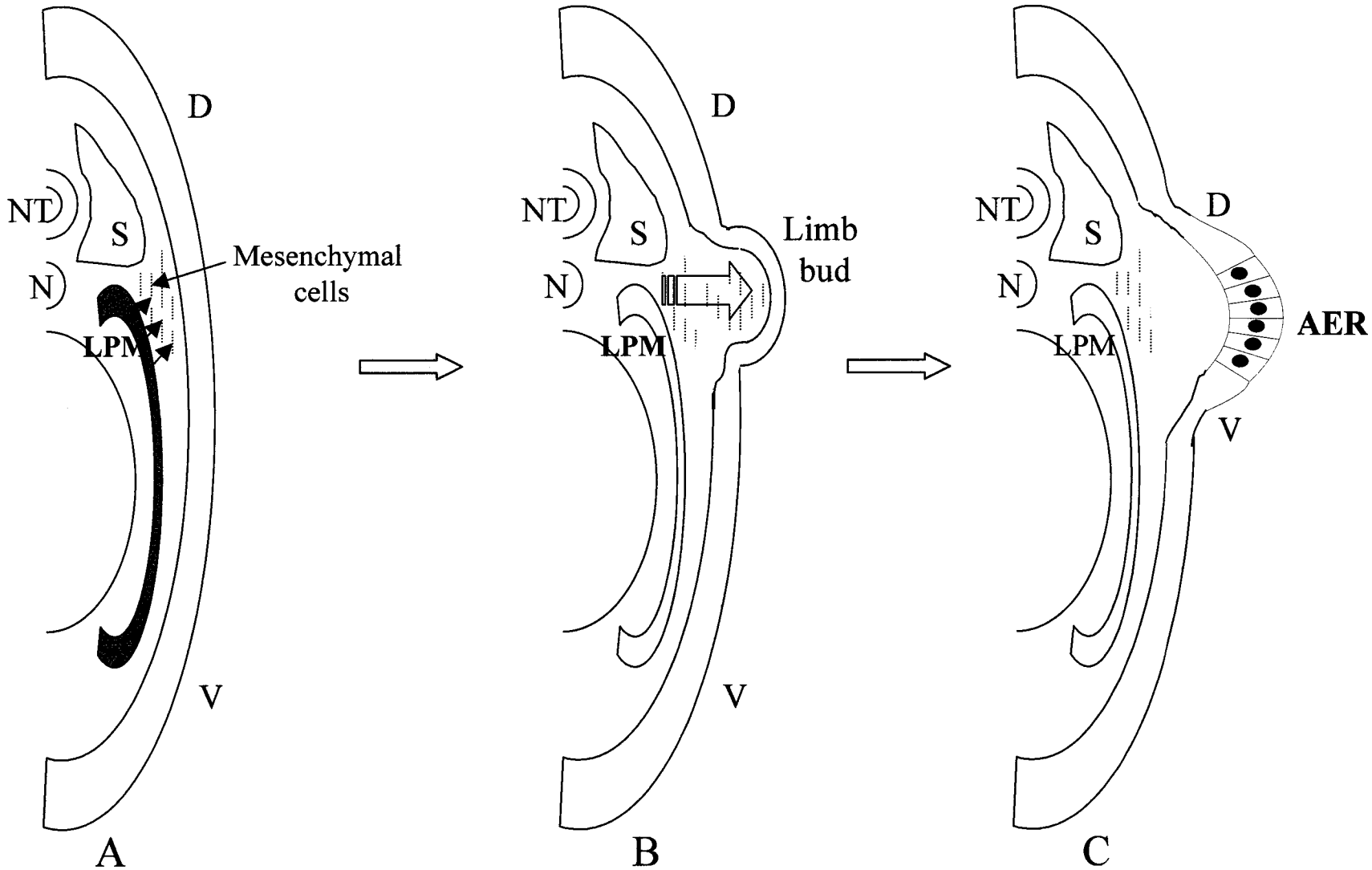

maintain the expression of signaling molecules involved in cell differentiation and the formation of the anterior-posterior (thumb-5th finger) and dorsal-ventral axes.

1.3.1 Dorso-ventral patterning:

Studies have shown that just prior to limb bud formation, the dorsal flank ectoderm synthesizes a secreted protein whose expression is exclusive to the dorsal cells and demarcates the dorsal-ventral (D-V) boundary (reviewed in Irvine and Vogt, 1997). This protein, Radical Fringe, was identified in chick as the signaling molecule involved in dorso-ventral patterning and directing the formation of the AER at the boundary between *radical fringe* expressing and non-expressing cells (Rodriguez-Esteban *et al.*, 1997). *Radical fringe* shows expression and sequence similarity to the gene responsible for wing margin formation in *Drosophila, fringe* (Irvine and Wieschaus, 1994), and another secreted gene product of *Xenopus*, *lunatic fringe* (Wu *et al.*, 1996). Ectopic expression of *radical fringe* in the limb results in a new boundary between cells expressing and not expressing the gene. At this boundary, a new AER forms. The ventral repression of *radical fringe* is caused by a homeobox-containing transcription factor *Engrailed-1* (*En-1*) (Loomis *et al.*, 1996). *En-1* assists the positioning of the AER by restricting *radical fringe* to the dorsal ectoderm (reviewed in Johnson and Tabin, 1997). The preservation of an evolutionary mechanism between insects and vertebrates leading to limb formation and outgrowth is further solidified by the identification of additional members of the pathway, namely Delta, Serrate and Notch, in higher vertebrates (Myat *et al.*, 1996; Shawber *et al.*, 1996).

The mesodermal specification of the dorsal-ventral (knuckles/nails-pads/soles) axis of the limb is dependent on the expression of the secreted factor, Wnt7a in the

ectoderm. The rotation of the ectoderm 180° within the axis leads to the reversal of the digits, i.e., the digit pads face upward (MacCabe *et al.*, 1974). In the chick and mouse, *Wnt7a* is expressed solely in the dorsal ectoderm and deletion of *Wnt7a* leads to the ventralization of the dorsal ectoderm causing sole pads to be present on both sides of the limb in mouse (Parr and McMahon, 1995), and the loss of posterior digits in both the mouse and chick (Parr and McMahon, 1995; Yang and Niswander, 1995). This mesodermal ventralization outcome does not affect the expression of either *radical fringe* or *En-1* since the AER is maintained and found in the correct position. *Wnt7a* induces the LIM-homeodomain protein, Lmx1, a transcription factor that plays a significant role in cell fate specification of dorsal mesenchyme. Ectopic expression of *lmx1* in the ventral mesenchyme leads to the development of the dorsal phenotype (Riddle *et al.*, 1995; Vogel *et al.*, 1995).

1.3.2 Proximal-distal patterning:

The mechanism behind the formation of the AER through *radical fringe* and *En-1* is still unknown, but it has now been shown that the cells at the D-V boundary begin to express Fibroblast Growth Factor 8 (*fgf8*) prior to the induction of the AER (Crossley *et al.*, 1996; Vogel *et al.*, 1996). The synthesis of members of the FGF family seems to be involved with the proliferation of the mesenchyme beneath the AER. This area of cell proliferation in known as the progress zone. *Fgf8* is the first molecule synthesized in the ectoderm that becomes the AER. Removal of the AER can be replaced by the implantation of beads soaked with *fgf2, fgf4* or *fgf8* (Niswander *et al.*, 1993; Cohn *et al.*, 1995; Crossley *et al.*, 1996). Therefore, these fibroblast growth factors appear to play a critical role in promoting growth of the limb bud.

1.3.3 Anterior-posterior patterning:

The specification of the limb anterior-posterior axis depends on the signals expressed in a region of posterior limb bud mesoderm known as the zone of polarizing activity (ZPA). The segment polarity gene *sonic hedgehog* (*shh*), homolog of the *hedgehog* gene in *Drosophila*, was found in the chick by Riddle and co-workers (Riddle *et* al., 1993). They showed that the expression of *shh* was found specifically in the ZPA and transfection of *shh* to an anterior portion of the limb bud resulted in the reversed polarity duplication of digits. It is still unknown how the ZPA establishes the anterior-posterior boundary. Current studies are focused on discovering the target genes of *shh* activity. Since the AER is required for ZPA function, it is known that *shh* expression is dependent on *fgf4* expression. *Shh* subsequently activates *fgf4* in the AER, creating a positive feedback loop between *shh* in the posterior mesoderm and *fgf4* in the AER (Niswander *et al.*, 1994). The localization of *shh* expression to the posterior limb bud mesenchyme and not the entire mesenchyme beneath the ridge may be explained by the expression of *hoxb-8* which is restricted to the posterior half of the limb in mouse forelimb buds (Charite *et al.*, 1994). Transgenic mice which express *hoxb-8* throughout the limb bud express sonic hedgehog in the anterior mesenchyme of the limb and the formation of a new ZPA subsequently results in the mirror-image duplication of forelimbs (Charite *et al.*, 1994).

On the other hand, loss of *Wnt7a* and subsequent reduction of *lmx1* in the dorsal limb mesenchyme results in the loss of both *shh* and *fgf4* expression. Viral-induced *Wnt7a* expression restores dorsal ectoderm function, *shh* expression and posterior digit patterning. It is still unclear how *lmx1* contributes to the determination of dorsal cell fate

specification, but it is possible that *lmx1* participates in the induction or maintenance of *shh* activation (Johnson and Tabin, 1997). These observations suggest that the synthesis of *shh* in the ZPA (anterior-posterior axis) is dependent on fgf8 and fgf4 (proximal-distal axis/AER) and Wnt7a/Lmx1 proteins (dorsal-ventral axis).

It can therefore be assumed that normal development of the vertebrate limb/wing is dependent on the specific interaction/communication of the major regulatory genes within all three defined axes of the limb. Although vertebrate limbs and wings are not homologous structures, these findings suggest that they recruit similar mechanisms during their development.

1.4 Forelimb Development in the Urodele

Urodeles, such as the newt, differ from other vertebrates in the mechanisms that set up the initial patterning of the limb. In urodeles, digits 1 and 2 are the first to appear followed by digits 3 and 4 (Figure 3A and B; adapted from Jarvik, 1980). Each digit appears to "grow out" from the limb palette. In higher vertebrates, a flattened palette grows outward from the AER, cartilage condensation of the individual digits occurs and this is followed by apoptosis of the interdigital tissues, or necrotic zones (Figure 3C). This interdigital apoptosis seems to be absent in the newt, although no study has actually addressed this issue. Morphological evidence from Liversage and Khan (unpublished results), suggests that the developing and regenerating limbs of embryonic *Notophthalmus viridescens* are similar. In both cases, the characteristic pattern of individual outgrowth of the digits occurs. However, during regeneration in the adult, the

Figure 3. Comparison between skeletal digit formation in the urodele and higher vertebrates.
During limb development in the urodele, digits form one at a time anterior to posteriorly in the forelimbs (A - digits 1 to 4), and hindlimbs (B - digits 1 to 5). In higher vertebrates, cartilage condensation of the digits occurs at the same time. The separation of the digits occurs by way of interdigital mesenchymal cell death of the interdigital necrotic zones (C). Image modified from Jarvik, 1980.

Comparison of digit formation in urodeles and higher vertebrates

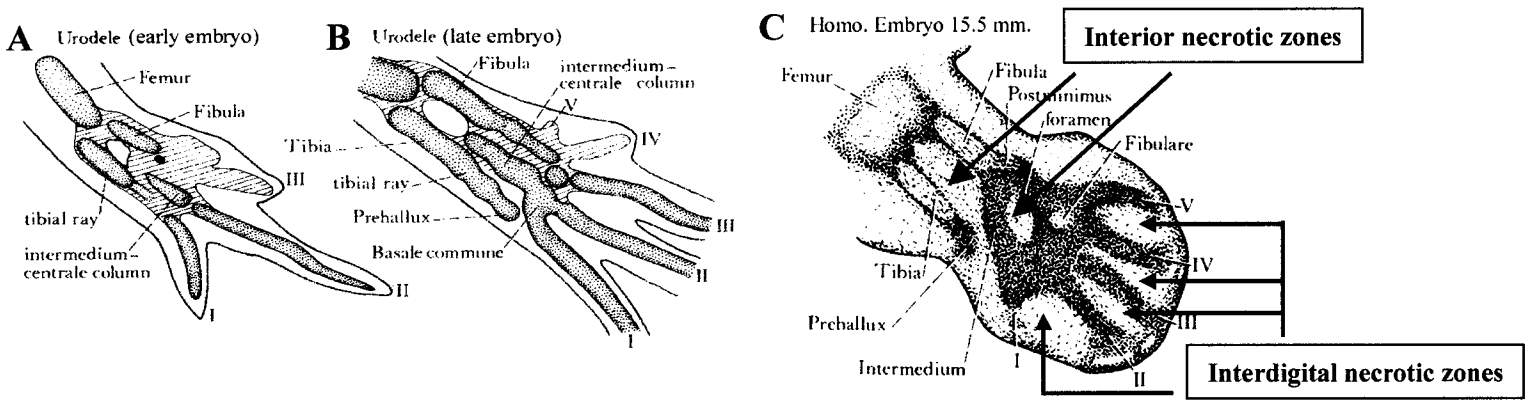

morphological appearance of the regenerate is quite different than that seen during development or embryonic regeneration. All the digits appear to form at once as seen through the condensation of digit cartilage and the existence of interdigital mesenchyme, a pattern reminiscent of that which occurs in higher vertebrates (Figure 4).

The mechanisms involved in the development of the urodele limb have only recently been brought into light. Some genes that have been identified in the early stages of higher vertebrate limb development have now also been identified in the urodele. These include homeobox genes (Beauchemin and Savard, 1993; Gardiner and Bryant, 1996; Khan *et al.*, 1999), T-box genes (Sone *et al.*, 1999; Khan *et al.*, 2002), genes associated with signaling pathways (Caubit *et al.*, 1997; Imokawa and Yoshizato, 1997; Stark *et al.*, 1998; Cadinouche *et al.*, 1999), and growth factors such as Fgf-8 (Han *et al.*, 2001). Since most of these genes were cloned in order to characterize their role in regeneration, they will be discussed in the next section in the context of newt forelimb regeneration.

1.5 Comparing forelimb regeneration and development

Before molecular experiments were employed for comparing the mechanisms of development and regeneration, results from classical transplantation experiments addressed the question of whether regenerating adult forelimbs utilized a mechanism similar to that occurring during embryonic development. Grafting experiments with axolotl embryonic developing and regenerating tissue performed by Muneoka and Bryant (1982), showed evidence that the patterning mechanisms in the developing and regenerating limb are the same. They transplanted embryonic palette stage regenerating

Figure 4. *N. viridescens* palette staged forelimb regenerate.
During forelimb regeneration in the adult, the cartilage of the four digits can be seen to develop prior to the individualization of the digits, a manner comparable to that seen in higher vertebrate limb development (refer to Figure 3c).

Palette staged newt adult forelimb regenerate

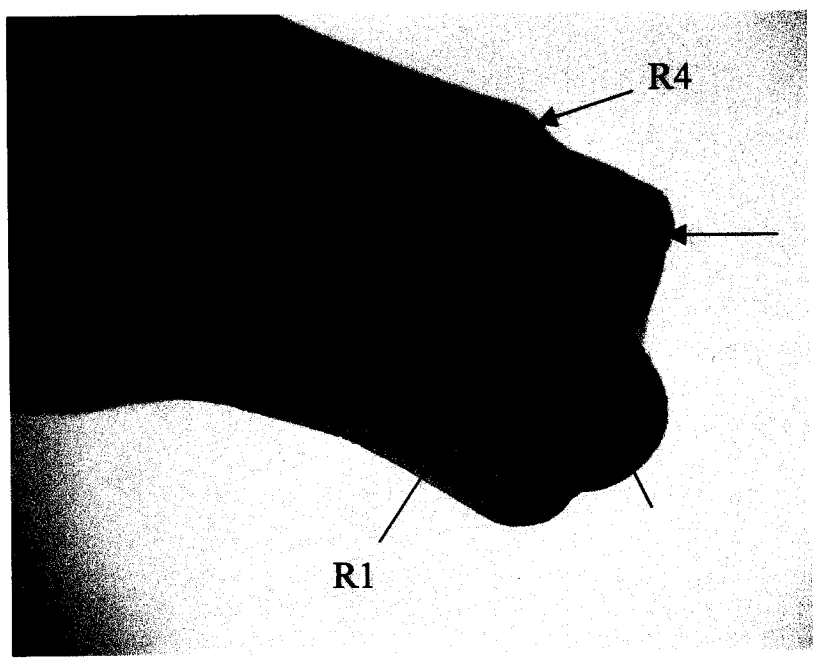

forelimb blastemas onto host amputated hindlimb buds either ipsilaterally (control), matching limb tissue axes or contralaterally, misaligning anterior and posterior limb tissue. Hindlimb developing buds were also either contralaterally transplanted onto the hindlimb or amputated and replaced onto their original sites (control). The results of their experiment showed that when transplanting either tissue types, normal developing hindlimb buds or regenerating blastemas, supernumerary digits form only in animals where the tissue is in a misaligned position with respect to the limb axis. Based on these observations they concluded that patterning mechanisms during both initial development and regeneration in urodeles are the same. However, since embryonic and not adult regenerating tissue was used, one could question whether this is true epimorphic regeneration or a re-initiation of development since not all cell types would have been fully formed.

With the use of molecular biology, understanding the pathways involved in both vertebrate and invertebrate limb development and patterning is becoming clear and it is also becoming more evident that many of the genes involved in the initial development of the higher vertebrate limb are also expressed during limb development in urodeles and furthermore, re-expressed during regeneration. This has supported the theory that the regeneration process is a recapitulation of development, and patterning of the regenerate mimics pattern formation in development.

Many of the genes expressed during development and regeneration of the newt limb have been evolutionarily conserved. Although these genes have been cloned and show high homology to genes that set up the limb during development in higher vertebrates, the functions of these genes have not been characterized to a degree

comparable to that in higher vertebrates and furthermore some fundamental differences are present when comparing these orthologues. The T-box genes encode a family of transcription factors that contain a conserved DNA-binding domain whose gene products are involved with either the activation or repression of downstream targets during early embryogenesis (Papaioannou and Silver, 1998). Four T-box genes, *Tbx2-Tbx5*, were found to be expressed during limb development, and their characteristic expression patterns have been shown to be conserved among jawed vertebrates (reviewed in Ruvinsky and Gibson-Brown, 2000). *Tbx4* and *Tbx5* are expressed throughout the lateral plate mesoderm within the forelimb and hindlimb fields prior to initiation of bud outgrowth. Subsequently, *Tbx5* expression is found exclusively in the forelimb/wing/pectoral fin and *Tbx4* expression becomes restricted to the hindlimb/leg/pelvic fin in mouse, chick, *Xenopus* and zebrafish (Gibson-Brown *et al.*, 1998; Tamura *et al.*, 1999; Isaac *et al.*, 1998; Takabatake *et al.*, 2000). These T-box genes are thought to specify limb identity during embryogenesis (Gibson-Brown *et al.*, 1996). T-box genes have also been identified in the newt. In the Japanese newt, *Cynops phyrrhogaster*, four novel T-box genes have been identified and shown to play a role during the development of the limbs, and three of these are continually expressed in normal adult appendages and show elevated expression during limb regeneration (Sone *et al.*, 1999). In the red-spotted newt, *Notophthalmus viridescens*, four T-box genes have also been identified. *Tbx5* (formerly *NvTbox1*) was shown to be expressed at low levels in normal adult forelimbs with a strong induction in the blastema during regeneration. As regeneration progresses, expression levels lower to the original basal amounts of non-regenerating limbs (Simon *et al.*, 1997). More recently, *Tbx4* has been cloned in *N.*

viridescens and shown to be expressed solely in the hindlimb during regeneration with basal level expression in non-regenerating hindlimbs, patterns mimicking *Tbx4* expression in higher vertebrates (Khan *et al.*, 2002). These findings suggest that at the molecular level, similar regulatory mechanisms exist between limb development in higher vertebrates and urodele limb regeneration. *Tbx5* and *Tbx4* have also been found to be expressed during the initiation of forelimb and hindlimb bud outgrowth similar to initial expression patterns of *Tbx5* and *Tbx4* during mouse and chick limb development (Gibson-Brown *et al.*, 1996; Simon *et al.*, 1997; Isaac *et al.*, 1998). Unlike expression patterns in higher vertebrates, Khan *et al.* (2002) presented data showing the expression of *Tbx5* and *Tbx4* in both developing forelimb and hindlimb mesenchyme in the newt and axolotl. In higher vertebrates *Tbx4* is expressed solely in hindlimbs and *Tbx5* only in forelimbs, showing that with these genes, the expression patterns appear to be different in urodele development in comparison to higher vertebrates.

Other evidence linking limb development in higher vertebrates to that of developing and regenerating limbs in urodeles is the identification of homeobox containing genes. *Hoxc-6* determines the position of forelimb and hindlimb bud outgrowth in higher vertebrates. During newt forelimb and hindlimb regeneration, *hoxc-6* transcripts are found in the mesenchymal cells of the blastema as well as mesenchymal cells of adult unamputated limbs (Savard *et al.*, 1988; Savard and Tremblay, 1995). These findings are consistent with the tissue-specific expression patterns of *hoxc-6* in developing limb buds of higher vertebrates including mouse, human, chick, *Xenopus* and zebrafish (Simeone *et al.*, 1987; Oliver *et al.*, 1988; Sharpe *et al.*, 1988; Molven *et al.*, 1990; Nelson *et al.*, 1996). This evidence suggests that the newt maintains a low level of

expression of developmental pattern regulating genes required for the replacement of lost appendages in adulthood. This is quite different than what is seen in developing limb buds of the newt. Although *hoxc-6* expression is similarly found in mesenchymal cells as in the adult, expression is restricted to the developing and regenerating forelimb in larval *N. viridescens* according to Khan et al. (1999). No *hoxc-6* expression is detected in developing hindlimbs, as compared to the regenerating hindlimb as shown by Savard and Tremblay (1995). This finding is quite significant and suggests that a developmental pattern regulating gene is expressed for the first time in adult differentiated tissue implying that a unique mechanism of hindlimb bud initiation may exist in urodeles that does not require *hoxc-6* expression as in higher vertebrates, or that an as yet unidentified homologue of *hox-6* is required for hindlimb bud outgrowth. Interestingly, in both these examples, Tbox genes and *hoxc-6*, regeneration seems to mimic higher vertebrate development while newt development is different from both newt regeneration and higher vertebrate development.

Further molecular evidence for similarities between limb development in higher vertebrates and limb regeneration in the newt involves the function of the AER in higher vertebrate limb development and the signaling centre homologous to the AER in regenerating newt forelimbs, the Apical Epithelial Cap (AEC). As of yet, there is no evidence for a functional equivalent of an AER in the developing urodele limb. Growth factors, such as Fgf-8, function to promote the continuous cell proliferation of mesenchyme beneath the AER. *Fgf-8* expression is commonly studied in parallel with the AER because of its role in both establishing the AER and substituting for the AER's role in anurans and amniotes. *Fgf-8* has been found to be involved in limb bud outgrowth

during development in urodeles, along with blastema formation and outgrowth of the regenerating limb. Unlike in *Xenopus* or in amniotes such as chick and mouse, *fgf-8* expression in the larval axolotl limb is localized mainly to the mesenchymal tissue rather than the epidermis (Han *et al.*, 2001). *Fgf-8* expression in the axolotl is localized to the basal layer of the AEC in a cap-like shape at the D-V boundary and within the underlying thin layer of mesenchyme, or the distal-most part of the blastema (Han *et al.*, 2001). Furthermore, *Xenopus fgf-8* was reported to be expressed in the basal layer of the AEC in regenerating tadpoles (Yokoyama *et al.*, 2000). This expression of *fgf-8* in the regenerating amphibian AEC is regarded as the mechanistic equivalent during regeneration, of the mesenchymal-epidermal interaction seen in the AER of higher vertebrates.

The *fringe* gene, first identified in *Drosophila*, was shown to code for a secretory signaling molecule that played a crucial role in wing margin formation and outgrowth (Irvine and Wieschaus, 1994; Kim *et al.*, 1995). In Drosophila, *fringe* modulates the interaction between the transmembrane receptor protein Notch, and its known ligands, Delta and Serrate, and restricts Notch activity to the D-V boundary to establish the wing margin (reviewed in Irvine and Vogt, 1997). Vertebrate homologues of the genes in the Notch-signaling pathway have been identified in chick, mouse, and *Xenopus*, showing their importance in establishing a D-V boundary necessary for the formation of the AER (Hayashi *et al.*, 1996; Shawber *et al.*, 1996; Blaumueller and Artavanis-Tsakonas, 1997; Laufer *et al.*, 1997; Rodriguez-Esteban *et al.*, 1997). A *fringe* homologue has also been identified during limb development and regeneration in the newt (Cadinouche *et al.*, 1999). Newt *radical fringe* (*nrFrg*) is first expressed during the limb field stage of

development, peaks during bud outgrowth and subsequently diminishes with the formation of digits. This expression pattern is similar to that seen in both *Drosophila* and chick. It is similarly expressed highly during the proliferative stages of adult regeneration when cell division is laying down the progenitor cells of the blastema. Although there seems to be a clearly evident role for *fringe* during both newt forelimb development and adult regeneration, one significant difference in the newt is that *nrFrg* does not seem to play a role in the formation of the AEC. Its expression is absent in the ectoderm at both the limb field and bud outgrowth stages during development and again within epidermal cells during active cell division and proliferation at the time of blastema formation (Cadinouche *et al.*, 1999). Furthermore, *nrFrg* expression is not restricted to the dorsal limb and so may not play a role in establishing the D-V boundary.

Investigation into the role of *fringe* during development and regeneration in the newt has identified yet other genes involved in the Notch-signaling pathway, including Notch and its two known ligands, NvSerrate and NvDelta (Vascotto and Tsilfidis, unpublished). Studies currently underway will address the roles of these genes during newt limb development and regeneration and how these roles correlate to that seen in higher vertebrates. These unique expression patterns of *radical fringe* and *fgf-8* in the urodele suggest regulatory mechanisms that are different during limb development between urodeles and other higher vertebrates.

Wnt genes display restricted expression patterns along the dorsal-ventral and proximal-distal axis of the limb bud during mouse development. For example, *Wnt-5A* is initially expressed in the overlying ectoderm of the limb bud but later displays a gradient of expression in the limb mesenchyme with highest expression at the distal tip of the

developing bud (Parr *et al.*, 1993). In urodeles, a similar gradient of expression is seen along the anterior-posterior axis of the tail regenerate with maximal expression detected in the mesenchyme beneath the AEC (Caubit *et al.*, 1997). These findings further support the theory that the molecular pathways used in higher vertebrate limb development are also utilized in the regeneration process in newt.

Further evidence that shows evolutionary conservation of limb development genes is the characterization of the zone of polarizing activity (ZPA) genes that are responsible for determining the anterior-posterior limb axis. A newt homologue of *shh* has been identified in the Japanese newt, *C. pyrrhogaster*. Studies have shown that *shh* expression is present in mesenchymal cells at the posterior region of the embryonic limb bud and likewise in the regenerating blastema of the adult limb (Imokawa and Yoshizato, 1997). These findings correlate with the expression pattern of *shh* in developing limbs of higher vertebrates and suggest the presence of a ZPA in the regenerating limb blastema and developing embryonic limb bud in the newt. Upon closer examination, this apparent similarity has some significant expression differences. Newt *sonic hedgehog* (*N-shh*) is expressed in the posterior limb mesenchyme in the developing limb bud and this expression is downregulated by the two to three digit stages. Although the comparison of newt and chick limb development can not be in a strict sense, *N-shh* expression in the developing newt limb bud seems to parallel that found in chick limbs where *shh* expression begins in the early limb bud and lasts until the cone to digit stage (Riddle *et al.*, 1993). In contrast, regenerating limbs of both the larva and adult are confined to a shorter expression period than that seen with both developing limbs of chick and urodeles. Unlike the drop in expression at digit stages as seen during newt limb

development and likewise in higher vertebrates, in the regenerating blastema *N-shh* expression is limited between medium bud stage and late bud to palette stages. This expression pattern can be explained by the fact that regenerating blastemas need only to replace the missing structure distal to the amputation plane whereas developing limbs need to construct whole limbs. A second member of the hedgehog family has been identified in *N. viridescens*. A newt homologue has been identified for *Xenopus banded hedgehog* (*bhh*), the anuran homologue of the avian *Indian hedgehog* (*Ihh*). *Bhh* and *Ihh* are involved in controlling chondrogenic differentiation in the later stages of limb development (Ekker *et al.*, 1995; Lanske *et al.*, 1996; Vortkamp *et al.*, 1996; Stark *et al.*, 1998). Although sequence homology is greater than 80%, the expression patterns of newt *banded hedgehog* (*N-bhh*) do not follow the profiles found in that of either frog or chick. It is evident that *shh* plays a role during the early stages of limb development, whereas in later stages, *Ihh* plays a role in the differentiation of prehypertrophic chondrocytes of cartilage elements (Lanske *et al.*, 1996; Vortkamp *et al.*, 1996). Unlike the expression patterns of that seen in chick and mouse, *N-bhh* is expressed underneath the wound epidermis within the first days of blastema cell accumulation and throughout proliferation suggesting its possible role during these periods of cell cycle re-entry. Expression is downregulated at the onset of differentiation and cartilage condensation (Stark *et al.*, 1998). This difference in expression is also seen during limb development where no detection of *N-bhh* is evident within developing cartilage. *N-bhh*, represents one gene that may play similar roles in the newt during both larval limb development *and* adult limb regeneration. These findings suggest a possible mechanism for the differentiation of prehypertrophic chondrocytes that is unique to urodeles, one that either does not involve

a family member of the hedgehog family or that involves an unidentified newt hedgehog gene that plays a more equivalent role to that of *Ihh*. The significance of these differences is currently not understood, but does raise questions as to whether the signalling mechanisms employed by newts and higher vertebrates are identical.

Adult regeneration requires the dedifferentiation of committed cell types whereas evidence of dedifferentiation in the regenerating larval limb has not been described in any animal that undergoes epimorphic regeneration. Since the origin of limb progenitor cells in an embryo differs fundamentally from the source of blastema cells in the adult, describing regeneration as a recapitulation of development would require greater evidence. Limb bud cells originate from the lateral plate mesoderm whereas limb blastema cells arise from the distal tip of the stump. Evidence has shown that numerous adult blastemal markers are not present in developing limb buds suggesting that the cells in the embryo and adult are fundamentally different (Geraudie and Ferretti, 1998). For example, Ferretti *et al.* (1989) showed the first demonstration of keratin expression in *mesenchymal* progenitor cells in an adult animal, the regenerating newt. Keratins are normally only expressed in epithelial cells. Antibodies against the human keratin intermediate filaments, K8 and K18, were used to identify keratin proteins in undifferentiated mesenchymal cells of the blastema. Although the progenitor cells of both developing and regenerating limb buds do express a mesenchymal intermediate filament, vimentin, the newt homologues to the human epithelial keratins NvKII, KvK8 and NvK18 are exclusively expressed in the regenerating blastema and no expression is found in the developing limb at either early bud stages or later digit stages (Corcoran and Ferretti, 1997). These results are consistent with observations made in another urodele

species, *P. waltl* (Ferretti *et al.*, 1989) suggesting that differences in keratin expression between developing and regenerating limbs may be a common feature among urodeles that undergo an epimorphic regenerative process in the adult involving dedifferentiation of mature tissues.

Overall, morphological and genetic data has suggested that the process of limb regeneration in the urodele is related to development in both urodeles and higher vertebrates, but clear differences are also present. Most of the genes cloned in urodeles have been examined either in the context of regeneration **or** development, but there are very few studies which examine gene expression in both development **and** regeneration to enable a direct comparison to be made. Notable exceptions are the studies with *Tbox* genes and *Hoxc-6*, which suggest that the urodele regeneration response may be more closely related to development in **higher** vertebrates than it is to urodele development. Clearly, additional research is warranted before any definitive conclusions can be drawn.

In limb development in higher vertebrates, individualization of the digits occurs through apoptosis of the interdigital mesenchyme. This mechanism is conserved from chick to mammals. In urodele limb development however, digits appear to grow out individually from the limb palette. Interestingly, the regenerating adult urodele limb morphologically more closely resembles the developing limb of higher vertebrates during chondrogenesis and digit formation than the developing urodele limb, in that all the digits seem to develop at once as opposed to individually. Since apoptosis between the digits is a major characteristic of morphogenesis and patterning in the higher vertebrate limb, examination of apoptotic patterns in urodele development and regeneration will help to

address the question of whether urodele regeneration is more closely related to development in urodeles or development in higher vertebrates.

1.6 The role of Apoptosis during limb development and regeneration

1.6.1 Apoptosis Introduction

Programmed cell death (PCD) or apoptosis (for the Greek meaning 'to fall off' - James Cormack as cited by Kerr *et al.*, 1972) is considered one of the most important cellular processes during the morphogenesis of tissues and organ systems in the developing animal. Apoptosis is a metabolic genetically programmed and evolutionarily selected cell death process that ensures proper development by maintaining tissue homeostasis and the removal of damaged or unwanted cells. This programmed cell death is so accurately regulated that in the nematode *Caenorhabditis elegans*, exactly 131 cells die during development in every animal (Hengartner and Horvitz, 1994). Apoptosis is distinguishable from necrosis by certain structural and molecular characteristics. Necrosis is a pathological cell death process that occurs in response to external inflammatory toxic factors or injury. Cells are characterized by the swelling of mitochondria and cytosol due to the loss of ion and water balance, and they undergo membrane and intracellular organelle disruption before they lyse (Wu *et al.*, 2001). In contrast, an apoptotic event is characterized by the cellular blebbing of the membrane and cytoplasmic condensation that normally shrinks the cell causing its loss of adherence with neighbouring cells. The nuclear DNA undergoes an endonuclease-mediated double-strand cleavage leaving fragments of approximately 180-200 base pairs long, the size of an oligonucleosomal unit (Wyllie *et al.*, 1980). These cellular events lead to the breakdown of the cell and are

morphologically referred to as 'apoptotic bodies'. These membrane-bound bodies are removed from their environment by neighbouring macrophages through phagocytosis and lysozymal enzyme degradation (Kerr *et al.*, 1972). A comparison between necrosis and apoptosis is shown in Figure 5. The DNA cleavage during apoptosis offers an enzymatic method of detecting apoptotic cells *in situ*. The double-stranded break in the DNA leaves free 3' terminal hydroxy ends that can be labelled and viewed through histochemistry. The DNA fragmentation in necrosis is in a non-specific manner and therefore *in situ* methods allow the identification of apoptotic bodies in contrast to necrotic cells. Apoptosis occurs as a single cell event and does not disrupt adjacent cells because the cellular membrane remains intact preventing the escape of any cellular debris that may normally lead to a leucocytic inflammatory response as seen in necrosis (Gobe and Harmon, 2001).

1.6.2 Executioners of apoptosis: caspases

Apoptosis is fundamental to many normal physiological processes such as homeostasis, differentiation and morphogenesis. However, misregulation of the apoptotic mechanism can lead to disease. For example, excess cell death can lead to neurodegenerative diseases such as Alzheimer and Parkinson syndromes, muscular dystrophies, myocardial infarctions due to ischaemic injury and AIDS. Too little cell death can result in persistent viral infection or cancer.

A large group of genes and proteins have been implicated in the control of apoptosis. Apoptosis can be activated at many steps throughout the apoptotic cascade but the point of irreversible execution is reached when caspases become enzymatically activated and cleave other apoptotic target proteins. Caspases (*c*ysteinyl *asp*artate-

Figure 5. A morphological comparison between necrosis and apoptosis.
Necrotic cells swell, heterochromatin is clumped throughout the nucleus, nuclear and cellular membranes become disrupted and the organelles break down (A). In contrast, apoptotic cells show heterochromatin condensation along the nuclear membrane, preservation of the organelles, mainly the mitochondria, shrinkage and convolution, and maintain themselves in discrete apoptotic bodies (B).

From: http://www.whfreeman.com/kuby/content/anm/kb04an01.htm

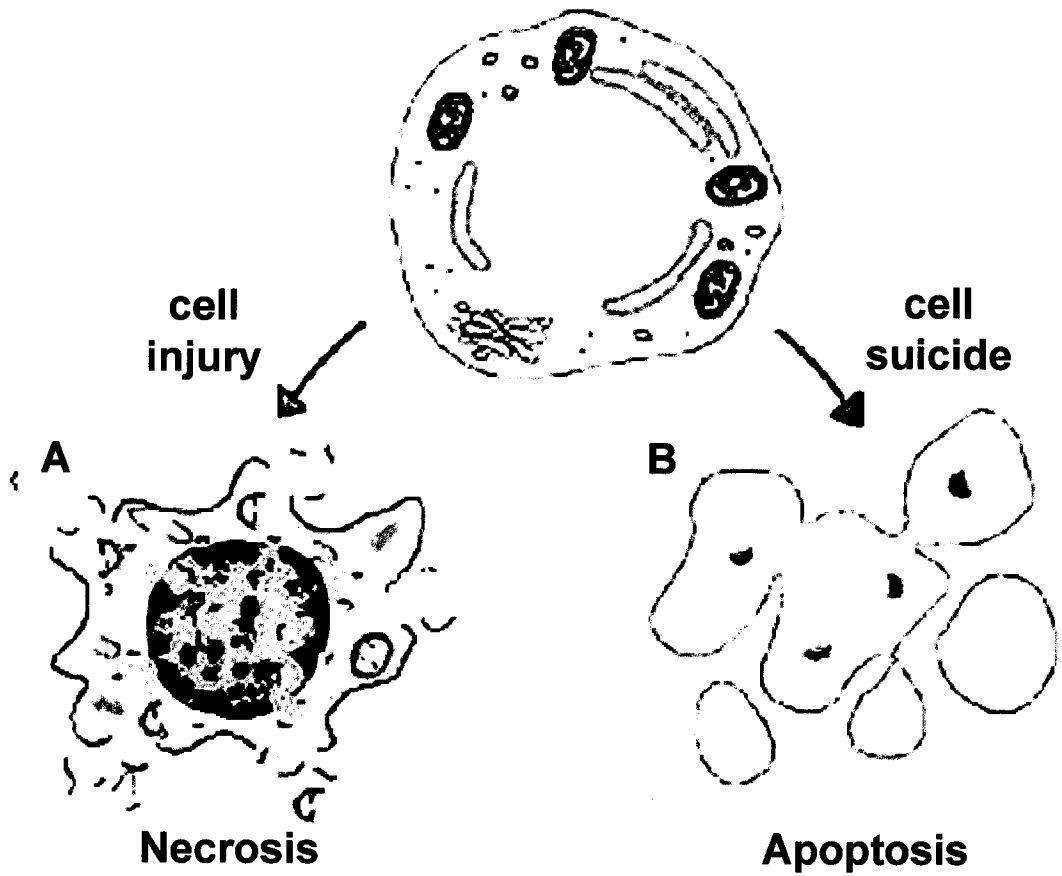
cell
injury
cell
suicide
A
B
Necrosis
Apoptosis

specific protein*ases*) are a family of proteases that become specifically activated to carry out the morphological changes seen in cells destined to an apoptotic fate. Because their key roles involve bringing about the biochemical characteristics of apoptosis, caspases have been regarded as the executioners of the apoptotic pathway (reviewed in Hengartner, 2000). Structurally, caspases have been evolutionarily conserved from nematodes to insects to mammals; functionally they possess a cysteine at their active site and cleave substrates C-terminal to aspartic acid residues. Caspases exist as proenzyme polypeptides or zymogens that become proteolytically activated and in turn activate downstream target proteins and other effector procaspases. The importance of caspases in apoptosis has been shown in knockout experiments in the mouse. Caspase-3 and caspase-9 knockout mice will normally die *in utero*, but the ones that survive are born with brain masses twice the size of normal volume due to ectopic cell masses that do not undergo apoptosis during normal neuronal central nervous system development (Yoshida *et al.*, 1998).

Recently the works of Nagata identified the caspase substrate responsible for the degradation of genomic DNA between nucleosomes which generate the DNA laddering effect first described by Wyllie (1980) now used extensively as a marker for apoptosis. They showed that this nuclease, caspase-activated DNase (CAD), exists as an inactive complex in living cells, inhibitory CAD (ICAD). The activation and release of the catalytic subunit occurs with the caspase-3-mediated cleavage of the inhibitory unit (Enari *et al.*, 1998; Sakahira *et al.*, 1998; Nagata *et al.*, 2003). Other characteristic features of apoptosis are also brought about by the activation of caspase substrates including the nuclear lamins involved in nuclear shrinking and budding, cytoskeletal

proteins that function to maintain cell shape and kinases involved in membrane blebbing (Rao *et al.*, 1996; Kothakota *et al.*, 1997; Rudel and Bokoch, 1997). Over 100 caspase substrates have been identified in recent years and although the mechanisms behind the activation of these substrates and the downstream effects of caspases are still poorly understood, it is clear that caspases play a crucial role during the regulation of apoptosis. Our understanding of how they are activated to exert their effects will be valuable to our implementation of their use in biological functions and the control of disease.

1.6.3 Inducers of Apoptotic signalling: Death receptor (DR) pathway

The activation of an apoptotic cascade highly depends on the initial stimulus that triggers the apoptotic event. Apoptosis can be initiated at the cell membrane through protein-protein binding and activation of specific protein kinase receptors that contain intracellular cytoplasmic domains known as 'death domains' (DD). Ligands to these death domain receptors respond to stress induced stimuli like heat shock and UV radiation or the activation of an inflammatory cytokine. Signal transduction proceeds from the cell membrane to the nucleus (Gobe and Harmon, 2001). Following interaction with the ligand, the DDs of death receptors such as Fas or TNFR1 recruit adaptor proteins which interact with a number of other proteins to complete the DR signalling pathway. Initiator caspases such as caspase-8 and –10 are activated and cleave subsequent effector caspases and cellular substrates that facilitate cell death (Figure 6) (Ashe and Berry, 2003).

1.6.4 Inducers of Apoptotic signalling: Mitochondrial pathway

Damaged DNA will either undergo repair before re-entering the cell cycle, or proceed through apoptosis if repair is ruled out for the cell. Depending on the type of

Figure 6. Apoptotic cell death initiation by death domain activation in the Death Receptor signaling pathway.
The Fas and TNF receptors contain a conserved cytoplasmic motif known as the death domain (DD), which upon activation by their ligands, binds adapter proteins like FADD and TRADD. These adaptor proteins recruit procaspases -8 and -10 through the death effector domain (DED). Initiator caspase activation leads to downstream effector caspase activation and subsequent cleavage of cell death and substrates.

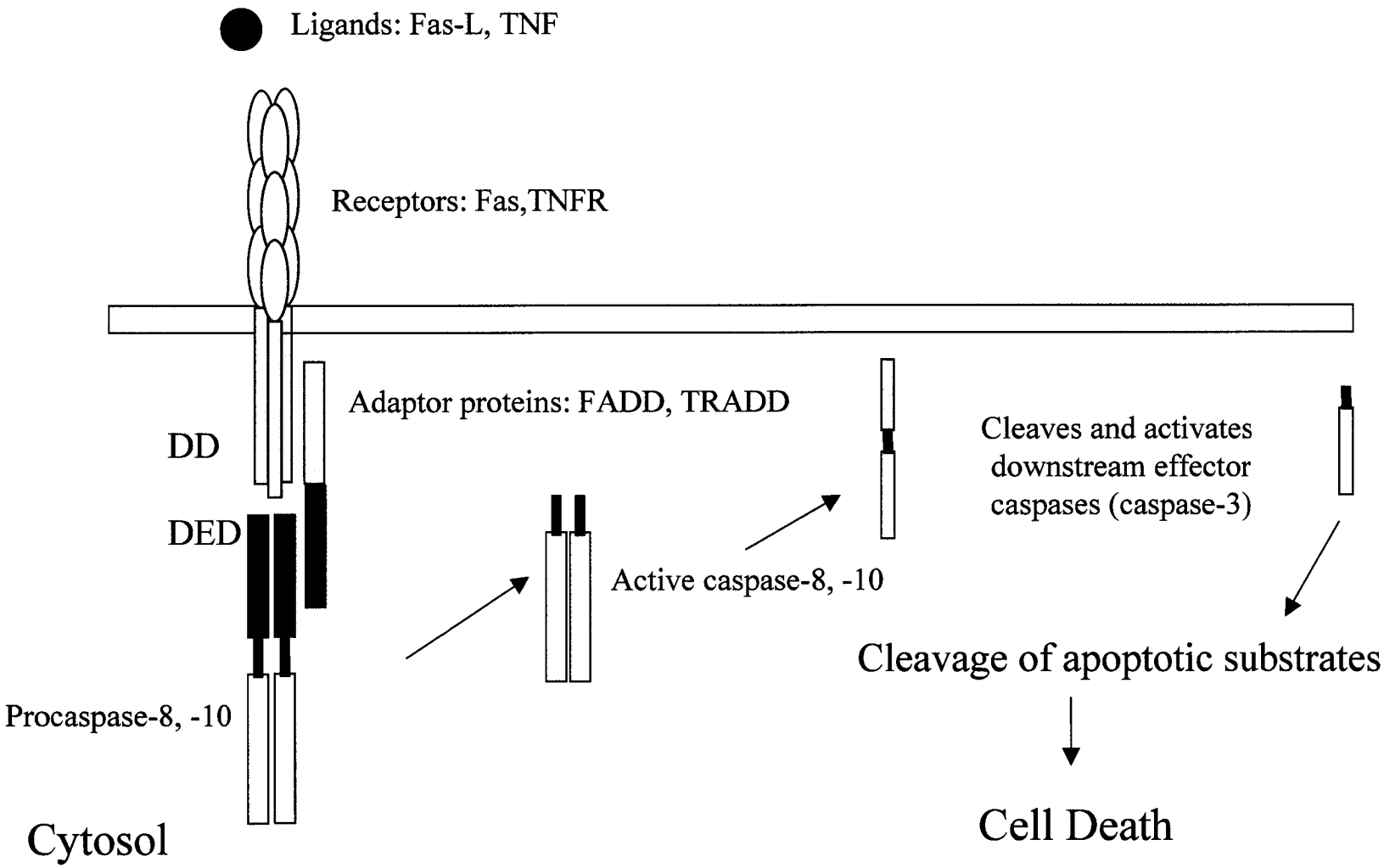
Ligands: Fas-L, TNF
Receptors: Fas,TNFR
Adaptor proteins: FADD, TRADD
DD
DED
Procaspase-8, -10
Active caspase-8, -10
Cleaves and activates downstream effector caspases (caspase-3)
Cleavage of apoptotic substrates
Cell Death
Cytosol

DNA damage and at what stage of the cell cycle the cell is in, repair or the apoptotic pathway can be activated by intracellular factors. These include checkpoint factors (Chk1, Chk2), repair factors (RAD50, RAD51), tumour suppressors (*p53*, ATM and BRCA1) and other signalling molecules (NF-kB). For example, chemical or ionizing radiation can lead to the cleavage of the Bcl-2 family member BID, or the nuclear activation of *p53*. Both pathways direct pro-apoptotic Bcl-2 member Bax to initiate the mitochondrial apoptotic pathway.

The Bcl-2 family of genes can be classified into three functional groups depending on their protein structure. Members of the first group, including Bcl-2 and Bcl-X_L contain four Bcl-2 homology (BH) domains (BH1-BH4) and have anti-apoptotic activity which protects the cell from death. The second group, which includes Bax and Bak, has similar structure to group I except they lack the fourth BH domain. This group has pro-apoptotic activity. Group III, which contains a diverse number of proteins, only shares sequence similarity to the other members of the family through the BH3 domain and also has pro-apoptotic activity. All members possess a C-terminal hydrophobic tail that localizes the proteins to the mitochondrial surface. Pro-apoptotic Bcl-2 members like Bax, regulate the release of other pro-apoptotic factors from the mitochondrial intermembrane compartment and into the cytosol, in particular cytochrome *c* (reviewed in Hengartner, 2000). Cytochrome *c* release results in its coupling with the apoptosis protease activating factor-1 (Apaf-1), and then procaspase-9 to form the apoptosome. This interaction leads to the activation of caspase-9 and subsequent cleavage of the effector caspase-3 (Figure 7). Both the death receptor and mitochondrial pathways converge at the level of caspase-3 leading to the cleavage of specific substrates that

Figure 7. The mitochondrial death pathway.
DNA damage triggers the activation of pro-apoptotic Bcl-2 family members, like Bax, and other upstream repair modulators like p53. These modulators regulate the release of Cytochrome *c* from the mitochondria which associates with Apaf-1 and than procaspase-9 to create the apoptosome which in turn activates caspase-3. Modified from Hengartner, 2000.

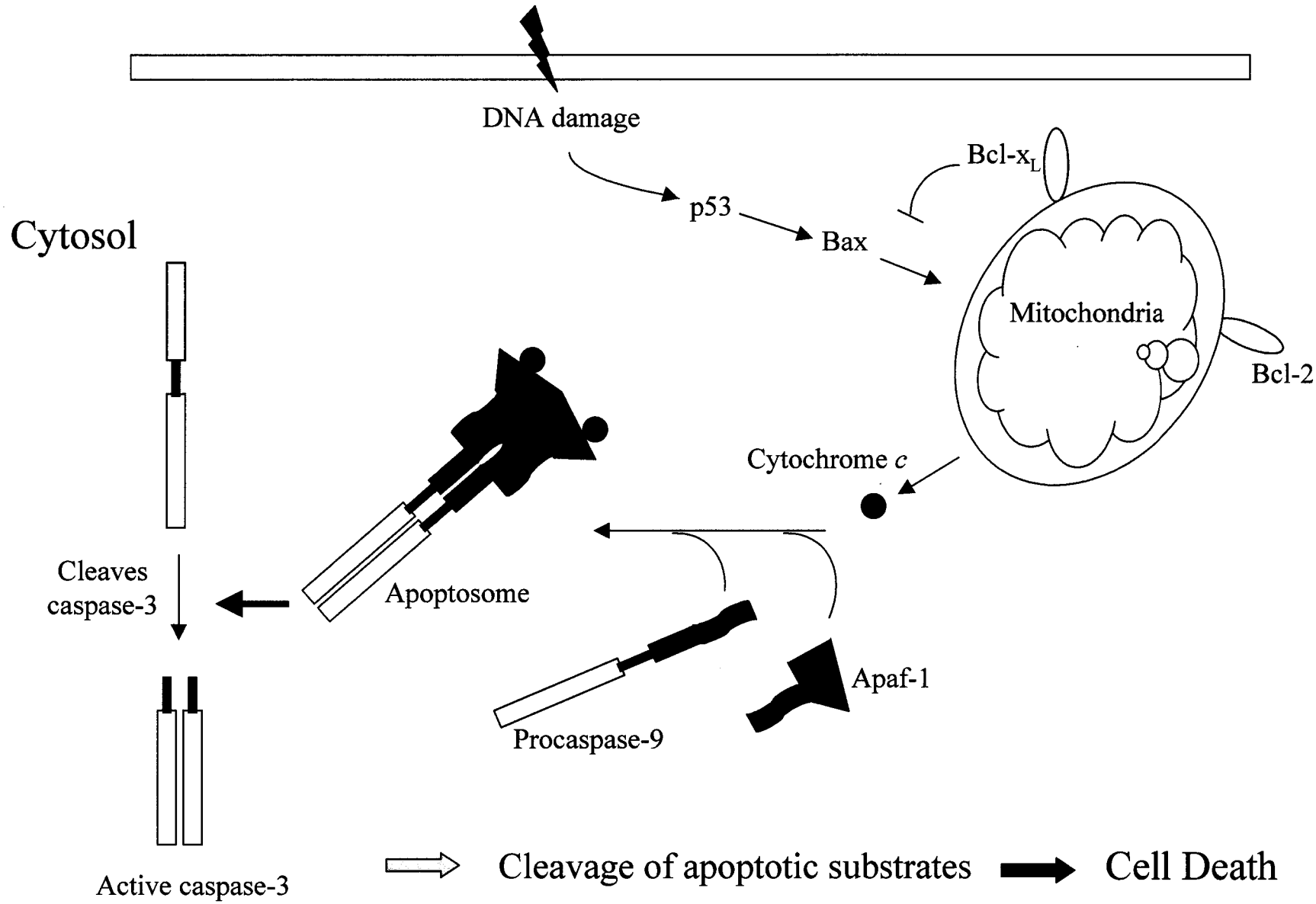
DNA damage
p53
Bax
Bcl-x_L
Mitochondria
Bcl-2
Cytosol
Cytochrome *c*
Apaf-1
Procaspase-9
Apoptosome
Cleaves caspase-3
Active caspase-3
Cleavage of apoptotic substrates
Cell Death

undertake the actions of disassembling the cell. It is this action that has characterized the caspases as the executioners of the apoptotic pathway.

Upstream modulators of apoptosis that seem to direct their action on downstream factors like Bcl-2 members include oncogenes and tumour suppressor genes whose normal function is important in the regulation of tumorigenesis and cancer. Gain of function mutations of oncogenes such as *c-myc*, *fos*, *jun* and *ras*, promote cell proliferation and neoplastic transformation indicating the importance of apoptosis in cancer cell biology. A loss of function mutation in a tumour suppressor like *p53* or *Rb*, can result in the inactivation of DNA repair genes and loss of the inhibitory signal that regulates cell cycle progression. *p53* mutations have been found in over 50% of cancers. An important characteristic of *p53* is its ability to induce either cell cycle arrest or apoptosis. *p53* modulates cell cycle arrest in response to DNA damage, therefore the loss of *p53* causes the progression of damaged cells through the cell cycle.

1.6.5 Antiapoptotic genes and Inhibitors of apoptosis

An increase in apoptotic resistance promotes tumor progression and therapeutic resistance to drug therapies. The most widely studied anti-apoptotic genes in vertebrates are *Bcl-2* and the recently identified family of proteins that inhibit caspases, the Inhibitors of Apoptosis proteins (IAPs). Bcl-2, the mammalian homologue of the anti-apoptotic *C. elegans* cell death protein CED-9, antagonizes apoptosis by competing with its pro-apoptotic family members to maintain mitochondrial membrane potential and inhibit cytochrome *c* release into the cytosol. In *C. elegans*, CED-9 guards the cell from death by directly binding the pro-apoptotic Apaf-1 homologue CED-4 (Metzstein *et al.*, 1998). Although this direct binding of Bcl-2 to Apaf-1 has not been detected in mammals, it is

clear that a conserved mechanism of antagonism between pro- and anti-apoptotic factors exists for the inhibition of apoptosis.

The inhibitors of apoptosis proteins (IAPs) are a family of cell death regulators that have been identified in a wide variety of eukaryotes, including yeast, flies birds and mammals. First identified in baculoviruses, these proteins were shown to suppress cell death in virally infected host cells (Crook *et al.*, 1993; Birnbaum *et al.*, 1994). Since their discovery, researchers have shown that the primary mechanism for IAP cell death suppression seems to be through the inhibition of caspases. Studies have demonstrated that several human IAPs can bind and directly inhibit caspases (Deveraux *et al.*, 1997; Roy *et al.*, 1997). In the death receptor apoptotic pathway, IAPs bind the caspase-8 substrate, effector caspase-3, inhibiting its proteolysis and arresting Fas receptor mediated apoptosis (Deveraux *et al.*, 1997; Roy *et al.*, 1997; Deveraux *et al.*, 1998) (Figure 8). In the mitochondrial death pathway, IAPs can bind processed caspase-9, inhibiting the activation of caspase-3 (Deveraux *et al.*, 1998) (Figure 8).

The IAPs are structurally characterized by the presence of a ~ 70 amino acid long domain of cysteine and histidine residues with a possible serine/threonine phosphorylation site, termed the baculoviral IAP repeat (BIR) (LaCasse *et al.*, 1998). There can be up to three conserved tandem BIR domains within an IAP family member and the spatial positioning of the domains suggests a novel zinc-binding fold configuration (Deveraux and Reed, 1999). Studies have found that the presence of at least one BIR domain is necessary for apoptotic suppression function. Furthermore, IAPs have been shown to inhibit more than one specific caspase (Suzuki *et al.*, 2001). Recently, the role for the BIR domains has been provided by Riedl and co-workers (Riedl *et al.*, 2001).

Figure 8. The IAPs antagonize caspase-3 activation resulting in the cessation of apoptosis.
Both the death receptor and mitochondrial death pathways converge at the level of caspase-3 activation. Caspase-3 activation leads to the activation of downstream targets that cause the ultimate breakdown and removal of the cell. IAPs regulate caspase activity through their interaction with the BIR and RING domains.

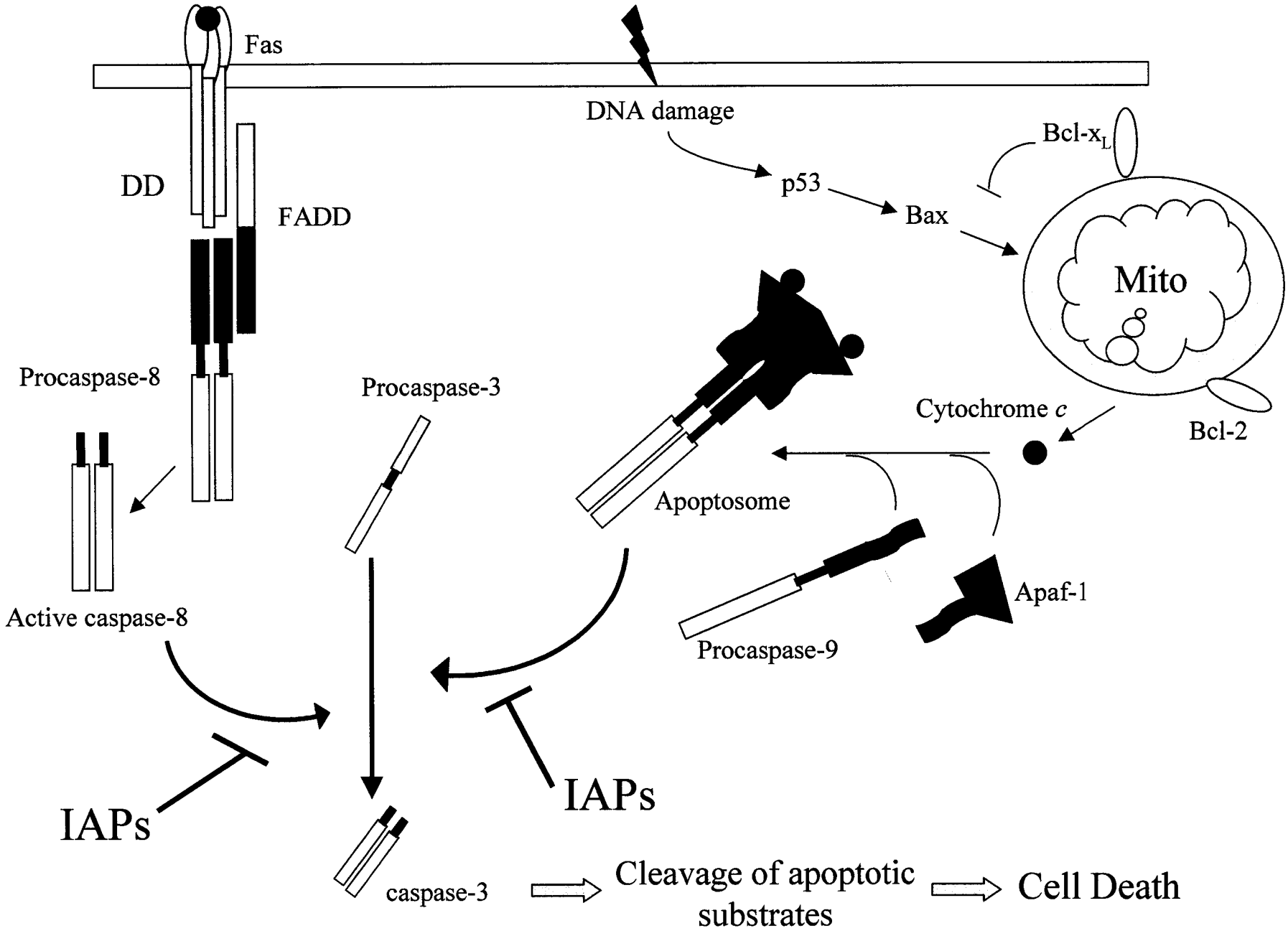
Fas
DNA damage
DD
FADD
p53
Bax
Bcl-x_L
Mito
Procaspase-8
Procaspase-3
Cytochrome *c*
Bcl-2
Apoptosome
Active caspase-8
Procaspase-9
Apaf-1
IAPs
IAPs
caspase-3
Cleavage of apoptotic substrates
Cell Death

They have shown that the BIR domain itself is not involved in the direct binding of the IAP to caspases, but instead critical amino acids residues surrounding the domain known as the 'hook, line and sinker' are responsible for the inhibitory effect. The BIR domain maintains and stabilizes the centrals bonds created by the hook, line and sinker showing a unique arrangement for a multi-purpose inhibitor (Riedl *et al.*, 2001). Several IAPs also possess a second defined motif at the carboxy-terminal, the RING Zn finger domain. In baculovirus IAPs, the presence of both the BIR and RING domains seem to be required for apoptotic suppression.

Recent evidence has uncovered the significance of the RING domain in metazoan IAPs. The presence of the RING finger domain is required for the ubiquitin-protein ligase activity of XIAP (X-linked inhibitor of apoptosis) to promote the proteasomal degradation of caspase-3 (Suzuki *et al.*, 2001). Several human IAPs contain an additional caspase recruitment domain (CARD) between the BIR and RING domains. Although the function of the CARD domain has to date been experimentally untested, CARD-containing IAPs have been found to bind caspase activators that contain CARD domains. CARDIAK/RIP2/RICK, a CARD domain containing protein, has been reported to bind and activate pro-caspase-1 (Thome *et al.*, 1998). It is known that pro-caspase-1 contains an amino-terminal CARD domain and caspase-1 can participate in apoptosis, as shown by caspase-1 knockout mice that resist pathological neuronal cell death in response to ischemia (Schielke *et al.*, 1998). Human c-IAP1 has been reported to bind CARDIAK/RIP2/RICK, but whether this interaction interferes with the activation of pro-caspase-1 by CARDIAK, has yet to be tested (Thome *et al.*, 1998). Understanding the

role of apoptotic inhibitors will play a key role in our understanding of both degenerative diseases and cancer.

1.6.6 Cell death during vertebrate limb development

The limb can be separated into three skeletal sections. The stylopodium consists of the humerus, the zeugopodium consists of the radius/ulna and the autopodium consists of the skeletal elements of the hand; the carpals, metacarpals and phalanges (digits). Patterning of the vertebrate limb has been the most widely studied model of apoptosis during embryonic development in amniotes. Apoptosis is important for the proper formation of skeletal elements, joints and separation of the digits. Early evidence for this cell degradation was shown in the chick, where at a specific time during autopod development, mesenchymal cells between the digit cartilage die leading to the individualization of the digits (Saunders *et al.*, 1962).

In the developing limb, there are three regions or zones that undergo cell death to pattern the limb. The interior necrotic zone (old nomenclature adapted prior to the discovery of apoptosis; now proven to be a genetically programmed process) undergoes apoptosis to separate the radius and ulna; the anterior and posterior necrotic zones shape the anterior and posterior part of the wrist; and the interdigital necrotic zones separate the digits (Figure 3C). The presence of the interdigital necrotic zones has been identified in most amniotes that have non-webbed feet suggesting a common mechanism is present for cell death.

The bone morphogenetic proteins (BMPs) are a family of secreted proteins originally identified because of their ability to induce ectopic bone formation when implanted into skeletal musculature of adult rats (Wozney *et al.*, 1988). BMPs have also

been shown to be involved in cell death during *Drosophila* embryogenesis (White *et al.*, 1994) and mullerian duct regression in the mouse (Behringer, 1994). In the developing limb, BMPs play a role in numerous morphogenetic processes including chondrogenesis (Zou *et al.*, 1997; Buckland *et al.*, 1998), joint formation (Storm and Kingsley, 1996), pattern specification (Laufer *et al.*, 1997), myogenesis (Duprez *et al.*, 1996), and apoptosis (Zou and Niswander, 1996). Yokouchi *et al.* (1996) showed that the expressions of the BMP2 and BMP4 proteins overlapped with the areas of PCD in the chick limb bud, and the overexpression of a dominant negative BMP receptor blocked endogeneous BMP2/4 signalling resulting in the suppression of mesenchyme regression in the interdigital regions. Implanting latex beads loaded with BMP2, 4 and 7 into the interdigital tissues of chick and duck induced precocious cell death in the interdigital mesenchyme (Ganan *et al.*, 1998; Merino *et al.*, 1998). Their findings suggest that BMP2, 4 and 7 are the apoptotic signalling molecules during PCD in the limb bud. However, whereas BMPs promote mouse undifferentiated mesenchymal cells to undergo apoptosis, prechondrogenic cells are induced to undergo chondrogenesis (Macias *et al.*, 1997). Lee *et al.* (1994) reported that undetermined mouse 12.5 day interdigital cells will revert their cell fate from the apoptotic pathway to the chondrogenic pathway when isolated from the limb and maintained in culture suggesting a dual role for BMPs during limb development. Interdigital explants will always produce cartilage in culture, but when cultured in the presence of digits, chondrogenesis can be inhibited. This conversion of cell fate has been attributed to *Bmp-4*. Tang *et al.* (2000) showed that the addition of exogenous *Bmp-4* to interdigital cultures *in vitro* does not induce apoptosis but instead causes the formation of bone. When a digit is left attached to the interdigital tissue, *Bmp-*

4 induces apoptosis. These results have also been demonstrated in the chick, duck and rat, signifying the dual function of BMPs for cell differentiation and apoptotic regulation at the level of the digits (Hurle *et al.*, 1989; Lee *et al.*, 1993; Ganan *et al.*, 1998).

Currently, the role of apoptosis during urodele limb regeneration is unknown. To date, one group of scientists has investigated the role of apoptosis during normal limb regeneration and denervated limb regression in the larval axolotl limb. Mescher *et al.* (2000) performed bilateral amputations with unilateral denervations (transections of brachial nerves 3, 4 and 5) in larval axolotl forelimbs and concluded that denervation increases the rate of apoptosis during limb regression. Whether apoptosis plays a role in this regression in the adult has yet to be identified. Similarly, the role of apoptosis during any stages of adult forelimb regeneration has yet to be identified.

1.7 Thesis hypothesis and rationale

Although differences exist, genetic and morphological evidence has led to the suggestion that limb development in regenerating animals such as the newt, and in higher vertebrates such as mouse and man, may follow the same evolutionarily conserved mechanisms. Muneoka and Bryant (1982) suggested that patterning mechanisms in the developing and regenerating urodele forelimb are the same. These pieces of evidence taken together, would suggest that the mechanisms involved in the development of the limb in higher vertebrates may be conserved in the regenerating limb of urodeles. In fact, studies involving Tbox genes ands HoxC6 suggest that the urodele regeneration response may be more closely related to development in higher vertebrates than it is to urodele development. My research will examine this hypothesis using apoptosis patterns during

development and adult forelimb regeneration in the newt, *Notophthalmus viridescens*. To date, apoptosis has been observed during the early phase of embryonic forelimb regeneration in the axolotl, and the rate of apoptosis is seen to increase in denervated, regenerating forelimbs, as would be expected during limb regression (Mescher *et al.*, 2000). No studies have examined apoptosis patterns in newt forelimb development or during advanced regeneration in the adult animal. My research will determine whether regeneration in the adult proceeds without cell death between the digits (as appears to be happening in development), or whether a mechanism employing interdigital cell death similar to that seen in higher vertebrates is occurring.

CHAPTER 2
MATERIALS AND METHODS

2.1 Animals and Tissue Preparation

2.1.1 Embryo collection and fixation

Notophthalmus viridescens embryos/larvae at various limb developmental stages were obtained from Christine Wong and R. A. Liversage (University of Toronto, Toronto, Canada). In brief, embryos were collected after natural or induced spawning as described by Khan and Liversage (1995). Embryos were maintained in Holtfreter's solution and allowed to develop to various stages of limb development (limb field, limb bud, cone, palette, early 2 digit to advanced 4 digit). Embryos/larvae were fixed overnight at room temperature in MEMFA (0.1 M MOPS, pH 7.4, 2 mM EGTA, 1 mM $MgSO_4$, 3.7% formaldehyde) with gentle agitation, dehydrated with 25, 50, 75 and 100% methanol/phosphate-buffered saline containing 0.1% Tween20 (PBT), and stored in 100% methanol at –20°C. Early stage embryos were dissected from their jelly coat prior to fixation. Developing limbs were staged according to a closely related species, *Triton taeniatus* (Glucksohn, 1931). No known staging has been reported for *Notophthalmus viridescens* limb development.

For histological assessment of embryonic tissues, embryos were brought to room temperature and rinsed twice in 100% ethanol for 20 minutes. Embryos were transferred to xylene and washed in xylene twice for 30 minutes at room temperature. This was followed by a 30 minute incubation in 1:1 xylene:paraplast at 60°C. Embryos were rinsed in hot paraplast for 30 minutes at 60°C and than transferred into molds with new paraplast and left overnight at 60°C. The following day, the embryos were oriented in the molds and allowed to set overnight at room temperature. 8-12 μm paraffin sections were

cut and adhered to slides pretreated with 0.01% aqueous solution of poly-L-lysine (Sigma Chemical Co., St. Louis, MO).

2.1.2 Haematoxylin-Eosin staining for Paraffin Embedded sections

For haematoxylin and Eosin staining, sections were deparaffinated and rehydrated in 2 x 3 minute changes of xylene at room temperature followed by 2 x 2 minute changes in absolute ethanol, and 2 minutes each in 95% ethanol, 70% ethanol and distilled water. Tissues were stained in filtered acidic Harris Haematoxylin (2 ml acetic acid/100 ml) for 1-3 minutes and rinsed in lukewarm tap water until the water went clear (approx. 2-3 minutes). Sections were transferred to 70% ethanol containing conc. HCl (4 drops/200 ml) for 3 dips, followed by 5 dips in tap water, 10 dips in filtered saturated Lithium Carbonate diluted 1:2 with distilled water, then transferred to lukewarm tap water for not less than 10 minutes. The tissues were counterstained for 1 minute in working Eosin solution followed by 3 dips in 95% ethanol and 5 dips in absolute ethanol. Tissues were dehydrated through 2 x 1 minute rinses in absolute ethanol followed by 3 x 1 minute rinses in xylene. Tissue sections were mounted with Permount and coverslips and let dry overnight at room temperature. Sections were viewed and photographed using a Zeiss Axioskop 2 microscope equipped with an AxioCam HRc camera.

2.1.3 Adult forelimb amputations and fixation

Adult newts (*Notophthalmus viridescens*) were obtained from Michael Tolley (Nashville, Tennessee, USA) and housed in aerated aquaria containing dechlorinated tap water. Newts were kept at room temperature on a 12L/12D photoperiod and fed ground

beef heart once weekly. All amputations were performed following anaesthesia in 0.05% 3-aminobenzoic acid ethyl ester (tricaine methane sulphonate – MS-222) (Sigma Chemical Co., St.Louis, MO, USA) adjusted to pH 7.0 with $NaHCO_3$. Post-amputation newts were maintained under similar conditions as stated above. Regenerating limbs were staged according to Iten and Bryant (1973).

Apoptosis patterns during regeneration:

Forty-eight animals were amputated through the right mid-zeugopodium and the protruding bone was trimmed back to the level of the soft tissue. Limbs were allowed to regenerate to different stages post-amputation (24hr, 3 day, 1 week, 2wk, 3wk, 4wk, 5wk, 6wk) and 6 limbs were re-sampled through the mid-stylopodium for each time point and fixed overnight in 4% buffered paraformaldehyde (PFA). Tissues were embedded in 50/50 sucrose/OCT compound, quick frozen in liquid nitrogen and stored at –80°C for cryosectioning. 10-16 μm sections were cut and adhered to positively charged slides (Superfrost Plus, Fisher Scientific), dried at room temperature for 2 hours and stored at –20°C prior to being used for TUNEL analysis.

Image superimpositions:

Five animals were unilaterally amputated through the right mid-zeugopodium, and 5 animals were bilaterally amputated through both mid-zeugopodia and the protruding bone was trimmed back to the level of the soft tissue. Limbs were photographed before and after amputation using the Nikon Coolpix 990 digital camera. Limbs were allowed to regenerate to a flattened palette stage when the formation of digits became visible (~ 5 weeks post-amputation). Subsequently, every 3-4 days thereafter,

animals were re-anaesthetized and photographed until the digits were visibly separated (~ 9 weeks post-amputation).

2.2 TUNEL/End Labeling

To identify cells containing apoptotic DNA fragments, a terminal deoxynucleotidyl transferase (TdT) –mediated dUTP nick end labeling (TUNEL) protocol modified from Gavrieli *et al.* (1992), and a Xenopus whole mount TUNEL protocol adapted from Veenstra *et al.* (1998) were used. Whole mount and tissue section immunohistochemistry protocols were adapted from Cadinouche et al. (1999), and Jensen and Wallace (1997).

2.2.1 Whole-mount TUNEL

Details of this protocol (including recipes for the reagents) are found in Appendix I. Embryos were rehydrated in PBT, treated with proteinase K (25 μg/mL) at 37°C for 20 min and washed twice with PBT. Positive controls were obtained by pretreating embryos in DNAse buffer (50 mM Tris-Cl, pH 7.5, 10 mM $MnCl_2$, 50 μg/ml BSA) containing10 units DNAse I (0.1 u/μl; Sigma Chemical Co.) for 30 min at 37°C. This treatment induces DNA nicking. After incubation, embryos were rinsed in 1X PBS and processed through the TUNEL protocol. Embryos were transferred to 1X terminal deoxynucleotidyl transferase (TdT) buffer (30 mM Trizma base, pH 7.2, 140 mM sodium cacodylate, 1 mM cobalt chloride; GibcoBRL) and equilibrated for 30 min at room temperature. End labeling was carried out overnight at room temperature in TdT buffer containing 150 units/mL TdT and 0.5 mM digoxygenin-dUTP (Boehringer Mannheim). The following day, embryos were washed 2 x 45 min in 1X PBS/1 mM EDTA at 65°C, followed by 4 x

45 min in 1X PBS at room temperature. Embryos were equilibrated in MAB-B for 30 min at room temperature and incubated in 1 mL blocking solution overnight at 4°C. Anti-digoxigenin antibody coupled to alkaline phosphatase (Anti-DIG-AP; 150U/mL; Boehringer Mannheim) was diluted 1:400 in blocking solution and 10 mg/mL newt powder and allowed to rotate overnight at 4°C. The following day, the newt powder was spun down and the anti-DIG was further diluted 1:1000 in block solution. Embryos were transferred to the block solution and gently agitated overnight at 4°C. To remove excess antibody, embryos were washed 10 x 15 min in MAB at room temperature. Embryos were equilibrated in alkaline phosphatase (AP) buffer (100 mM Tris-Cl, pH 9.5, 100 mM NaCl, 50 mM $MgCl_2$) 2 x 5 min at room temperature. The chromogenic reaction with alkaline phosphatase was carried out in AP buffer containing Nitro blue tetrazolium chloride, 100 mg/ml and 5-bromo-4-chloro-3-indolylphosphate, 50 mg/ml. The reaction was monitored (10-30 min) and stopped by transferring the embryos to Bouin's fixative overnight at 4°C. Embryos were cleared in several changes of 70% ethanol and 80%MeOH/20%H_2O_2. Embryos were viewed following dehydration in methanol and photographed with the Nikon Coolpix 990 digital camera mounted on a dissecting scope. Negative controls were obtained by omitting the TdT enzyme.

2.2.2 TUNEL Staining of Tissue Cryosections

Details of this protocol (including recipes for the reagents) are found in Appendix I. Frozen tissue sections of different staged regenerates (see section 2.1.3) were rehydrated in tap water, fixed in 1% PFA for 10 min at room temperature and washed 2 x 5 min in 1X PBS. Sections were post-fixed in pre-cooled Ethanol/Acetic acid (2:1) for 5

min and washed 2 x 5 min in PBS followed by a 5 min wash in PBT (0.2% Tween-20 in PBS). In a humidified chamber, sections were incubated for 20 minutes in PBT containing 20 μg/ml Proteinase K (Sigma) at room temperature and rinsed in 3 x 1 min PBS. Positive controls were obtained by pretreating sections in DNAse buffer (50 mM Tris-Cl, pH 7.5, 10 mM $MnCl_2$, 50 mg/ml BSA) containing10 units DNAse I for 10 minutes at room temperature. Following incubation, slides were rinsed in PBS and processed through DNA nick end labeling. Tissues were equilibrated in 1X TdT buffer for 5 minutes and end labeling was carried out by incubating the sections in TdT buffer containing 150 units/mL TdT and 0.5 mM digoxygenin-dUTP for 1 hour in a slide moat (Boekel Scientific) at 37°C. End labeling was stopped by transferring the sections into 1X PBS/1 mM EDTA for 10 min at room temperature, followed by 2 x 2 min rinses in PBS. Cryosections were equilibrated for 5 min in MABT (MAB; 0.1% Tween-20), and incubated in blocking solution for 1 hr at room temperature. Tissues were blocked overnight at 4°C in blocking solution containing a 1:1500 dilution of anti-digoxygenin antibody conjugated to alkaline phosphatase. The following day, sections were rinsed in MABT and equilibrated 5 min in AP buffer. The chromogenic reaction with alkaline phosphatase was carried out in AP buffer containing Nitro blue tetrazolium chloride (100 mg/ml) and 5-bromo-4-chloro-3-indolylphosphate (50 mg/ml). The reaction was monitored for up to 2.5 hrs and stopped by several washes in 1X PBS. Slides were dried and mounted in 50:50 1X PBS/glycerol. Images were taken on a Zeiss Axioskop 2 microscope equipped with an AxioCam HRc camera. Negative controls were obtained by omitting the TdT enzyme.

2.3 Image analysis

2.3.1 Image superimpositions

Superimposition of digital limb images was performed from an adapted protocol (Salas-Vidal *et al.*, 1998; Salas-Vidal *et al.*, 2001). Images were displayed using Abode Photoshop software, version 7.0. Images from all the regenerate stages (amputation-day 0 to 9 weeks-day 63), were superimposed (by dropping opacity of the overlying image by 50%) and the overlying images were positioned until they were completely aligned with underlying images at earlier stages. Images were aligned by locating corresponding pigment epithelium spots closest to the original plane of amputation within each image. Outlines of each regenerate stage were drawn and each stage was assigned a different colour. Contour images were overlapped and analyzed for interdigital tissue elongation or regression.

2.3.2 Statistical Analysis of image superimpositions

To account for the photographing variability at each time point and variability during superimposition, absolute values of control lengths and variable lengths along the newt limb were taken for statistical analysis. Digital and interdigital lengths were taken for each animal (6 different limb samples) and at each stage (7 different time points). The Law of Cosines was used to obtain the lengths of each digit at the midline (Figure 9). Interdigital lengths were measured from the most proximal interdigital point between two digits to the plane of amputation (Figure 9). Growth rate changes were statistically analyzed using the Microsoft Excel programme and significant differences between and

Figure 9. Digital and interdigital measurements.

The **Law of Cosines** calculates a side of a triangle when the angle opposite and the other two sides are known. Measurements were taken from the distal tip to either side of the interdigital grooves of digit 3 (a and c), along with the width of the base of the digit between the interdigital grooves (b). These 3 known values were used to calculate an unknown angle (C) using the law of cosines: $c^2 = a^2 + b^2 - 2ab \cos C$. Knowing the value for cos C, it was applied to the formula $\mathbf{x^2} = a^2 + b^2/4 - abcosC$ to get the digital length (**x**) of digit 3 (**D3**) which represented the most accurate digital length for digit 3 along the digital midline. This was similarly done for digit 2.

Interdigital length (D2-3) was measured as the distance between the interdigital groove between digits 2 and 3 to the midline at the plane of amputation. Control values were measured at each time point for each animal to normalize values for statistical analyses (C1, C2, C3).

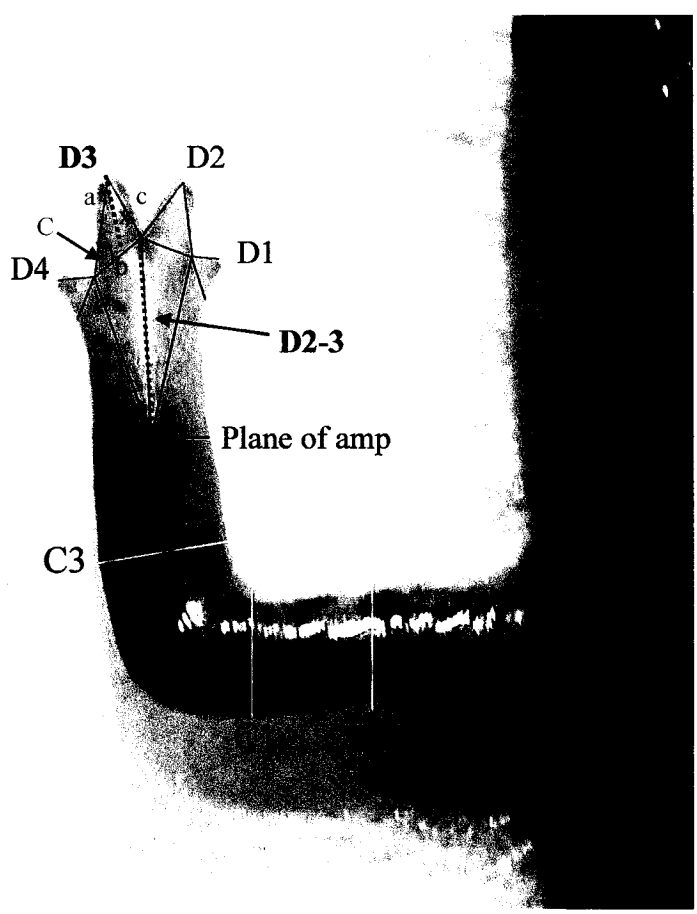
D3
D2
a
c
C
D4
D1
D2-3
Plane of amp
C3

among groups was calculated using a multiple analysis of variance at $p<0.05$ confidence interval.

CHAPTER 3
RESULTS

3.1 Apoptotic patterning

The terminal deoxynucleotidyl transferase (TdT) –mediated dUTP nick end labeling (TUNEL) staining technique demonstrates in situ DNA fragmentation in cells that have been destined to die by apoptosis (Gavrieli *et al.*, 1992). To examine the expression profile of apoptosis during newt forelimb development and regeneration, developing forelimbs of *Notophthalmus viridescens* embryos from the presumptive limb field to the four-digit stage, and regenerating adult limbs from the wound healing to the 6-week digit formation and cartilage condensation stages were put through the TUNEL staining techniques.

3.1.1 The role of apoptosis during *Notophthalmus viridescens* forelimb development

Apoptosis plays an important role during the normal development and patterning of the limb in higher vertebrates. To study the role of apoptosis during newt forelimb development, embryos with limbs at various developmental stages were fixed and put through a whole-mount TUNEL protocol. This protocol originally developed by Gavrieli et al (1992) was modified for use with newt tissue.

Positive Controls:

As a positive control, DNAse treatments were performed on embryos prior to TdT end labelling, which resulted in extensive DNA fragmentation and widespread positive cell staining (Figure 10A,B). Internal positive controls for TUNEL staining were provided by the labeling of the embryonic gills at all stages of limb development and the dorsal tailfin, two structures that are known to undergo regression from embryonic aquatic stages to eft land stages (gills seen in figure 11 F) (Khan and Liversage, 1995).

Negative controls omitted the TdT enzyme and showed no positive staining as expected (Figure 10C,D). As a final verification for specificity of this protocol, 13.5 day mouse embryos were fixed in a similar manner to the fixation procedure for newt embryos, and were put through the whole mount TUNEL protocol. TUNEL positive staining was found in the interdigital mesenchyme cells of 13.5 day mouse embryonic limb palettes (Figure 10F). Apoptotic activity is expected at this time point during mouse limb development, based on the studies of others (Martin and Cotter, 1990; Mirkes *et al.*, 2001; Salas-Vidal *et al.*, 2001).

Haematoxylin and Eosin staining of embryonic tissue sections shows that cell diameter in the developing embryonic limb (including nuclei) is very large (Figure 10G,H). As such the apoptotic events described for the developing limb below are probably indicative of a single positive cell and not a group or cluster of cells. The relevance of this apoptosis in establishing pattern is therefore questionable, and will be considered further in the Discussion.

Apoptosis patterns in Limb Development:

In the developing newt forelimb, the first TUNEL positive cells were detected during the cone stage of development. Prior to this stage, no positive cells were visible at either the limb field or limb bud stages (data not shown). As the limb bud develops and elongates to form a cone, positive signal is sometimes evident in the distal-most tissue of the cone (Figure 11A). Since this is not always detected, it is difficult to say whether it is an isolated event due to cell damage or whether the event is so short-lived that it is not detectable throughout the entire cone stage of development.

Figure 10. TUNEL controls in the developing forelimb of the newt, *Notophthalmus viridescens*.

Positive controls for the end labelling reaction were performed by treating the embryos with Dnase I to fragment the DNA which resulted in alkaline phosphatase staining of the entire embryo (A), and specifically the forelimb (B). Negative controls were performed by omitting the TdT enzyme during end labelling (C,D). To further verify that our TUNEL protocol adapted for newt tissues labelled apoptotic cells, 13.5 day mouse embryos were put through the protocol and resulted in interdigital staining which is consistent with the findings of interdigital apoptosis during mouse limb development at this stage (F). (E) Mouse negative control. Haematoxylin and eosin staining of an early 2 digit (G) and early 3 digit (H) limb shows that the diameter of newt cells at these stages is very large and that the nucleus usually occupies the entire diameter of the cell. Similar cell and nucleus diameters were seen at the other stages of forelimb development studied (data not shown).

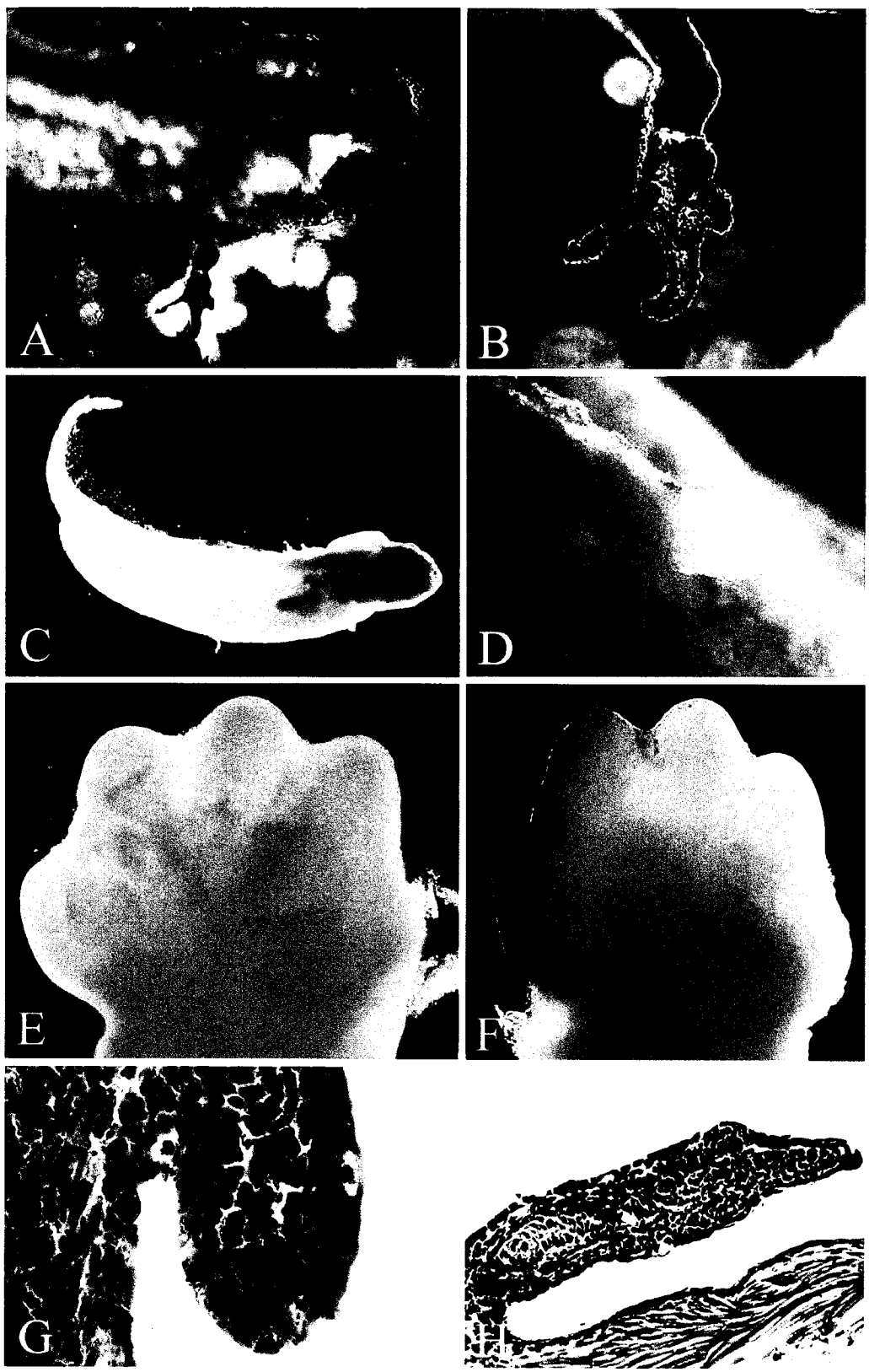
A
B
C
D
E
F
G

Staining found in embryos of palette staged limbs or older, was seen in posterior regions of the forearm at the future site of joints, like the presumptive wrist or elbow joint (Figure 11B). During the stages of digit outgrowth, positive signal was seen within digit and non-digit regions, digit tips, presumptive future wrist joints and occasionally interdigitally (Figure 11C-F). TUNEL positive staining was primarily within the ectoderm and immediate underlying mesoderm. Interdigital mesenchyme can be seen in embryos from the 2-digit to mid 3-digit stages (Figure 11D, F). Interestingly, interdigital staining was seen between digit 2 and the protuberance at the future site of digit 3 in an early 3-digit embryo (Figure 11E, white arrowhead). Staining was also seen just posterior to the projection of the emerging 3rd digit (Figure 11E, black arrowhead). This staining may be dying cells within the mesenchyme in between the 3rd and 4th digits. Furthermore, staining which at this stage would be observed at a presumptive wrist joint (Figure 11E, arrow), may in fact be mesenchymal apoptosis posterior to the future site of finger 4. Cell death anteriorly and posteriorly to finger 4 (Figure 11E, black arrowhead and white arrow) would contribute to the individualization of that finger. At the mid 3-digit stage (Figure 11F), positive TUNEL staining was seen at the digit tip of digit 2, interdigitally between digits 1 and 2 (Figure 11F, arrowhead), and just proximal to the digits in the developing autopodium (Figure 11F, arrow). Strong signal was seen within the embryonic gills at this stage and at other stages of limb development signifying a good positive control for apoptosis since the embryonic gills, along with the tailfin, are two structures know to undergo regression during the water to land eft stages. As with the cone-staged embryos, TUNEL positive staining seemed to identify isolated single cell

Figure 11. TUNEL labelling in the early developing forelimb of the newt, *Notophthalmus viridescens*.

Newt embryos were fixed at different stages of forelimb development and put through the TUNEL protocol. The first observation of TUNEL positive cell staining was found in the cone stage embryo. A positive single cell was seen at the most distal tip of the cone (A). At a later early 2 digit stage, positive cell staining was seen at the posterior margin of the limb in the presumptive wrist and elbow joint (B). At the 2 digit stage, a single positive cell was seen in the dorsal ectoderm of the first finger (C). An early 3 digit forelimb contained positive cell staining at both a presumptive wrist joint (arrow) and within the interdigital tissue between digits 2 and 3 (arrowhead). Interdigital mesenchyme was clearly visible in between digits 1 and 2 at this stage (D). Another limb at the early 3 digit stage (E) showed positive cell staining at the digit tip of digit 2 and at the presumptive wrist or elbow joint (white arrow). Interdigital staining was seen between digits 2 and 3 (white arrowhead) *and* just posterior to the projection of emerging digit 3 (black arrowhead). This staining posterior to the 3rd digit may be the future interdigital site between digits 3 and 4. By the mid 3 digit stage (F), TUNEL positive staining was observed at the distal tip of digit 2, interdigital tissue between digits 1 and 2 (arrowhead) and within the developing autopodium just proximal to the digits (arrow). Strong cell staining was seen in the embryonic gills (EG), a structure known to undergo regression during the water to land eft stages of this species. D1-D4: digits 1 through 4.

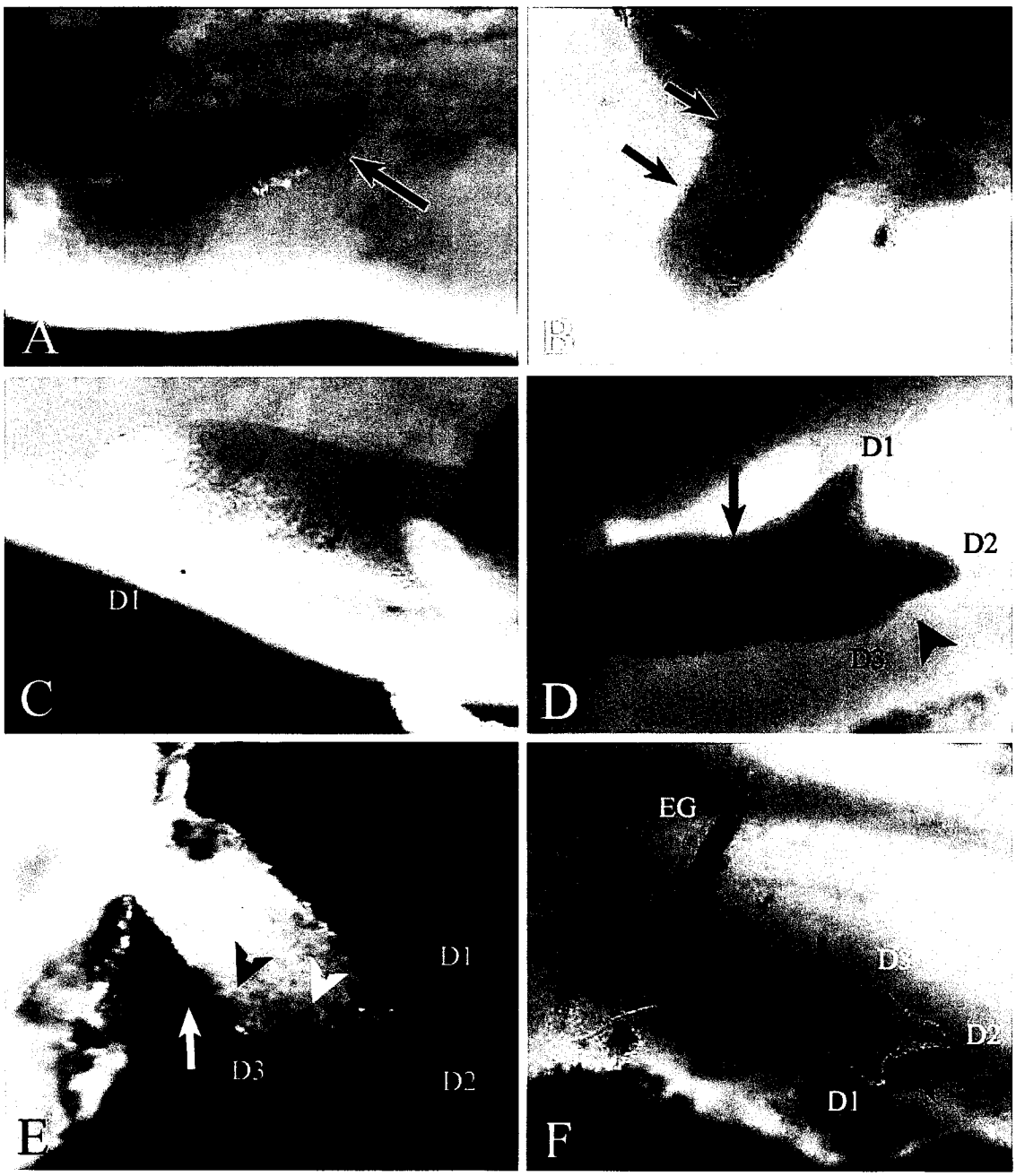
A
B
C
D1
D
D1
D2
D3
E
D1
D3
D2
F
EG
D3
D2
D1

events and did not identify cell clusters, as would be expected if apoptosis were involved in establishing pattern.

TUNEL staining during the advanced digit stages did not identify any distinct pattern of interdigital apoptosis (Figure 12) as would be expected if compared to mouse limb development. Interdigital mesenchyme was absent between digits 1 and 2, and digits 2 and 3 at the 3-digit stage although positive cell staining was seen interdigitally and occasionally at digit tips at this stage (Figure 12A,B). Positive cells were seen in presumptive digital joint sites (Figure 12B,E) and again ventrally and posteriorly at the presumptive wrist/elbow joints (Figure 12C,D). Occasional positive staining was seen within the digits of one hand (Figure 12F), but in the contralateral hand there was no similar staining at that stage (Figure 12G). Overall, positive staining in an individual cell or a small population of cells was seen, but no extensive apoptosis was present at any particular stage to suggest interdigital mesenchyme regression. One isolated case showed extensive TUNEL positive staining along the entire shaft of digits 2 and 3 in a 4-digit embryo (Figure 12H). Since this was an isolated incident, it was most likely not developmentally regulated but resulting from damage to the tissue.

The observations described above were typical results obtained from multiple TUNEL experiments. Whenever TUNEL positive cells were seen, they were almost always at presumptive elbow, wrist or phalangeal joints. However, they did not always appear in embryos of apparently similar stages. This may suggest that the apoptotic event is non-specific and due to cellular damage as opposed to developmentally regulated. It may also be transient, so that unless embryos of the exact age (within an hour) are

Figure 12. TUNEL labelling in the late developing forelimb of the newt, *Notophthalmus viridescens*.
By the 3-digit stage (A,B), interdigital mesenchymal tissue was absent and TUNEL positive staining was seen at the digit tips (black arrows), and occasionally interdigitally (A, arrowhead). Positive staining was still identified at the presumptive elbow joints (blue arrows; C, ventral view; D, posterior view). The 3-digit stage represented the first digital stage where positive cell staining was seen within the digits of an elongated and differentiated finger, digit 2 (B, blue arrow). This staining may represent the location of the digital joints. Positive staining was also seen within digit 2 at the early 4-digit stage (E, blue arrow). By the late 4-digit stage, interdigital mesenchyme was absent in between all the digits (E, F), and unequal positive staining was seen between the two forelimbs in the same animal (F, right hand; G, left hand). An isolated result showed positive TUNEL staining along the entire shaft of fingers 2 and 3 in a 4-digit embryo (H, anterior-dorsal view of F). D1-D4: digits 1 through 4.

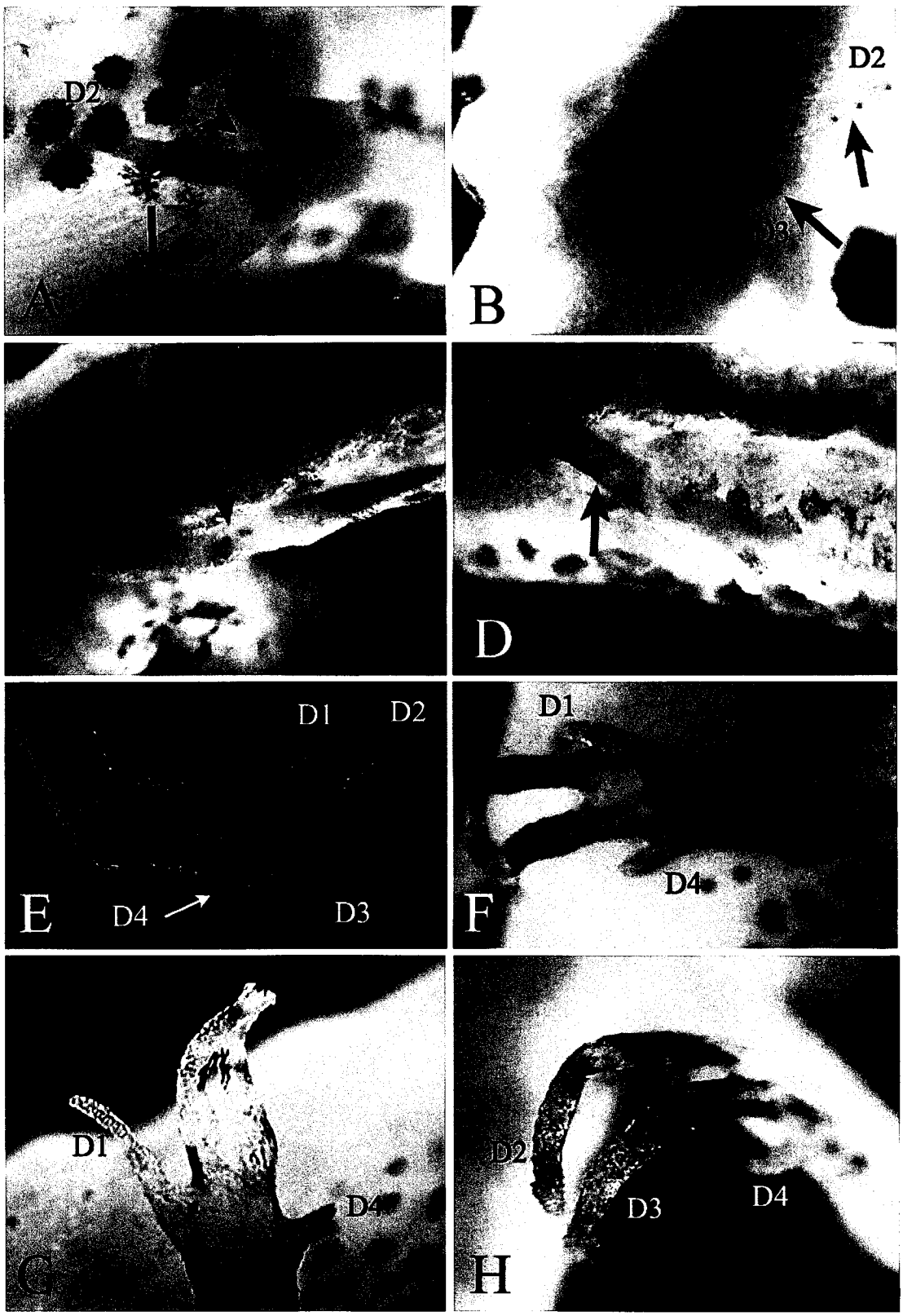
D2
A
D2
B
D
D1
D2
E
D4
D3
D1
F
D4
D1
G
D4
D2
D3
D4
H

examined, the same profiles may not be seen. The relevance of the positive cell staining seen interdigitally will be addressed in the discussion.

3.1.2 The role of apoptosis during *Notophthalmus viridescens* forelimb regeneration

To study the role of apoptosis during adult forelimb regeneration in the newt, and in particular during digit patterning and formation, longitudinal tissue sections of adult forelimb regenerates from amputation to 6 weeks post-amputation were fixed and stained using a TUNEL protocol adapted for newt tissue (see Appendix I).

Morphological detail described for each stage of regeneration is reviewed by Iten and Bryant, (1973). At 24 hrs post-amputation, the distal portion of the stump becomes swollen and the cut surface becomes completely covered by a thin transparent layer of epidermal cells known as the wound epidermis. At this wound healing stage, the sub-epidermal blood vessels become engorged and the distal stump tissues become disorganized. Our results showed weak TUNEL positive staining throughout the epidermal and dermal cell layers at the plane of amputation (Figure 13A,B). Proximal to the epithelial layer, individual positively staining cells were seen. Identification of cell types was difficult under higher magnification due to the thickness of the tissue sections. Possible tissue types include white blood cells and red blood cells, both of which would be located throughout the limb stump and damaged following amputation. In the newt, red blood cells are nucleated and would therefore stain for apoptosis. Strong TUNEL positive staining was seen within the bone in the longitudinal plane of the radius or ulna (Figure 13A). Furthermore, strong positive signal was also seen within the periostium along the edges of the bone (Figure 13A, arrowheads). Connective tissue and

degenerating, fragmented muscle surrounding the bone were also strongly positive. Dorsally and ventrally from the level of the radius and ulna, individual positive muscle cells were seen to have separated from the surrounding longitudinal muscle fibres (Figure 13B). It should be noted that tattered or damaged areas of bone or tissue, seemed to pick up strong staining even in negative controls that excluded the TdT enzyme (data not shown). These areas were considered false-positive and were not considered at any of the stages.

By 3 days post-amputation, the wound epithelium thickens to 5-7 cell layers and no dermal pigment cells can be found beneath the wound epithelium. Laterally, the presence of pigmented melanocytes identifies the plane of amputation. Further degeneration of the muscle, erythrocytes and nerves takes place (Iten and Bryant, 1973). At this stage, TUNEL positive staining remained within areas of muscle breakdown but fewer positive cells were found in the epidermis and dermis (Figure 13C).

At 1-week post-amputation, the apical wound epithelium becomes a bulbous 6-11 cell layer structure known as the apical epithelial cap (AEC). No basement membrane is seen beneath the AEC. Further tissue damage exists at this stage of regeneration although less debris can be seen. Dedifferentiation of the stump tissue including bone is taking place and blastema cells are forming (Iten and Bryant, 1973). At this stage, fragmented muscle was seen as short segments of myotubes containing single nuclei (Figure 13D) along with multinucleate osteoclasts around the distal tips of the humerus (plane of humerus not shown). Sparse individual TUNEL positive nuclei were identified throughout the regenerating tissue, which had begun to undergo dedifferentiation. The

Figure 13. TUNEL staining in the regenerating forelimb of the newt, *Notophthalmus viridescens*, during wound healing.
24hrs post-amputation (A), extensive TUNEL positive staining was seen throughout the distal stump of the wound. Weak staining was found within the wound epidermis (epi). Fragmented muscle (m), bone (b) and connective tissue (ct), was identified among the debris. Apoptotic cells were seen along the periostium outlining the bone (arrowheads). Dorsally and ventrally from the plane of the radius/ulna, fragmented muscle fibers were seen with strong single nuclei staining (B). Pigmented epithelial cells (PE) indicated non-regenerating dermis, which identified the regenerating/non-regenerating boundary (plane of amputation). 3 days post-amputation (C), positive cell staining was seen in the fragmented muscle, but became absent in the epidermal layers. By 1 week post-amputation, very few TUNEL positive cells could be identified in the stump, and the cells had begun to undergo dedifferentiation in distal tip (D; inset: TUNEL positive nuclei). Dnase I treated sections were used as a positive control (E), and the TdT enzyme was omitted during end labelling as a negative control (F). Dotted line: plane of amputation.

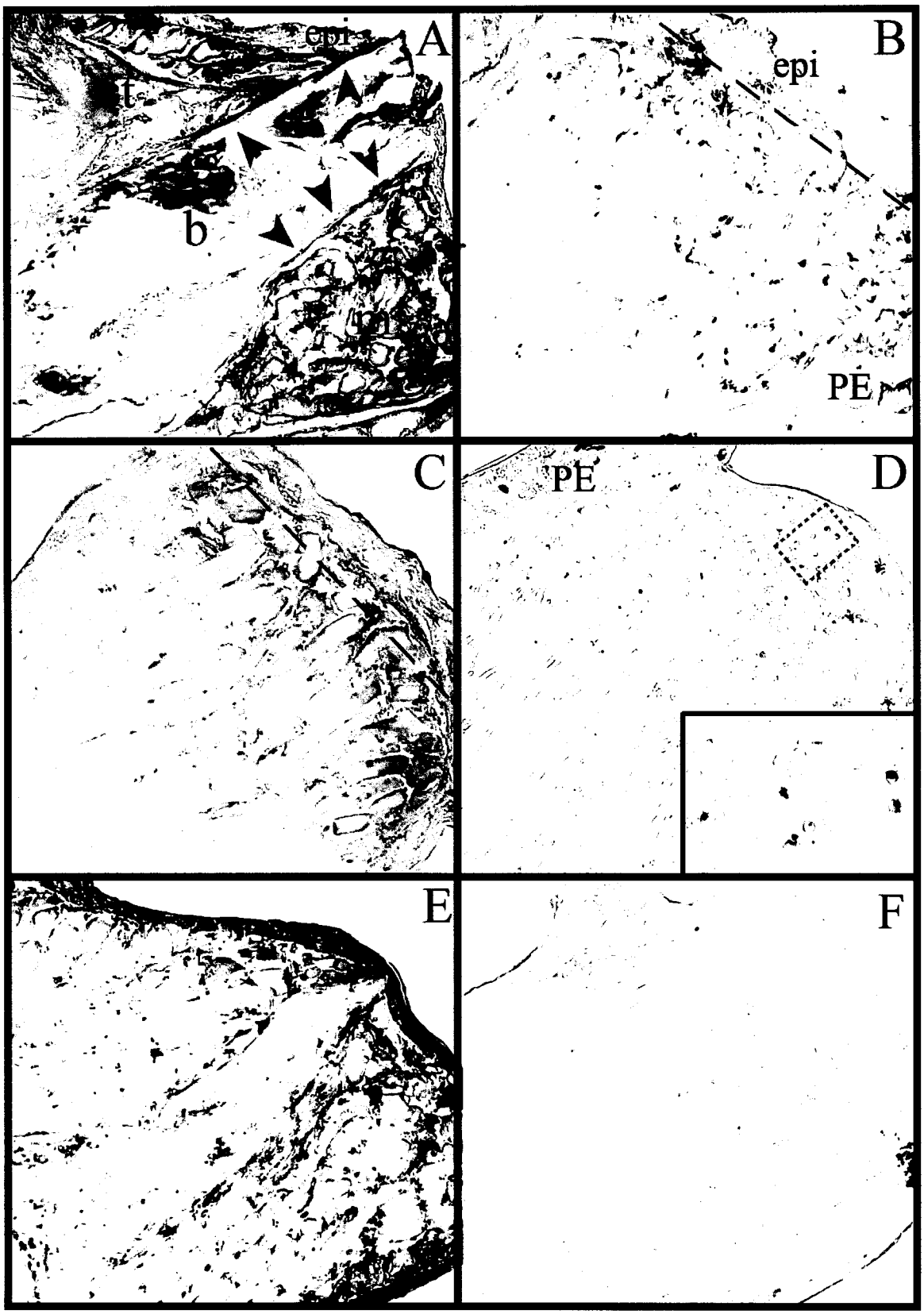
epi
A
t
b
B
epi
PE
C
PE
D
E
F

labeled cells represented approximately 1-2 % of the total cells within the regenerating tissue (Figure 13D).

By 2-weeks post-amputation, the blastema becomes established through the dense accumulation of blastemal cells at the distal tip of the stump. Blood vessels begin to form within the blastema and the regenerate visibly begins to look cone-shaped (Iten and Bryant, 1973). At this time point, the number of TUNEL positive cells had diminished to undetectable levels.

At 3-weeks post amputation, the regenerate begins to flatten at the cone apex (palette shaped). Chondrogenesis begins and is the most important change at this stage. Cartilage condensation takes place at the most distal tip of the radius/ulna proximal to the blastemal mass. Dedifferentiation is usually complete by this stage and capillary formation is underway throughout the regenerate (Iten and Bryant, 1973). Similar to the 2-week regenerates, 3-weeks post amputation, no TUNEL positive cells were detectable distal to the plane of amputation (data not shown).

At 4-weeks post amputation, chondrogenesis continues with the distal arrangement of the blastemal cells patterning the autopodium (hand). Four digital projections are evident at the distal tip along with three interdigital grooves. The zeugopodium (radius and ulna) has not separated from the autopodium whose elements are still fused. This stage marks the beginning of myogenesis (Iten and Bryant, 1973). At this stage longitudinal sections through the condensing cartilage of the regenerating distal tip contained TUNEL positive chondrocytes within the digital elements of the limb suggesting the possible turnover of cartilage to bone (Figure 14A). This positive staining of chondrocytes within the regenerating hand became more abundant in tissue sections at

Figure 14. TUNEL staining in the regenerating forelimb of the newt, *Notophthalmus viridescens*, during early digit cartilage condensation.
A) At 4 weeks post-amputation, the dermal layer (d) contained differentiated dermal glands (dg) and pigmented epithelial cells (PE). Cartilage condensation of the digits was seen within the distal tip of the regenerate. TUNEL positive cells were seen mainly within the condensing cartilage of the digits (inset). B) Dnase I treated positive control. C) Negative control.

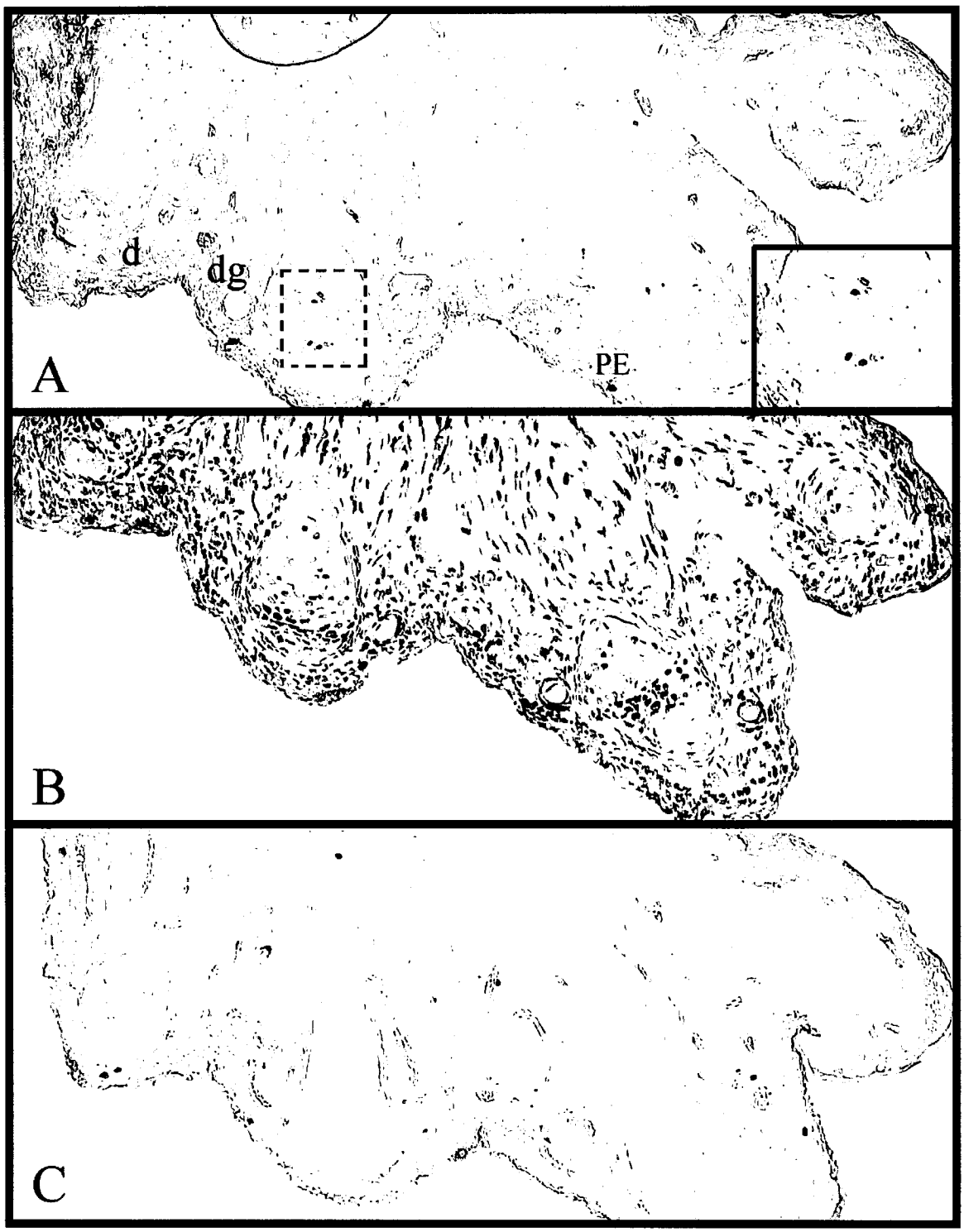
d
dg
PE
A
B
C

both 5 and 6-weeks post amputation when patterning and the separation of the digits was evident (Figure 15). Normally at 5-weeks post-amputation, complete separation occurs between digits 2 and 3 and few blastemal cells remain since most of the regenerate is made up of cartilage, bone and connective tissue. The elements of the autopodium (carpals and metacarpals) begin to separate from each other, and the formation of joints within the phalanges becomes present at 6 weeks post amputation (Figure 15A). No TUNEL positive cell staining was seen contributing to the demarcation of either the phalangeal joints or the individualized carpal and metacarpal bones at this stage of morphogenesis (Figure 15B-D). Digits had thinned out and were elongated with both digits 1 and 4 separated from their neighbouring digits along the interdigital grooves. According to Iten and Bryant (1973), at this stage the stump tissue is usually completely differentiated. The cartilage of the zeugopod and autopod becomes hypertrophic and some ossification is taking place (Iten and Bryant, 1973). Our observations identified individual TUNEL positive cells within the digit cartilage (Figure 15B,C). Close examination of interdigital tissue showed no TUNEL positive staining of mesenchymal cells during any stages of early or late digit formation in sections through the plane of the condensing cartilage of the autopod (Figure 15B,C). These same results were seen in multiple TUNEL assays conducted on six animals per stage.

Figure 15. TUNEL staining in the regenerating forelimb of the newt, *Notophthalmus viridescens*, during late digitation.
At 6 weeks post-amputation, the skeletal elements of the autopod, the carpals (c), metacarpals (m) and phalanges (p) are undergoing differentiation. The joints between the phalanges are forming without any positive TUNEL staining within the condensing cartilage (A). Positive cell staining was observed within the phalange and metacarpal cartilage (B and C, arrows). No interdigital mesenchymal cells (im) were found to be TUNEL positive in any of the sections studied at this stage (B,C). No positive cell staining was found with the separations of the carpal and metacarpal bones (D). Dnase I treated positive control (E). Negative control (F).

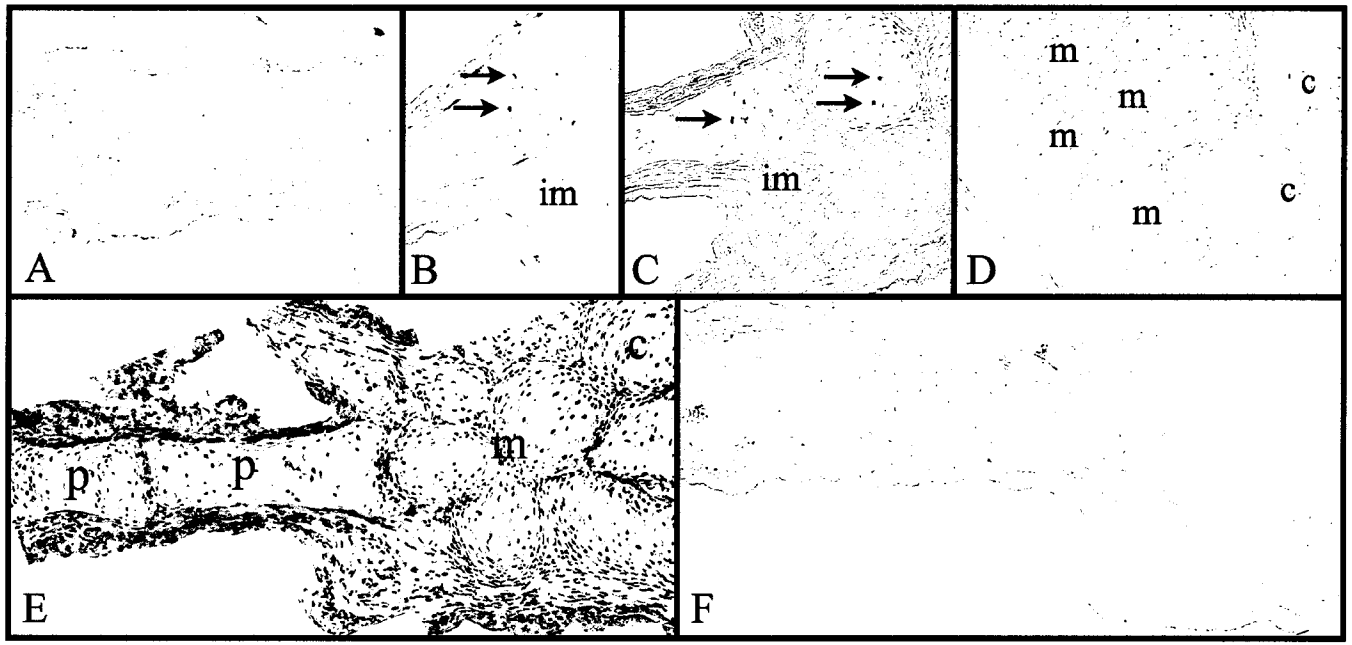
A
B
im
C
im
D
m
m
m
m
c
c
E
p
p
m
c
F

3.2 Image Analysis on adult forelimb regeneration

3.2.1 Superimposition analysis reveals no interdigital regression during adult forelimb regeneration

Salas-Vidal et al. (1998; 2001) used superimposition of forelimb images at various stages to show that interdigital regression was occurring during forelimb development in higher vertebrates. We used the same strategy to examine digital elongation in regenerating forelimbs of *Notophthalmus viridescens*. Individual regenerates were followed for a period of 9 weeks and pictures were taken at various stages in the regeneration process. Image contours of the regenerating limbs showing digit formation and individualization were superimposed and analyzed for digital elongation or interdigital regression as shown by Salas-Vidal et al. (1998; 2001). Superimpositions (Figure 16) revealed that digit elongation and individualization appears to result from growth of the individual digits as opposed to interdigital regression. This conclusion is based on the fact that in all 6 limbs examined there was very little overlap between the contours from one stage to the next.

3.2.2 Statistical analysis reveals that interdigital length plateaus at 8 weeks post-amputation

To further study the contribution of elongation versus regression during digit separation and individualization in newt forelimb regeneration, measurements were taken of interdigital lengths from the plane of amputation and individual digit lengths during each time point used for the superimposition analysis previously described (refer to Figure 9). In order to eliminate any intra-animal variations in size, all measurements for a

Figure 16. Limb contour superimpositions show interdigital regression does not contribute to digit individualization.
Limb contours were drawn for 6 random limbs at 7 different time points starting from day 39 (~ 5 weeks) and ending at day 63 (9 weeks). Contours were superimposed using pigmented epithelial landmarks as guides. Superimpositions showed that digits elongated from 5 weeks to 9 weeks and there was no interdigital regression based on the result that no overlap existed between earlier and later time points.

Day 39 - 5wks4dys
Day 42 - 6wks
Day 45 - 6wks3dys
Day 49 - 7wks

Day 63 - 9wks

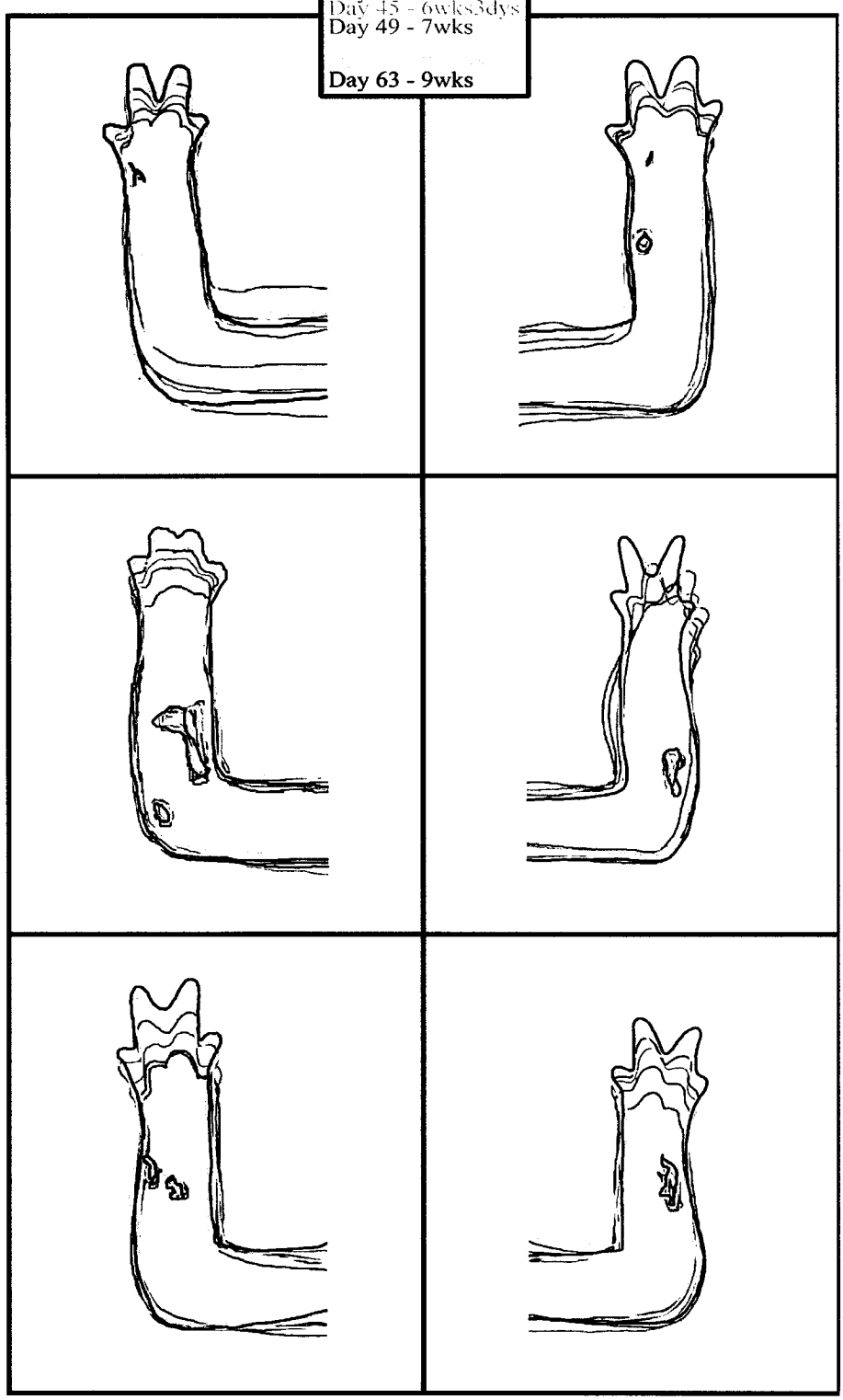

particular animal were normalized to a control value for that animal (eg. cross-sectional width of the stylopod; see Figure 9). Validation that this control value would remain constant throughout the study period (throughout regeneration) was shown by comparing ratios between 3 different control values within the newt limb over time (Figure 17). Control value C1 was chosen as the normalizing value over the other two controls based on the result that the ratios C1/C2 and C3/C1 were a tighter fit over time as compared to C3/C2 (see appendix II, Figure 20). Normalization of the measurements also eliminated any variability in limb sizes from one stage to another due to changes in magnification of images by the digital camera. Measurements of digital lengths was based on the ability to estimate the delineation between fingers. Since the lateral border of digits 1 and 4 were not visible, lengths were taken of digits 2 (D2) and 3 (D3) exclusively. Digital length was the distance from the most distal tip of the digit to the midpoint of the base of the digit as determined by the law of cosines (see Figure 9). Since digits 2 and 3 were used to analyse digit growth, the interdigital length between digits 2 and 3 (D2-3) was used exclusively to analyse interdigital growth. Interdigital length was the distance between the most proximal point between digits 2 and 3 and the midpoint at the plane of amputation (see Figure 9).

Digital lengths were seen to increase for both digit 2 and digit 3 from the first time point measured to the last time point measured when the digits were fully separated. However the length of digit 3 seemed to increase at a faster rate from day 49 to day 63 as compared to digit 2. Both digit lengths appeared to plateau by day 63 (9 weeks). Averages for the normalized digital lengths for the 6 animals are shown in Figure 18. Interdigital length between digits 2 and 3 was seen to increase from the first time point

Figure 17. Comparing controls between animals using averaged standardized ratios for 7 time points.
In order to account for variability between animals, controls were chosen in limb areas unaffected by the regenerating tissue (eg. the cross-section of the stylopod), and used to normalize absolute values taken at each timepoint. Averaged standardized ratios for the 7 time points were calculated using 3 control values (see Figure 9 for location of controls) which helped determine the best control to use for normalization. Since ratios C1/C2, and C3/C1 had the tightest fit compared to C3/C2, C1 was chosen as the value for normalization (trendlines are shown in appendix II, figure 20). Normalization also eliminated any variability in the measurements from one stage to another due to magnification effects caused by the digital camera. Numbers in x-axis represent individual animals.

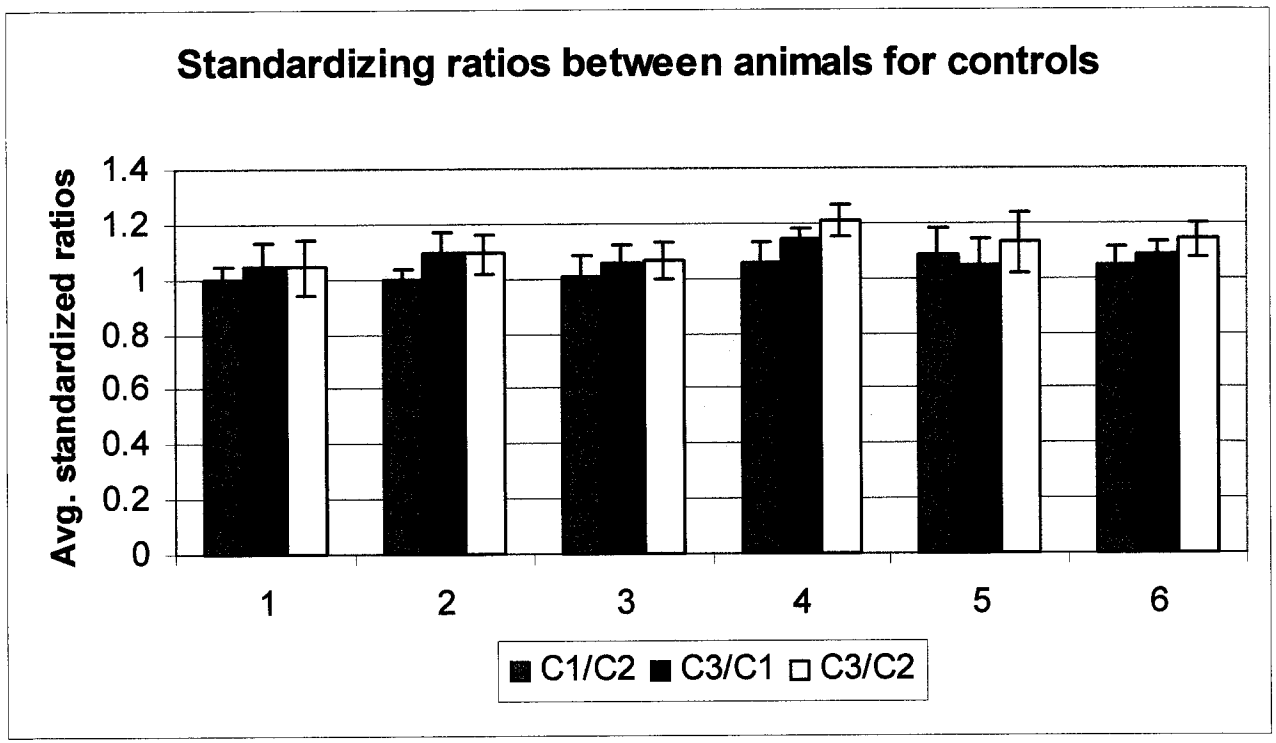
Standardizing ratios between animals for controls
Avg. standardized ratios
1.4
1.2
1
0.8
0.6
0.4
0.2
0
1
2
3
4
5
6
C1/C2
C3/C1
C3/C2

Figure 18. Digital length increases over time.
Normalization of lengths of digits 2 and 3 (digit length/C1 length) showed that the digits elongated from day 39 (~ 5 weeks) to day 63 (9 weeks). Digit 3 seemed to grow out at a faster rate from day 49 to day 63 as compared to digit 2, but both the lengths seem to plateau by day 63.

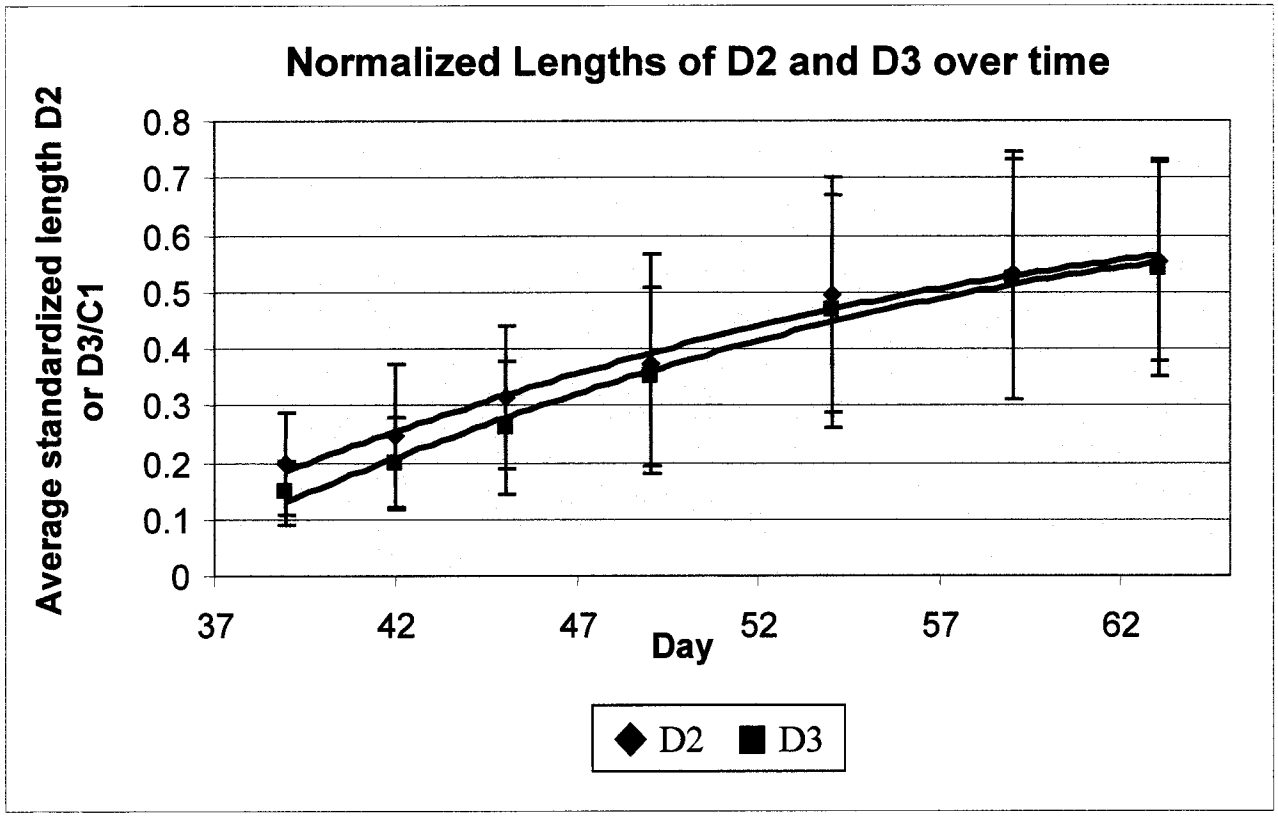
Normalized Lengths of D2 and D3 over time
Average standardized length D2 or D3/C1
0.8
0.7
0.6
0.5
0.4
0.3
0.2
0.1
0
37
42
47
52
57
62
Day
D2
D3

(day 39) to the fifth time point (day 54), and then plateau for the last two time points measured (days 59 and 63), (Figure 19, top trendline). Averages of normalized interdigital lengths between all digits is shown in appendix II, figure 21. Comparing digital and interdigital lengths over time revealed that interdigital length plateaued at approximately 8 weeks while digital lengths continued to increase suggesting that up until 8 weeks post-amputation, the digits *and* the carpals/metacarpals elongate to contribute to the growth of the entire hand (Figure 19). It appears therefore, that digit individualization during forelimb regeneration in the newt is a result of digit elongation and not mesenchymal regression between the digits.

Figure 19. Interdigital regression does not contribute to digit individualization during adult forelimb regeneration in the newt, *Notophthalmus viridescens*.
Comparing digital and interdigital lengths in the regenerating autopod showed that interdigital length increased from day 39 to day 54 where it peeked and then plateaued until day 63 (A,B). A multiple analysis of variance (ANOVA) test showed no significant difference between the value at ~ 8 weeks) and the final time point at 9 weeks (*p=<0.05). Digital length increased at all time points for both digit 2 (A) and digit 3 (B).

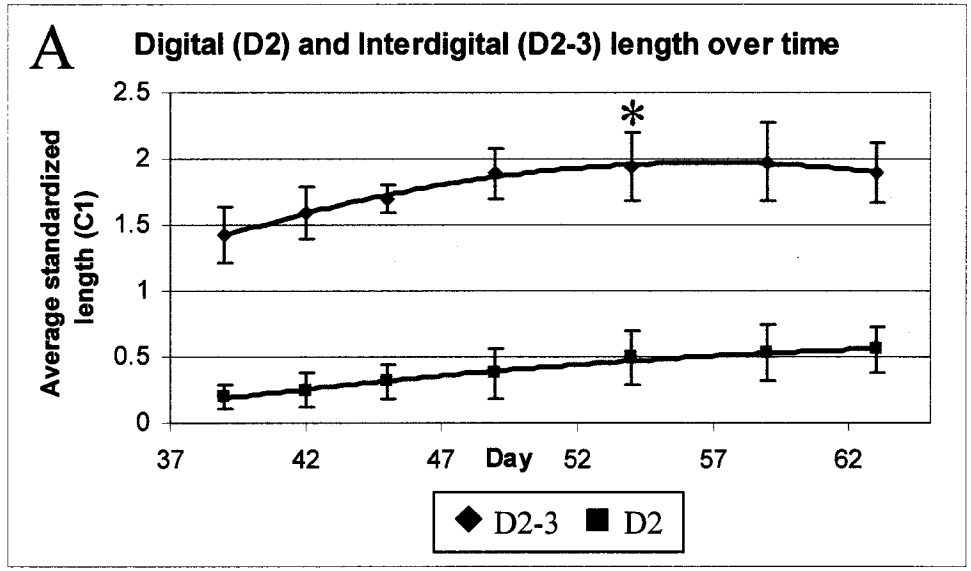
A
Digital (D2) and Interdigital (D2-3) length over time
Average standardized length (C1)
2.5
2
1.5
1
0.5
0
37
42
47
Day
52
57
62
*
D2-3
D2

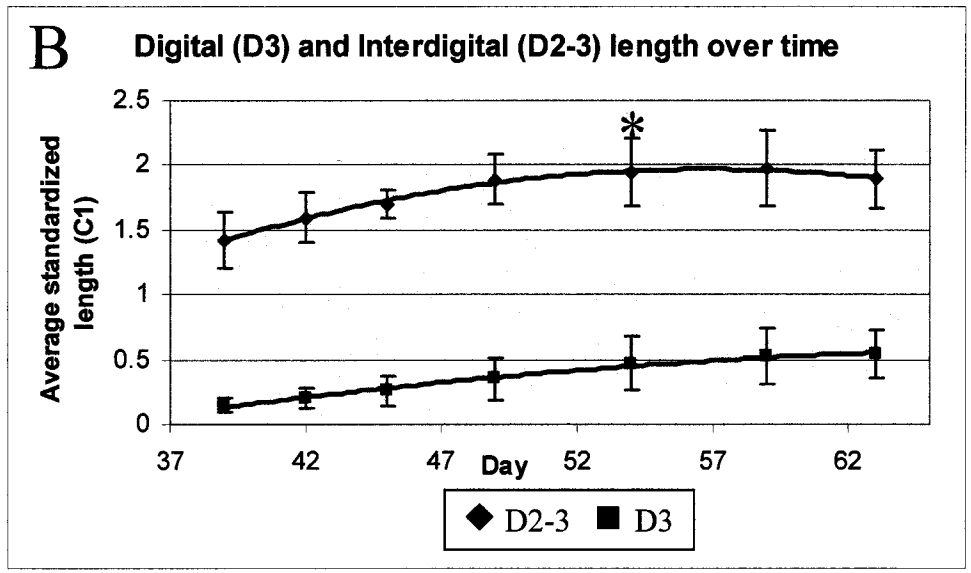
B
Digital (D3) and Interdigital (D2-3) length over time
Average standardized length (C1)
2.5
2
1.5
1
0.5
0
37
42
47
Day
52
57
62
*
D2-3
D3

CHAPTER 4
DISCUSSION

4.1 General Discussion

Regeneration in the red-spotted newt, *Notophthalmus viridescens*, proceeds through the dedifferentiation and proliferation of stump tissue to give rise to the cell mass required for the complete replacement of the lost structure. This type of epimorphic regeneration is unique to urodeles and results in the re-growth of a replacement that is morphologically and functionally equivalent to the original.

Many studies have suggested that the regeneration of the forelimb in newt is a recapitulation of newt forelimb development. Muneoka and Bryant (1982) performed transplantation graft experiments in the axolotl and concluded that patterning mechanisms during limb development and regeneration are the same. Their conclusion was based on the result that the developing limb responded to embryonic regenerating tissue by forming supernumerary digits following tissue misalignment, the same response seen when other developing tissue was grafted misaligned. At the molecular level, many developmental genes have been shown to be re-expressed during the regeneration process. These same genes are involved in the development of the limb in higher vertebrates such as mouse or chick. However, even though the same genes are involved in patterning both the newt and the mouse limb, there are clear differences in the way the limbs develop. Mouse limbs develop as a palette, with all the digits forming at the same time, and apoptosis between digits leading to digit individualization. In the developing newt limb, digits develop one at a time and appear to grow out from the limb palette. Even though newt forelimb regeneration has been called a recapitulation of development, the regenerating adult newt limb morphologically more closely resembles the developing limb of higher vertebrates during chondrogenesis and digit formation in that all the digits

seem to develop at once as opposed to individually. Genetic studies also support this observation. For example, even though Tbox genes are expressed in both development and regeneration, their expression profiles differ. During newt development, *Tbx4* and *Tbx5* gene expression is found in both forelimbs and hindlimbs. However, during regeneration *Tbx4* is restricted to the hindlimb and *Tbx5* is restricted to the forelimb, in a pattern which is reminiscent of that found in higher vertebrate development. Another example is provided by the expression of *HoxC6*. In chick, *HoxC6* is expressed in both the development of the forelimb and hindlimb. A similar profile is seen during urodele regeneration, but in urodele development, expression of *HoxC6* is restricted to the developing forelimb only.

All these studies clearly show that more research needs to be done before we can definitively determine whether regeneration is a recapitulation of development. My work addressed the question of whether forelimb regeneration is more closely related to limb development in the newt or limb development in higher vertebrates such as chick and mouse. To examine this question, I looked at apoptotic patterns during newt forelimb development and adult forelimb regeneration and compared the results with known patterns of apoptosis during limb development in the chick and mouse.

For newt forelimb development, TUNEL analysis was performed on newt embryos at different stages of development to identify apoptotic cell patterns. The results showed that apoptotic cells were first seen at the cone stage of limb development. TUNEL positive nuclei were identified at the distal tip of the cone, an area which would be undergoing differentiation of the mesenchymal cells to form the digits. The cone subsequently flattens out into a palette and the formation of the first and second digits

becomes visible. Throughout the digital stages, single cell apoptotic events were found within interdigital mesenchyme and in areas adjacent to where digits were *just* beginning to appear. Another location where apoptotic cells were found was in presumptive joint areas, like the future site of the wrist or elbow. Since the cartilage was not completely differentiated in the entire stylopod and zeugopod, no concrete conclusion could be made as to whether these locations were definite joints.

The results of the development studies can be interpreted in two ways. On the one hand, the fact that all embryos of the "same" stage did not show the same patterns might suggest that the apoptotic cells seen were single-cell events which were unrelated to pattern formation. Haematoxylin and eosin staining showed that the size of the cells in the embryo is very large and that the nucleus takes up the bulk of the cytosol in the cell. Most of the apoptotic cells we identified were single cells, and may have been isolated events related to cell damage in the embryo prior to the fixation protocol.

On the other hand, apoptotic cells were almost always seen next to areas of future digits, in interdigital regions, or at sites of future joints such as the elbow or wrist joint. These are the expected sites of apoptotic cells which might be involved in limb patterning. If these cells were involved in patterning, why would embryos of the "same" stage not always show the same pattern of apoptosis? A possible explanation may be that staging of *Notophthalmus viridescens* development has not been previously carried out and is very difficult to do. In mouse development, there is very specific timing of developmental events. The moment when fertilization occurs can be accurately predicted, and the identical morphological and genetic patterns are found at specific times post-fertilization. In newt, the precise timing of developmental events is not possible.

The mating procedure involves the deposition of a spermatophore by the male into the water. This spermatophore is taken up by the female, and can be retained in her body for up to a year, during which time the sperm remain viable and can be used at any time to fertilize the egg. Fertilized eggs are deposited onto plants at variable times during the day and unless the deposition is viewed directly, it is very difficult to identify the precise time of fertilization or deposition. Furthermore, development of the embryo and larva progresses at variable rates, depending on environmental conditions such as temperature. So, even eggs fertilized at the same time can develop at different rates depending on their immediate environment. For this reason, staging of development is very difficult. To date, there is no staging protocol for forelimb development in *N. viridescens*. This makes it difficult to determine the exact beginning and end of each stage of limb development. Consequently, embryos classified as being at the "same" stage are morphologically similar but may have been fertilized at different times. As such, a "three-digit embryo" might be in the early or late three-digit stage, and if the apoptotic event was transient, the apoptotic window may have been missed in some embryos while seen in others.

In higher vertebrates like chick and mouse, all the digits are formed together and then become separated through apoptosis (regression) of the interdigital mesenchyme. In our newt embryos, morphologically it was observed that the digits elongated individually anterior to posterior. We identified single apoptotic cells at digit tips, in interdigital mesenchyme and at prospective elbow and wrist joints. While there clearly is not the same mechanism as in higher vertebrates, apoptosis at these sites in the newt embryo may have been involved in controlling growth (as opposed to inducing regression) and may have thus contributed to pattern formation.

During adult forelimb regeneration, our results showed that apoptosis played a major role within the first week post-amputation during the wound healing stage. Apoptotic cells were found throughout the stump tissue from 24 hrs post-amputation to 3 days post-amputation, suggesting that apoptosis was the key mechanism for the removal of debris in the stump tissue. During cell proliferation and the formation of the blastema, apoptosis did not seem to play any apparent role. Similarly, apoptosis did not seem to play a significant role during the morphogenesis of the limb. No visible apoptotic cell patterning events were found within mesenchyme outlining the condensing cartilage of the radius/ulna or autopod skeletal elements in the regenerate. Individual single apoptotic cells were found within condensed cartilage of the carpal, metacarpals and phalanges suggesting a role for apoptosis in cartilage cell turnover to bone. It is known that during embryonic cartilage development, mesenchymal cells condense and differentiate into chondrocytes. During the final stages of chondrocyte maturation, the chondrocytes undergo apoptosis and are replaced by the formation of bone through the action of osteoblasts (Hickok, 1998). Our identification of these apoptotic cells signified the beginning of ossification in the regenerating limb.

Previous work by Mescher and co-workers (2000) on apoptosis in regenerating axolotl larval forelimbs found that during the first week post-amputation, positive mesenchymal cells were found within the distal areas of the regenerate and represented ~ 1-2 % of the cells among the dedifferentiating tissue. While direct comparisons cannot be made between newt and larval axolotl because of differences in timing of regeneration events, these results were similar to our findings in adult newt regenerating forelimbs at one week-post amputation in that Mescher's group similarly found that the cells were in

small clusters or singly distributed near the tip of the stump beneath the wound epidermis. Their experiments only studied the role of apoptosis within the first 11 days post-amputation, and except for TUNEL positive chondrocytes in the distal areas of the cartilage, they too were unable to identify/classify most of the labeled cells as to their tissue origin. An earlier study of apoptosis in regenerating newt adult forelimbs reported that 8 days post-amputation, only a very small number of positive labeled mesenchymal cells could be identified remaining in the stump tissue (Geraudie and Ferretti, 1997).

The differences between our studies and those of Mescher (2000) and Geraudie and Ferretti (1997) are that we examined apoptosis profiles throughout regeneration, as opposed to only at a specific time in the regeneration process. We show that apoptosis plays a major role during wound healing in the newt up until the first week post-amputation. At intermediate stages in the regeneration process, our results support the findings of Mescher (2000) and Geraudie and Ferretti (1997). At later stages of regeneration, we show that apoptosis is not involved in pattern formation and is mainly involve in cartilage turnover to bone.

The most significant finding of our TUNEL analysis during adult forelimb regeneration was that no single cell or cell cluster apoptosis was found within interdigital mesenchyme during digit formation in regeneration. This result contrasts what is seen during limb development in higher vertebrates like chick and mouse. Thus, while all the digits appear to form at the same time in the regenerate (as in higher vertebrates), the individualization of the digits appears to result from growth and elongation of the digits rather than by the apoptosis of the preformed interdigital tissue. We created 2D models of forelimb regeneration based on the work done by Salas-Vidal et *al.* (2001). This involved

the drawing of contour outlines of the regenerates at different stages during the regeneration process and the overlapping of the contours to examine whether there was any evidence to support the possibility of interdigital regression (apoptosis). Our results showed that no interdigital regression occurred in regenerating autopods based on the observation that contour images did not overlap in the interdigital regions from earlier stages of regeneration when digits begin to appear until later stages when the digits are separated. Our findings showed that digit outgrowth, rather than cell death of the interdigital mesenchyme leads to the individualization of the digits. Statistical analysis performed on digit and interdigital lengths (see Figure 19) in the regenerating forelimb revealed that digital lengths increase throughout regeneration whereas interdigital length plateaus.

Our finding that no apoptosis contributes to the growth and protrusion of the digits is not surprising based on the results of previous studies. Although it has been long proposed that interdigital apoptosis is the major contributor during digit individualization is birds (Saunders, 1966) and mammals (Ballard and Holt, 1968; Mori *et al.*, 1995), it has also been shown that programmed cell death does not occur during limb development in several amphibians (Cameron and F., 1977). Cell death may play a role in maintaining balance within the interdigital tissues by limiting cell proliferation, restricting interdigital growth and allowing for more prominent digit projection. Proximal-distal digit cell proliferation by BrdU incorporation was shown to exist in mouse during stages of interdigital cell death (Mori *et al.*, 1995). This evidence supports what we saw during forelimb development in our animals. Positive apoptotic staining was found interdigitally during digit outgrowth and within mesenchyme adjacent to digits that were only

beginning to protrude. Apoptosis may regulate the digit-interdigit boundary by limiting cell proliferation in sites adjacent to future digits.

The aim of this study was to examine whether regeneration in the newt more closely resembles development in the newt or development in higher vertebrates. Our results show that even though the digits in a regenerate appear to develop all at the same time (similar to higher vertebrates), the apoptotic patterns seen in higher vertebrates are clearly absent in the regenerate. Digit individualization occurs through proliferation of the digit tips as opposed to regression of interdigital mesenchyme. In this respect, regeneration is more similar to development in newts than it is to development in higher vertebrates. Overall, it appears that the regenerating forelimb shares some things in common with development in the newt and some things in common with development in higher vertebrates.

Our research shows that apoptosis is present to some extent in both the developing embryo and the regenerating adult, although the contribution to pattern formation is unclear. This work indicates the need for identifying a more accurate method for staging newt embryos so that timing of developmental events can be more closely monitored. Future experiments should address identifying and characterizing genes involved in the apoptotic pathway. This will aid in our understanding of the apoptotic pathways being utilized for the removal of damaged cells or patterning of the limb. It will also give us tools for identifying transient apoptotic events involved in patterning that may have been missed by the TUNEL protocol.

Summary

In summary, forelimb regeneration in the urodele proceeds through a number of complex processes including wound healing, cell dedifferentiation and blastema formation and the morphogenesis of the lost structures including the muscles, nerves and bones. Our work shows that apoptosis may be the key mechanism involved in the removal of damaged tissue in the stump following amputation. Besides wound healing, apoptosis is also involved in the turnover of mature cartilage to bone during ossification. Digit separation and elongation proceeds through the growth of the digits. Patterning of the newt limb during regeneration does not involve apoptosis of the interdigital mesenchyme as seen in higher vertebrates like chick and mouse. Although morphologically the regenerating adult newt limb resembles that of the developing limb of higher vertebrates, different mechanisms seem to be employed for the individualization of the digits.

Our work also suggests that limb development in the urodele proceeds through a unique mechanism which seems to be an intermediate between limb regeneration in the adult and limb development in higher vertebrates. Digits grow outward individually anterior to posteriorly in a manner unique to urodele development, but the presence of apoptosis in between the digits and in areas adjacent to future sites of protruding digits suggests that a developmental patterning mechanism may be conserved between urodeles and higher vertebrates involving a limited degree of interdigital apoptosis.

In conclusion, our work suggests that the pattering mechanisms during urodele forelimb development and adult forelimb regeneration are different by the comparison of patterns of apoptosis during digit growth and separation. Furthermore, our apoptotic

results suggest that forelimb regeneration in the adult proceeds through a mechanism unlike that of limb development in higher vertebrates. Thus it appears that the regeneration mechanism is unique, sharing both similarities and differences with developing newt forelimbs and developing higher vertebrates.

REFERENCES CITED

Ashe, P.C. and M. D. Berry (2003). "Apoptotic signaling cascades." Prog Neuropsychopharmacol Biol Psychiatry **27**(2): 199-214.

Ballard, K. J. and S. J. Holt (1968). "Cytological and cytochemical studies on cell death and digestion in the foetal rat foot: the role of macrophages and hydrolytic enzymes." Journal of Cell Science **3**(2): 245-262.

Beauchemin, M. and P. Savard (1993). "Expression of five homeobox genes in the adult newt appendages and regeneration blastemas." Prog Clin Biol Res: 41-50.

Behringer, R. R. (1994). "The in vivo roles of mullerian-inhibiting substance." Curr Top Dev Biol **29**: 171-87.

Birnbaum, M. J., *et al.* (1994). "An apoptosis-inhibiting gene from a nuclear polyhedrosis virus encoding a polypeptide with Cys/His sequence motifs." J Virol **68**(4): 2521-8.

Blaumueller, C. M. and S. Artavanis-Tsakonas (1997). "Comparative aspects of Notch signalling in lower and higher eukaryotes." Perspect Dev Neurobiol **4**(4): 325-43.

Buckland, R. A., *et al.* (1998). "Antagonistic effects of FGF4 on BMP induction of apoptosis and chondrogenesis in the chick limb bud." Mech Dev **71**(1-2): 143-50.

Butler, E. G. (1935). "Studies on limb regeneration in X-rayed Amblystoma larvae." The Anatomical Record **62**: 295-307.

Cadinouche, M. Z., *et al.* (1999). "Molecular cloning of the Notophthalmus viridescens radical fringe cDNA and characterization of its expression during forelimb development and adult forelimb regeneration." Dev Dyn **214**(3): 259-68.

Cameron, C. B., *et al.* (1986). "Cardiovascular effects of d-tubocurarine and pancuronium in newborn lambs during normoxia and hypoxia." Pediatric Research **20**(3): 246-252.

Cameron, J. A. and F. J. F. (1977). "The absence of cell death during development of free digits in amphibians." Developmental Biology **55**(2): 331-338.

Caubit, X., *et al.* (1997). "Reactivation and graded axial expression pattern of Wnt-10a gene during early regeneration stages of adult tail in amphibian urodele Pleurodeles waltl." Dev Dyn **208**(2): 139-48.

Chalkely, D. T. (1959). The cellular basis of limb regeneration. In Regeneration in Vertebrates. Chicago, University of Chicago Press.

Chalkley, D. T. (1954). "A quantitative histological analysis of forelimb regeneration in *Triturus viridescens*." Journal of Morphology **94**: 21-70.

Charite, J., *et al.* (1994). "Ectopic expression of Hoxb-8 causes duplication of the ZPA in the forelimb and homeotic transformation of axial structures." Cell **78**(4): 589-601.

Cohn, M. J., *et al.* (1995). "Fibroblast growth factors induce additional limb development from the flank of chick embryos." Cell **80**(5): 739-46.

Corcoran, J. P. and P. Ferretti (1997). "Keratin 8 and 18 expression in mesenchymal progenitor cells of regenerating limbs is associated with cell proliferation and differentiation." Dev Dyn **210**(4): 355-70.

Corcoran, J. P. and P. Ferretti (1999). "RA regulation of keratin expression and myogenesis suggests different ways of regenerating muscle in adult amphibian limbs." J Cell Sci **112**(Pt 9): 1385-94.

Crook, N. E., *et al.* (1993). "An apoptosis-inhibiting baculovirus gene with a zinc finger-like motif." J Virol **67**(4): 2168-74.

Crossley, P. H., *et al.* (1996). "Roles for FGF8 in the induction, initiation, and maintenance of chick limb development." Cell **84**(1): 127-36.

Deveraux, Q. L. and J. C. Reed (1999). "IAP family proteins--suppressors of apoptosis." Genes Dev **13**(3): 239-52.

Deveraux, Q. L., *et al.* (1998). "IAPs block apoptotic events induced by caspase-8 and cytochrome c by direct inhibition of distinct caspases." Embo J **17**(8): 2215-23.

Deveraux, Q. L., *et al.* (1997). "X-linked IAP is a direct inhibitor of cell-death proteases." Nature **388**(6639): 300-4.

Duboule, D. (1992). "The vertebrate limb: a model system to study the Hox/HOM gene network during development and evolution." Bioessays **14**(6): 375-84.

Dunis, D. A. and M. Namenwirth (1977). "The role of grafted skin in the regeneration of x-irradiated axolotl limbs." Dev Biol **56**(1): 97-109.

Duprez, D. M., *et al.* (1996). "Bone morphogenetic protein-2 (BMP-2) inhibits muscle development and promotes cartilage formation in chick limb bud cultures." Dev Biol **174**(2): 448-52.

Ekker, S. C., *et al.* (1995). "Distinct expression and shared activities of members of the hedgehog gene family of Xenopus laevis." Development **121**(8): 2337-47.

Enari, M., *et al.* (1998). "A caspase-activated DNase that degrades DNA during apoptosis, and its inhibitor ICAD." Nature **391**(6662): 43-50.

Ferretti, P. (2001). Regeneration of vertebrate appendages. Encyclopedia of Life Sciences. Basingstoke Hampshire, Macmillan Publishing.

Ferretti, P., *et al.* (1989). "Transient expression of simple epithelial keratins by mesenchymal cells of regenerating newt limb." Dev Biol **133**(2): 415-24.

Ganan, Y., *et al.* (1998). "Morphological diversity of the avian foot is related with the pattern of msx gene expression in the developing autopod." Dev Biol **196**(1): 33-41.

Gardiner, D. M. and S. V. Bryant (1996). "Molecular mechanisms in the control of limb regeneration: the role of homeobox genes." Int J Dev Biol **40**(4): 797-805.

Gavrieli, Y., *et al.* (1992). "Identification of programmed cell death in situ via specific labeling of nuclear DNA fragmentation." J Cell Biol **119**(3): 493-501.

Geraudie, J. and P. Ferretti (1997). "Correlation between RA-induced apoptosis and patterning defects in regenerating fins and limbs." International Journal of Developmental Biology **41**: 529-532.

Geraudie, J. and P. Ferretti (1998). "Gene expression during amphibian limb regeneration." Int Rev Cytol **180**: 1-50.

Gibson-Brown, J. J., *et al.* (1996). "Evidence of a role for T-box genes in the evolution of limb morphogenesis and the specification of forelimb/hindlimb identity." Mech Dev **56**(1-2): 93-101.

Gibson-Brown, J. J., *et al.* (1998). "Expression of T-box genes Tbx2-Tbx5 during chick organogenesis." Mech Dev **74**(1-2): 165-9.

Glucksohn, S. (1931). "Aussere Entwicklung der Extremitaten und Stadieneinteilung der Larvenperiode von Triton taeniatus LEYD. und Triton cristatus LAUR." Wilhelm Roux' Archiv fur Entwicklungsmechanik der Organismen **125**: 341-406.

Gobe, G. and B. Harmon (2001). "Apoptosis: Morphological Criteria and Other Assays." Encyclopedia of Life Sciences: 1-6.

Goss, R. J. (1969). Principles of regeneration. New York, Academic Press.

Han, M. J., *et al.* (2001). "Expression patterns of Fgf-8 during development and limb regeneration of the axolotl." Dev Dyn **220**(1): 40-8.

Hay, E. D. (1952). "The role of epithelium in amphibian limb regeneration, studies by haploid and triploid transplants." American Journal of Anatomy **91**: 447-481.

Hay, E. D. and D. A. Fischman (1961). "Origin of the blastema in regenerating limbs of the newt *Triturus viridescens*: an autoradiographic study using tritiated thymidine to follow cell proliferation and migration." Dev Biol **3**: 26-59.

Hayashi, H., *et al.* (1996). "Isolation of a novel chick homolog of Serrate and its coexpression with C-Notch-1 in chick development." Int J Dev Biol **40**(6): 1089-96.

Hengartner, M. O. (2000). "The biochemistry of apoptosis." Nature **407**(6805): 770-6.

Hengartner, M. O. and H. R. Horvitz (1994). "Programmed cell death in Caenorhabditis elegans." Curr Opin Genet Dev **4**(4): 581-6.

Hickok, N. J., Haas, A. R., and Tuan, R. S. (1998). "Regulation of chondrocyte differentiation and maturation." Microscopy Research and Technique **43**(2): 174-190.

Hurle, J. M., *et al.* (1989). "Experimental analysis of the in vivo chondrogenic potential of the interdigital mesenchyme of the chick leg bud subjected to local ectodermal removal." Dev Biol **132**(2): 368-74.

Imokawa, Y. and K. Yoshizato (1997). "Expression of Sonic hedgehog gene in regenerating newt limb blastemas recapitulates that in developing limb buds." Proc Natl Acad Sci U S A **94**(17): 9159-64.

Irvine, K. D. and T. F. Vogt (1997). "Dorsal-ventral signalling in limb development." Curr Opin Cell Biol **9**(6): 867-76.

Irvine, K. D. and E. Wieschaus (1994). "fringe, a Boundary-specific signalling molecule, mediates interactions between dorsal and ventral cells during Drosophila wing development." Cell **79**(4): 595-606.

Isaac, A., *et al.* (1998). "Tbx genes and limb identity in chick embryo development." Development **125**(10): 1867-75.

Iten, L. E. and S. V. Bryant (1973). "Forelimb regeneration from different levels of amputation in the newt, *Notophthalmus viridescens*: Length, rate and stages." Wilhelm Roux' Archiv **173**: 263-282.

Jarvik, E. (1980). Basic structure and evolution of vertebrates. London, Academic Press.

Jensen, A. M. and V. A. Wallace (1997). "Expression of Sonic hedgehog and its putative role as a precursor cell mitogen in the developing mouse retina." Development **124**(2): 363-71.

Johnson, R. L. and C. J. Tabin (1997). "Molecular models for vertebrate limb development." Cell **90**(6): 979-90.

Kerr, J. F., *et al.* (1972). "Apoptosis: a basic biological phenomenon with wide-ranging implications in tissue kinetics." Br J Cancer **26**(4): 239-57.

Khan, P., *et al.* (2002). "Different regulation of T-box genes Tbx4 and Tbx5 during limb development and limb regeneration." Dev Biol **250**(2): 383-92.

Khan, P. A. and R. A. Liversage (1995). "Spawning of *Notophthalmus viridescens* and rearing of embryos under laboratory conditions." Herpetol. Review **26**: 95-96.

Khan, P. A., *et al.* (1999). "Hox C6 expression during development and regeneration of forelimbs in larval Notophthalmus viridescens." Dev Genes Evol **209**(6): 323-9.

Kim, J., *et al.* (1995). "Cell recognition, signal induction, and symmetrical gene activation at the dorsal-ventral boundary of the developing Drosophila wing." Cell **82**(5): 795-802.

Kothakota, S., *et al.* (1997). "Caspase-3-generated fragment of gelsolin: effector of morphological change in apoptosis." Science **278**(5336): 294-8.

Kumar, A., *et al.* (2000). "Plasticity of retrovirus-labelled myotubes in the newt limb regeneration blastema." Dev Biol **218**(2): 125-36.

LaCasse, E. C., *et al.* (1998). "The inhibitors of apoptosis (IAPs) and their emerging role in cancer." Oncogene **17**(25): 3247-59.

Lanske, B., *et al.* (1996). "PTH/PTHrP receptor in early development and Indian hedgehog-regulated bone growth." Science **273**(5275): 663-6.

Laufer, E., *et al.* (1997). "Expression of Radical fringe in limb-bud ectoderm regulates apical ectodermal ridge formation." Nature **386**(6623): 366-73.

Lee, K. K., *et al.* (1993). "Histogenetic potential of rat hind-limb interdigital tissues prior to and during the onset of programmed cell death." Anat Rec **236**(3): 568-72.

Lee, K. K., *et al.* (1994). "Influence of digits, ectoderm, and retinoic acid on chondrogenesis by mouse interdigital mesoderm in culture." Dev Dyn **201**(4): 297-309.

Lo, D. C., *et al.* (1993). "Reversal of muscle differentiation during urodele limb regeneration." Proc Natl Acad Sci U S A **90**(15): 7230-4.

Loomis, C. A., *et al.* (1996). "The mouse Engrailed-1 gene and ventral limb patterning." Nature **382**(6589): 360-3.

MacCabe, J. A., *et al.* (1974). "Ectodermal control of the dorsoventral axis in the leg bud of the chick embryo." Dev Biol **39**(1): 69-82.

Macias, D., *et al.* (1997). "Role of BMP-2 and OP-1 (BMP-7) in programmed cell death and skeletogenesis during chick limb development." Development **124**(6): 1109-17.

Martin, S. J. and T. G. Cotter (1990). "Specific loss of microtubules in HL-60 cells leads to programmed cell death (apoptosis)." Biochem Soc Trans **18**(2): 299-301.

Merino, R., *et al.* (1998). "Morphogenesis of digits in the avian limb is controlled by FGFs, TGFbetas, and noggin through BMP signalling." Dev Biol **200**(1): 35-45.

Mescher, A. L., *et al.* (2000). "Apoptosis in regenerating and denervated, nonregenerating urodele forelimbs." Wound Repair Regen **8**(2): 110-6.

Metzstein, M. M., *et al.* (1998). "Genetics of programmed cell death in C. elegans: past, present and future." Trends Genet **14**(10): 410-6.

Mirkes, P. E., *et al.* (2001). "Co-localization of active caspase-3 and DNA fragmentation (TUNEL) in normal and hyperthermia-induced abnormal mouse development." Teratology **63**(3): 134-43.

Molven, A., *et al.* (1990). "Expression of a homeobox gene product in normal and mutant zebrafish embryos: evolution of the tetrapod body plan." Development **109**(2): 279-88.

Mori, C., *et al.* (1995). "Programmed cell death in the interdigital tissue of the fetal mouse limb is apoptosis with DNA fragmentation." Anat. Rec. **242**(1): 103-110.

Muneoka, K. and S. V. Bryant (1982). "Evidence that patterning mechanisms in developing and regenerating limbs are the same." Nature **298**(5872): 369-71.

Myat, A., *et al.* (1996). "A chick homologue of Serrate and its relationship with Notch and Delta homologues during central neurogenesis." Dev Biol **174**(2): 233-47.

Nagata, S., *et al.* (2003). "Degradation of chromosomal DNA during apoptosis." Cell Death Differ **10**(1): 108-116.

Namenwirth, M. (1974). "The inheritance of cell differentiation during limb regeneration in the axolotl." Dev Biol **41**(1): 42-56.

Nelson, C. E., *et al.* (1996). "Analysis of Hox gene expression in the chick limb bud." Development **122**(5): 1449-66.

Niswander, L., *et al.* (1994). "A positive feedback loop coordinates growth and patterning in the vertebrate limb." Nature **371**(6498): 609-12.

Niswander, L., *et al.* (1993). "FGF-4 replaces the apical ectodermal ridge and directs outgrowth and patterning of the limb." Cell **75**(3): 579-87.

Oliver, G., *et al.* (1988). "A gradient of homeodomain protein in developing forelimbs of Xenopus and mouse embryos." Cell **55**(6): 1017-24.

Papaioannou, V. E. and L. M. Silver (1998). "The T-box gene family." Bioessays **20**(1): 9-19.

Parr, B. A. and A. P. McMahon (1995). "Dorsalizing signal Wnt-7a required for normal polarity of D-V and A-P axes of mouse limb." Nature **374**(6520): 350-3.

Parr, B. A., *et al.* (1993). "Mouse Wnt genes exhibit discrete domains of expression in the early embryonic CNS and limb buds." Development **119**(1): 247-61.

Rao, L., *et al.* (1996). "Lamin proteolysis facilitates nuclear events during apoptosis." J Cell Biol **135**(6 Pt 1): 1441-55.

Repesh, L. A. and J. C. Oberpriller (1978). "Scanning electron microscopy of epidermal cell migration in wound healing during limb regeneration in the adult newt, Notophthalmus viridescens." Am J Anat **151**(4): 539-55.

Riddle, R. D., *et al.* (1995). "Induction of the LIM homeobox gene Lmx1 by WNT7a establishes dorsoventral pattern in the vertebrate limb." Cell **83**(4): 631-40.

Riddle, R. D., *et al.* (1993). "Sonic hedgehog mediates the polarizing activity of the ZPA." Cell **75**(7): 1401-16.

Riedl, S. J., *et al.* (2001). "Structural basis for the inhibition of caspase-3 by XIAP." Cell **104**(5): 791-800.

Rodriguez-Esteban, C., *et al.* (1997). "Radical fringe positions the apical ectodermal ridge at the dorsoventral boundary of the vertebrate limb." Nature **386**(6623): 360-6.

Rose, F. C., and Rose, S. M. (1965). "The role of normal epidermis in recovery of regenerative ability in X-rayed limbs of *Triturus viridescens*." Growth **29**: 361-393.

Roy, N., *et al.* (1997). "The c-IAP-1 and c-IAP-2 proteins are direct inhibitors of specific caspases." Embo J **16**(23): 6914-25.

Rudel, T. and G. M. Bokoch (1997). "Membrane and morphological changes in apoptotic cells regulated by caspase-mediated activation of PAK2." Science **276**(5318): 1571-4.

Ruvinsky, I. and J. J. Gibson-Brown (2000). "Genetic and developmental bases of serial homology in vertebrate limb evolution." Development **127**(24): 5233-44.

Sakahira, H., *et al.* (1998). "Cleavage of CAD inhibitor in CAD activation and DNA degradation during apoptosis." Nature **391**(6662): 96-9.

Salas-Vidal, E., *et al.* (1998). "Reactive oxygen species participate in the control of mouse embryonic cell death." Exp Cell Res **238**(1): 136-47.

Salas-Vidal, E., *et al.* (2001). "Differential tissue growth and patterns of cell death in mouse limb autopod morphogenesis." Dev Dyn **220**(4): 295-306.

Salpeter, M. M. and M. Singer (1960a). "Differentiation of the submicroscopic adepidermal membrane during limb regeneration in adult Triturus, including a note on the use of the term basement membrane." The Anatomical Record **136**: 27-40.

Saunders, J. W., Jr. (1948). "The proximo-distal sequence of the origin of the parts of the chick wing and the role of the ectoderm." Journal of Experimental Zoology **108**: 363-404.

Saunders, J. W., Jr. and C. Reuss (1974). "Inductive and axial properties of prospective wing-bud mesoderm in the chick embryo." Dev Biol **38**(1): 41-50.

Saunders, J. W. J. (1966). "Death in embryonic systems." Science **154**(749): 604-612.

Saunders, J. W. J., *et al.* (1962). "Cellular death in morphogenesis of the avian wing." Developmental Biology **5**: 147-178.

Savard, P., *et al.* (1988). "Position dependent expression of a homeobox gene transcript in relation to amphibian limb regeneration." Embo J **7**(13): 4275-82.

Savard, P. and M. Tremblay (1995). "Differential regulation of Hox C6 in the appendages of adult urodeles and anurans." J Mol Biol **249**(5): 879-89.

Schielke, G. P., *et al.* (1998). "Reduced ischemic brain injury in interleukin-1 beta converting enzyme- deficient mice." J Cereb Blood Flow Metab **18**(2): 180-5.

Schmidt, A. J. (1968). Cellular biology of vertebrate regeneration and repair. Chicago, University of Chicago Press.

Schotte, O. E. and E. G. Butler (1944). "Phases in regeneration of urodele limbs and dependence on the nervous system." Journal of Experimental Zoology **97**: 95-121.

Sharpe, P. T., *et al.* (1988). "Isolation and expression of a new mouse homeobox gene." Development **102**(2): 397-407.

Shawber, C., *et al.* (1996). "Jagged2: a serrate-like gene expressed during rat embryogenesis." Dev Biol **180**(1): 370-6.

Simeone, A., *et al.* (1987). "Two human homeobox genes, c1 and c8: structure analysis and expression in embryonic development." Proc Natl Acad Sci U S A **84**(14): 4914-8.

Simon, H. G., *et al.* (1997). "A novel family of T-box genes in urodele amphibian limb development and regeneration: candidate genes involved in vertebrate forelimb/hindlimb patterning." Development **124**(7): 1355-66.

Singer, M. (1952). "The influence of the nerve in regeneration of the amphibian extremity." Quart Rev Biol **27**: 169-200.

Sone, K., *et al.* (1999). "Expression of five novel T-box genes and brachyury during embryogenesis, and in developing and regenerating limbs and tails of newts." Dev Growth Differ **41**(3): 321-33.

Stark, D. R., *et al.* (1998). "Hedgehog family member is expressed throughout regenerating and developing limbs." Dev Dyn **212**(3): 352-63.

Steen, T. P. (1968). "Stability of chondrocyte differentiation and contribution of muscle to cartilage during limb regeneration in the axolotl (*Siredon mexicanum*)." J Exp Zool **167**(1): 49-78.

Stocum, D. L. (1985). "Role of the skin in urodele limb regeneration." Regulation of Vertebrate Limb Regeneration. R. E. Sicard. New York, Oxford University Press: 32-53.

Storm, E. E. and D. M. Kingsley (1996). "Joint patterning defects caused by single and double mutations in members of the bone morphogenetic protein (BMP) family." Development **122**(12): 3969-79.

Summerbell, D., *et al.* (1973). "Positional information in chick limb morphogenesis." Nature **244**(5417): 492-6.

Suzuki, Y., *et al.* (2001). "X-linked inhibitor of apoptosis protein (XIAP) inhibits caspase-3 and -7 in distinct modes." J Biol Chem **276**(29): 27058-63.

Suzuki, Y., *et al.* (2001). "Ubiquitin-protein ligase activity of X-linked inhibitor of apoptosis protein promotes proteasomal degradation of caspase-3 and enhances its anti-apoptotic effect in Fas-induced cell death." Proc Natl Acad Sci U S A **98**(15): 8662-7.

Takabatake, Y., *et al.* (2000). "Conserved and divergent expression of T-box genes Tbx2-Tbx5 in Xenopus." Mech Dev **91**(1-2): 433-7.

Tamura, K., *et al.* (1999). "Differential expression of Tbx4 and Tbx5 in Zebrafish fin buds." Mech Dev **87**(1-2): 181-4.

Tanaka, E. M., *et al.* (1999). "Thrombin regulates S-phase re-entry by cultured newt myotubes." Curr Biol **9**(15): 792-9.

Tang, M. K., *et al.* (2000). "Bmp-4 requires the presence of the digits to initiate programmed cell death in limb interdigital tissues." Dev Biol **218**(1): 89-98.

Thome, M., *et al.* (1998). "Identification of CARDIAK, a RIP-like kinase that associates with caspase-1." Curr Biol **8**(15): 885-8.

Veenstra, G. J., *et al.* (1998). "Non-cell autonomous induction of apoptosis and loss of posterior structures by activation domain-specific interactions of Oct-1 in the Xenopus embryo." Cell Death Differ **5**(9): 774-84.

Vogel, A., *et al.* (1996). "Involvement of FGF-8 in initiation, outgrowth and patterning of the vertebrate limb." Development **122**(6): 1737-50.

Vogel, A., *et al.* (1995). "Dorsal cell fate specified by chick Lmx1 during vertebrate limb development." Nature **378**(6558): 716-20.

Vortkamp, A., *et al.* (1996). "Regulation of rate of cartilage differentiation by Indian hedgehog and PTH-related protein." Science **273**(5275): 613-22.

White, K., *et al.* (1994). "Genetic Control of Programmed Cell Death in *Drosophila*." Science **264**: 677-683.

Wozney, J. M., *et al.* (1988). "Novel regulators of bone formation: molecular clones and activities." Science **242**(4885): 1528-34.

Wu, J., *et al.* (2001). "Cepharanthine activates caspases and induces apoptosis in Jurkat and K562 human leukemia cell lines." J Cell Biochem **82**(2): 200-14.

Wu, J. Y., *et al.* (1996). "The secreted product of Xenopus gene lunatic Fringe, a vertebrate signalling molecule." Science **273**(5273): 355-8.

Wyllie, A. H., *et al.* (1980). "Cell death: the significance of apoptosis." Int Rev Cytol **68**: 251-306.

Yang, Y. and L. Niswander (1995). "Interaction between the signalling molecules WNT7a and SHH during vertebrate limb development: dorsal signals regulate anteroposterior patterning." Cell **80**(6): 939-47.

Yokouchi, Y., *et al.* (1996). "BMP-2/-4 mediate programmed cell death in chicken limb buds." Development **122**(12): 3725-34.

Yokoyama, H., *et al.* (2000). "Mesenchyme with fgf-10 expression is responsible for regenerative capacity in Xenopus limb buds." Dev Biol **219**(1): 18-29.

Yoshida, H., *et al.* (1998). "Apaf1 is required for mitochondrial pathways of apoptosis and brain development." Cell **94**(6): 739-50.

Zou, H. and L. Niswander (1996). "Requirement for BMP signalling in interdigital apoptosis and scale formation." Science **272**(5262): 738-41.

Zou, H., *et al.* (1997). "Distinct roles of type I bone morphogenetic protein receptors in the formation and differentiation of cartilage." Genes Dev **11**(17): 2191-203.

APPENDIX I
PROTOCOLS

HAEMATOXYLIN-EOSIN STAINING OF TISSUE SECTIONS

TISSUE DEPARRAFINIZATION AND REHYDRATION

1. Deparaffinized tissue sections in Xylene → 2 X 3 min at RT.
2. Rehydrate tissue in 100% Ethanol → 2 x 2 min.
3. Wash in 95% Ethanol 2 min.
4. Wash in 70% Ethanol 2 min.
5. Rinse in tap water 2 min.

HARRIS HAEMATOXYLIN STAINING

1. Stain tissue sections in acidic Harris Haematoxylin (2 ml acetic acid/200 ml haemotoxylin) for 1-3 min.
2. Rinse in lukewarm running tap water until water is no longer blue 2-3 min.
3. Transfer to 70% EtOH containing conc. HCl (4 drops HCl/200 ml EtOH) → 3 dips.
4. Rinse sections in lukewarm tap water → 5 dips.
5. Dip into filtered saturated Lithium Carbonate diluted 1:2 in distilled water → 10 dips.
6. Rinse in lukewarm tap water no less than 10 min.

COUNTERSTAIN

1. Counterstain tissue sections in Working Eosin solution for 1 min.
2. Remove excess Eosin by transferring sections to 95% EtOH → 3 dips.
3. Dehydrate tissue in 100% EtOH → 5 dips.
4. Incubate in 100% EtOH → 2 X 1 min.
5. Incubate in Xylene → 3 X 1 min.
6. Mount tissue sections with a coverslip and Permount and let dry O/N at RT.

TUNEL STAINING OF TISSUE CRYOSECTIONS

TISSUE REHYDRATION AND FIXATION

1. Dip slides in dH_2O and air dry 2 min.
2. Fix cryosections in 1% PFA → 10 min at RT.
3. Wash in PBS → 2 X 5 min.
4. Post-fix in precooled (–20°C) Ethanol:Acetic acid (2:1) → 5 min at RT.
5. Wash in PBS 5 min.

PROTEINASE K TREATMENT

1. Rinse in PBT 5 min.
2. In a humidified chamber, incubate slides in Proteinase K (20µg/ml) → 15 min at RT.
3. Rinse in PBS → 2 X 2 min.
4. Wash in PBS → 10 min at RT.

DNASE REACTION (POSITIVE CONTROL ONLY)

1. Following first PBS rinse above, incubate positive control slides in Dnase reaction buffer containing DNase I enzyme (10u/100 µl) → 10 at RT.
2. Wash in PBS 2 min.
3. Resume end labeling.

END LABELING/TdT REACTION

1. Equilabrate cryosections in 1X TdT buffer → 5 min RT.
2. Incubate slides in 1X TdT buffer containing 150U/ml TdT and 0.5 µM DIG-dUTP → 1h in 37°C chamber eg. 100 µl per slide covered with a coverslip:

10 µl	Terminal transferase (15u/µl)
0.5 µl	Dig-dUTP (0.5 µM)
200 µl	5X TdT Buffer
790 µl	ddH_2O
1000 µl	Total

3. Rinse slides in PBS/EDTA (1 mM) to lift coverslips.
4. Incubate in PBS/EDTA (1 mM) → 10 min at RT
5. Wash in PBS → 2 X 2 min.

IMMUNOHISTOCHEMISTRY

1. Equilabrate cryosections in MABT → 10 min RT.
2. In a humidified chamber, block cryosections in Blocking solution → 1 hr at RT.
3. Incubate slides in blocking solution containing Anti-digoxigenin antibody <anti-DIG-AP> (1:1500 dilution) covered with a coverslip → O/N at 4°C.

Following day:

4. Rinse slides in MABT to lift coverslips.
5. Incubate in MABT → 2 X 10 min at RT.

ALKALINE PHOSPHATASE (AP) REACTION

1. Equilabrate cryosections in AP buffer → 5 min at RT.
2. Incubate cryosections in AP buffer w/substrate (~300 ml/slide) → monitor Rx 30 min to 3 hrs.
3. Wash in PBS → 3 X 5 min.
4. Mount slides under a glass coverslip with 50/50 glycerol:PBS.
5. Seal slides with nail polish and store at 4°C in slide holder.

WHOLE MOUNT TUNEL PROTOCOL

TISSUE REHYDRATION

1. 75% MeOH/25% H_2O → 10 min RT.
2. 50% MeOH/50% H_2O → 10 min.
3. 25% MeOH/75% PBT → 10 min.
4. 100% PBT → 3 X 10 min.

PROTEINASE K TREATMENT

1. Incubate embryos in 1ml of 25 μg/ml Proteinase K in PBT → 20 min at 37°C.
2. Wash in PBT → 2 X 15 min at RT.
3. Wash in PBS → 2 X 15 min at RT.

DNASE REACTION (POSITIVE CONTROL ONLY)

1. Following PBT wash above, incubate positive control embryos in Dnase reaction buffer containing DNase I enzyme (10u/100 μl) → 20 min at 37°C.
2. Wash embryos in PBS → 2 X 5 min at RT.
3. Resume end labeling.

END LABELING/TdT REACTION

1. Equilibrate embryos in 1X TdT buffer → 30 min at RT.
2. Incubate embryos in 1X TdT buffer containing 150U/ml TdT and 0.5 μM DIG-dUTP → O/N at RT.

Following Day:

3. Wash in PBS/EDTA (1 mM) → 2 X 45 min at 65°C.
4. Wash in PBS → 4 X 45 min at RT.

IMMUNOHISTOCHEMISTRY

1. Equilabrate embryos in MAB-B → 30 min RT.
2. Add 1ml Blocking Solution and incubate → O/N at 4°C.
3. Dilute Anti-digoxigenin antibody <anti-DIG-AP> in 1:400 blocking solution.
4. Add 10 mg/ml newt powder and rotate → O/N 4°C.

Following Day:

5. Spin down newt powder and dilute <anti-DIG-AP> 1:400 solution to 1:1000.
6. Add 0.5 ml to embryos and gently agitate → O/N at 4°C.

Following Day:

7. Wash in MAB → 10 X 15 min RT.

ALKALINE PHOSPHATASE (AP) REACTION

1. Equilabrate embryos with AP Buffer → 2 X 5 min.
2. Incubate embryos in 1.5 ml AP Buffer w/ substrate → monitor Rx 10-30 min.
3. Rinse by adding Bouin's Fixative and fix → O/N 4°C.
4. Rinse in several changes of 70% EtOH to remove yellow (picric acid).

*If tissue appears to dark, transfer tissue to 80% MeOH/20% H_2O_2 in a glass vial → 4°C O/N.

5. Tissues are stored in 100% MeOH at –20°C.

REAGENTS/SOLUTIONS

10X MEM SALTS

MOPS (MW=209.3)	41.85 g	1 M
$MgSO_4$ (MW=246.5)	0.5 g	10 mM

ddH_2O up to 200 ml total volume
Adjust pH to 7.4 Add:

EGTA (MW=380.4)	1.5 g	20 mM

Autoclave, and store at RT in dark bottle/in dark. *Discard if solution turns bright yellow.*

MEMFA FIXATIVE (Fresh)

10X MEM salts	2 ml
37% Formaldehyde	2 ml

ddH_2O up to 20 ml total volume

10X PBS (Phosphate Buffered Saline)

NaCl	40 g
KCl	1 g
Na_2HPO_4	7.2 g
KH_2PO_4	1.2 g

ddH_2O up to 500 ml total volume
Autoclave and store at RT

PBT (Phosphate Buffered Tween)

10X PBS	50 ml
Tween-20	500 µl

ddH_2O up to 500 ml total volume
Store at RT

DNASE REACTION BUFFER

1 M Tris-Cl pH 7.5	10 µl	50 mM
0.5 M $MnCl_2$	4 µl	10 mM
1 mg/ml BSA	10 µl	50 µg/ml

ddH_2O up to 200 µl total volume

MAB (Maleic Acid Buffer)

Maleic anhydride	4.9 g	100 mM
NaCl	4.38 g	150 mM

Adjust pH to 7.5
ddH_2O up to 500 ml total volume, Store at RT

MAB-B (MAB with Bovine Serum Albumin-BSA; Fresh)

BSA-fraction V	100 mg	0.2 mg/ml BSA

MAB up to 500 ml total volume
Store at RT

MABT (MAB with 0.1% Tween-20)

MAB	200 ml
Tween-20	200 µl

ANTIBODY BLOCKING SOLUTION (whole mount)

MAB-B	4 ml
Sheep Serum	1 ml

Inactivate Sheep serum at 55°C for 1 hr prior to use

BLOCKING SOLUTION (cryosections)

Sheep Serum	1 ml
Blocking Reagent (BM)	1 ml
MABT	3 ml
	5 ml

BLOCKING REAGENT (BM)

Blocking reagent (cat. # 1096176) is prepared as 10% stocks in MABT
Aliquots stored at –20°C
Heat at 37°C to dissolve prior to use

AP REATION BUFFER (Fresh)

1 M Tris pH 9.5	5 ml	100 mM
5 M NaCl	1 ml	100 mM
1 M MgCl2	2.5 ml	50 mM

ddH_2O up to 500 ml total volume

AP BUFFER WITH SUBSTRATE

AP Reaction Buffer	1 ml	
NBT (100 mg/ml)	3.375 µl	p-Nitro Blue Tetrazolium chloride
BCIP (50 mg/ml)	3.5 µl	5-Bromo-4-Chloro-3-Indolyl-Phosphate

G-BOUIN'S FIXATIVE

Saturated aqueous picric acid	85 ml
37 % formaldehyde (formalin)	12 ml
Glacial acetic acid	3 ml
	100 ml

Solutions: 0.01 M PBS (pH7.4); BCIP and NBT (Invitrogen); Terminal Deoxynucleotidyl Transferase, Recombinant (10533-065, 500 units, 15U/µl, Invitrogen); Digoxigenin-11-dUTP (1 093 088, 25 nmol/25 µl, 1 mM, Roche); Anti-Digoxigenin-AP, Fab fragments 150U/ml dH_2O (1 207 733, 150U, Roche).

APPENDIX II
SUPPLEMENTAL STATISTICAL DATA

Figure 20. Trendlines showing the tightness of fit in standardizing ratios between animals.

A comparison between the best-fit trendlines based on the average ratios for control values between animals over time. Trendlines were based on the ratios for C1/C2 (A), C3/C1 (B), and C3/C2 (C). Since the ratios for C1/C2 and C3/C1 had the least variability over time, C1 was chosen as the normalizing value for digital and interdigital lengths between animals.

Trendline based on C1/C2

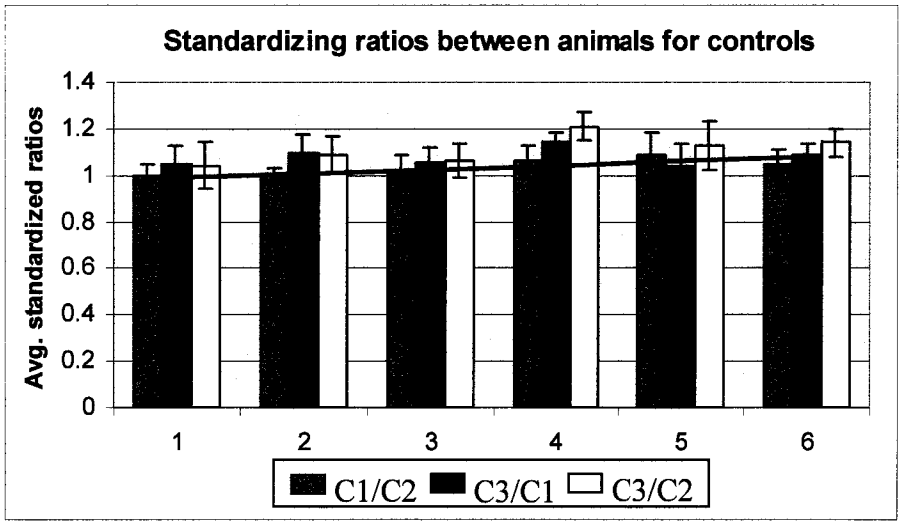

Trendline based on C3/C1

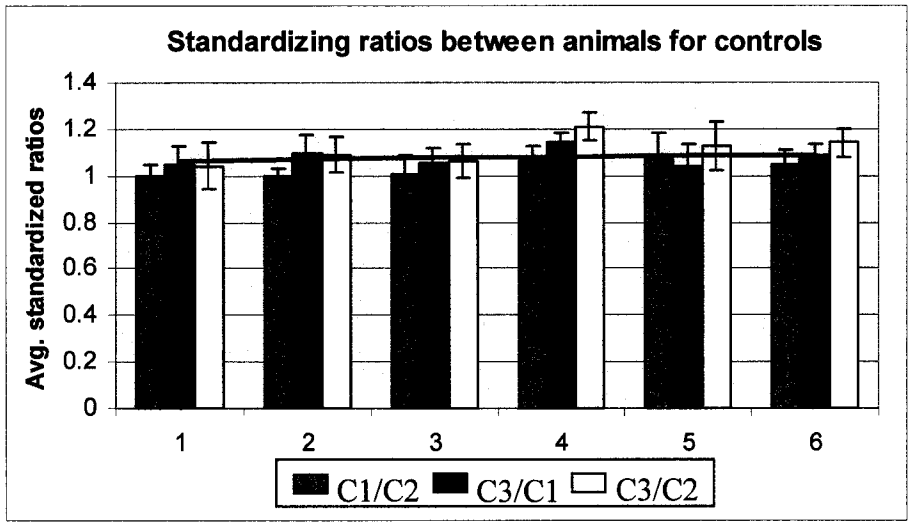

Trendline based on C3/C2

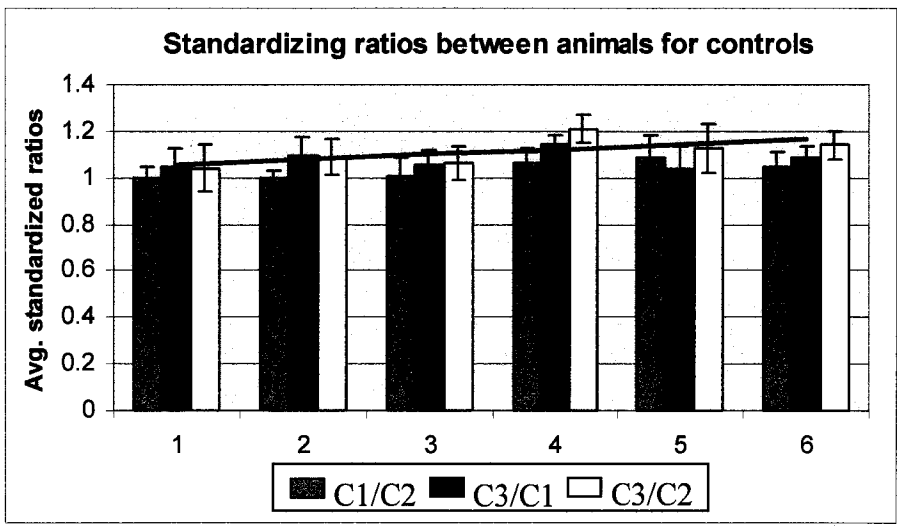

Figure 21. Average interdigital lengths between animals over time.
A) A representation of average interdigital growth between animals for digits 1 and 2 (D1-2); B) digits 2 and 3 (D2-3); C) digits 3-4 (D3-4). For all three interdigital measurements, lengths increased from the first time point (day 39) until day 54 (~ 8 weeks) and then the lengths plateaued for the last two time points.

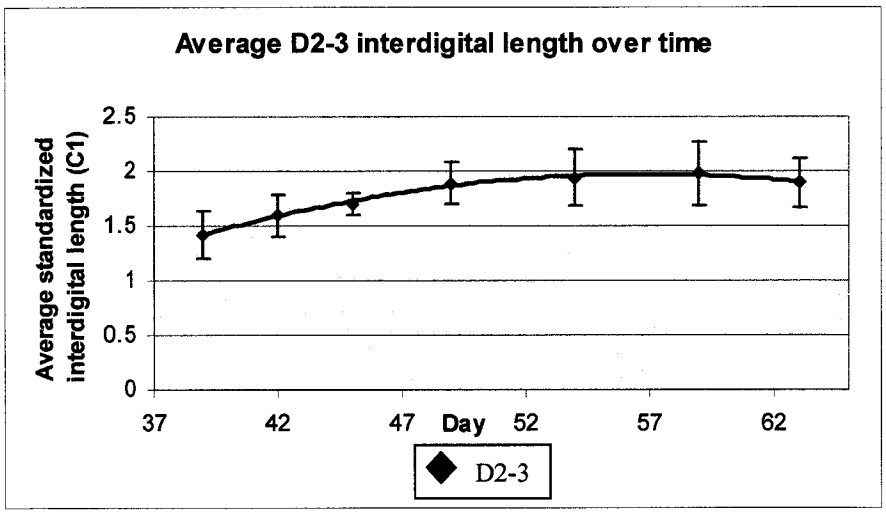
Average D2-3 interdigital length over time
Average standardized interdigital length (C1)
2.5
2
1.5
1
0.5
0
37
42
47
Day
52
57
62
D2-3

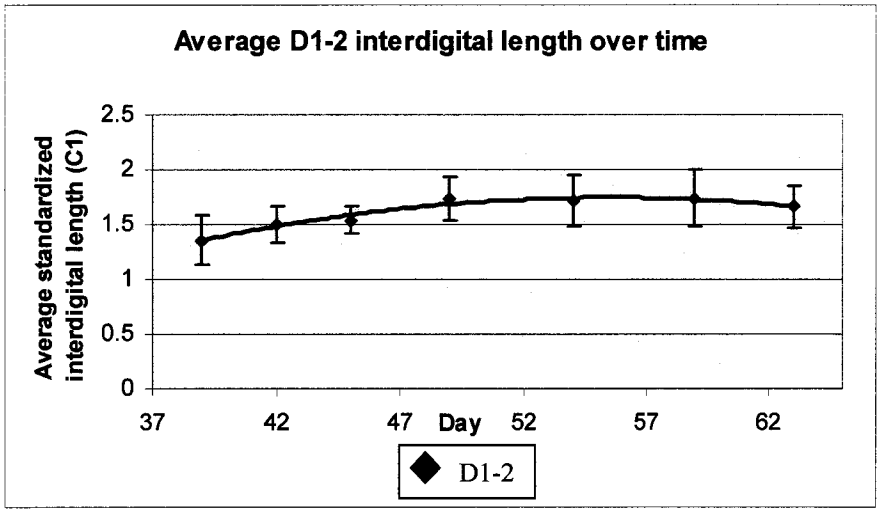
Average D1-2 interdigital length over time
Average standardized interdigital length (C1)
2.5
2
1.5
1
0.5
0
37
42
47
Day
52
57
62
D1-2

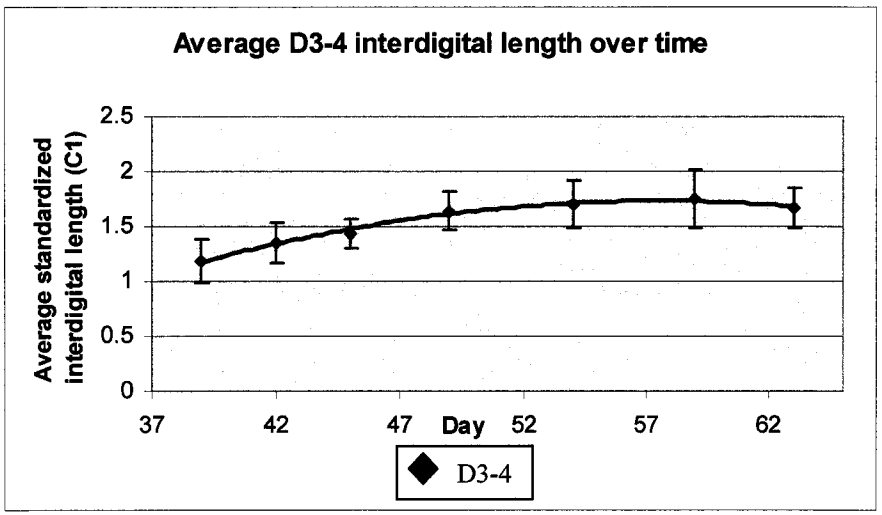
Average D3-4 interdigital length over time
Average standardized interdigital length (C1)
2.5
2
1.5
1
0.5
0
37
42
47
Day
52
57
62
D3-4